

Nature and Evolution of a Soil Toposequence at Coloso Valley Agricultural Reserve

by
Geraldine N. Vega Pizarro

A thesis submitted in partial fulfillment of the requirements for the degree of
MASTER OF SCIENCE
in
SOIL SCIENCES
UNIVERSITY OF PUERTO RICO
MAYAGÜEZ CAMPUS
2017

Approved by:

Miguel A. Muñoz, PhD
President, Graduate Committee

Date

Julia M. O'Hallorans, PhD
Member, Graduate Committee

Date

Hernán Santos, PhD
Member, Graduate Committee

Date

Roberto Vargas, PhD
Director Department of Agroenvironmental Sciences

Date

Ricardo R. López Rodríguez, PhD
Graduate School Representative

Date

Abstract

Soil physical, chemical and mineralogical properties of four profiles in a Rio Piedras-Bajura toposequence at Coloso Valley Agricultural Reserve were evaluated to theorize about the nature and evolution of these soil series over the last 49 million years. Rio Piedras soil series (Ultisol) formed from manganese enriched volcanoclastic and stratified sedimentary rocks, deformed by the compressive movement of tectonic uplift in western Puerto Rico. Bajura soil series (Mollisol) formed from alluvial deposits eroded from adjacent rocks. The Ultisol predominates in the highest parts of the valley, and the Mollisol in the lower parts. Soil profiles along the toposequence, at shoulder, backslope, footslope and valley landscape positions were evaluated. In the area occupied by the Rio Piedras soil series at shoulder position, a profile with an atypical vertical stratification was identified. Soil texture, aggregate stability, structure, color, pH, cation exchange capacity, organic matter content, presence of manganese masses or concretions, iron and aluminum oxides and the mineralogy of the clay fraction were evaluated. Yellowish and redish hues (2.5YR, 5YR, 7.5YR, 10YR and 10R), dominant in Rio Piedras profiles, were associated with an increase in iron and aluminum oxides with soil ageing. Brownish to yellowish and gley colors that dominated Bajura (2.5YR, 10YR and Gley) were associated to redox reactions during water table fluctuations. A clayey texture predominates along the toposequence, but a higher content of sand and silt was observed in Bajura, soil located at the lowest position in the toposequence. Aggregate stability (62% - 76%) and organic matter (0 - 3.3%) content in soil surface increased downslope, as we move from the Ultisol to the Mollisol. Surface pH also increased downslope (3.8 - 6.6). Soil exchangeable Al^{3+} content was very high in Rio Piedras profiles, reaching values over $30 \text{ cmol}_c \text{ kg}^{-1}$ in some instances. Bajura had a cation exchange capacity over $20 \text{ cmol}_c \text{ kg}^{-1}$ as expected for a Mollisol. The oxides content in the

crystalline fraction was considerably higher than amorphous fraction. X-ray diffraction analysis of the clay fraction indicated the presence of micas, expansive (2:1) clays, chlorite, kaolinite, gibbsite, goethite, hematite and quartz minerals in all soil profiles and possible presence of manganese minerals pyrolusite or birnesite in Bajura, Rio Piedras footslope and some strata of the vertically stratified profile. Oxides ratios, mineralogy and color reflect the advanced weathering stage of Rio Piedras Ultisol. Main differences in soil properties are attributed to differences in parent materials and topography. Nature and evolution of Coloso Valley is associated to geological processes of Cerrillos Belt, Eocene in age (~49 Ma). Manganese nodules occurrence in Rio Piedras soil may be a weathering product from these rocks while masses of Bajura are of more recent origin due to water table fluctuations. Geological and pedological processes of the area resulted in the properties and evolution of this soil toposquence over time.

Resumen

Las propiedades físicas, químicas y mineralógicas de cuatro perfiles de suelos en una toposecuencia de Rio Piedras-Bajura en la Reserva Agrícola del Valle de Coloso fueron evaluadas con el propósito de teorizar sobre la naturaleza y evolución de estas series de suelos en los últimos 49 millones de años. La serie de suelos Rio Piedras (Ultisol) se formó de rocas volcanoclásticas y sedimentarias estratificadas enriquecidas con manganeso, deformadas por los movimientos compresivos del levantamiento tectónico en el oeste de Puerto Rico. La serie de suelos Bajura (Molisol) se formó de los depósitos aluviales erodados de rocas adyacentes. El Ultisol predomina en las partes más altas del valle, y el Molisol en las partes más bajas. Los perfiles de suelos a lo largo de la toposecuencia fueron evaluados en las posiciones del hombro, ladera, falda y pie de la vertiente en el paisaje. En el área ocupada por el suelo Rio Piedras, en la posición del hombro de la pendiente, se identificó un perfil con una estratificación vertical atípica. La textura del suelo, estabilidad de agregados, estructura, color, pH, capacidad de intercambio catiónico, contenido de materia orgánica, presencia de masas o concreciones de manganeso, óxidos de hierro y aluminio y la mineralogía de la fracción de arcilla fueron evaluadas. Matices amarillentos y rojos (2.5YR, 5YR, 7.5YR, 10YR y 10R), dominantes en los perfiles de Rio Piedras, están asociados con un incremento en los óxidos de hierro y aluminio con el envejecimiento del suelo. Colores marrón a amarillento y gley (2.5YR, 10YR y Gley) que dominaron Bajura, están asociados a reacciones de oxidación y reducción durante fluctuaciones en el nivel freático. Una textura arcillosa predomina a lo largo de la toposecuencia, pero un contenido más alto de arena y limo se observó en el suelo Bajura localizado en la posición más baja de la toposecuencia. La estabilidad de agregados (62% - 76%) y contenido de materia orgánica (0 - 3.3%) en la superficie del suelo aumentaron pendiente abajo al moverse del Ultisol al Molisol. El pH de la superficie también aumentó pendiente abajo (3.8 - 6.6). El contenido de

Al^{3+} intercambiable del suelo fue muy alto en los perfiles de Rio Piedras, alcanzando en ocasiones valores sobre 30 cmolc kg^{-1} . Bajura tuvo una capacidad de intercambio catiónico sobre 20 cmolc kg^{-1} , esperado para un Molisol. El contenido de óxidos cristalinos fue considerablemente más alto que en la fracción amorfa. Los resultados de difracción de rayos x para la fracción de arcilla indicaron la presencia minerales de mica, arcillas expandibles (2:1), clorita, caolinita, gibsita, goetita, hematita y cuarzo en todos los perfiles de suelos y la posible presencia de los minerales de manganeso pirolusita y birnesita en Bajura, Rio Piedras en la falda de la pendiente y algunos estratos del perfil verticalmente estratificado. La proporción de óxidos, mineralogía y color reflejan el avanzado estado de meteorización para el Ultisol. Las diferencias principales en las propiedades de los suelos son atribuidas a las diferencias en material parental y topografía. La naturaleza y evolución del Valle de Coloso es asociado a los procesos geológicos del Cinturón de Cerrillos, del Eoceno en edad ($\sim 49 \text{ Ma}$). La ocurrencia de los nódulos de manganeso en Rio Piedras pudiera ser producto de la meteorización de estas rocas, mientras que las masas de Bajura, producto de las fluctuaciones en el nivel freático, son de un origen más reciente. Los procesos geológicos y pedológicos en el área han resultado en las propiedades y evolución de esta toposecuencia de suelos a través del tiempo.

To My Beloved Victor Manuel, family and friends who inspired me to accomplish this goal.

Acknowledgements

I am very grateful to Dr. Miguel A. Muñoz for sharing this original research, for his guidance, patience and countless teaching in the last years.

Thanks to Sigfredo (Freddie) Patiño for allowing me to use his land to conduct my research and for his great support during field visits and sampling process. Without your help, this research would not have been possible.

Hernán Santos and Julia O'Hallorans thanks for being member of my committee. Your guidance is priceless. Integration of two scientific disciplines is not easy but your role as mentors have been fundamental in the result of this research.

I wish to thank my beloved husband Victor Manuel for all the love, patience and support during my college years. You inspire me to keep fighting and not to give up when I feel faint.

Special thanks to Dr. Ricardo Goenaga and Delvis Pérez from the Tropical Agriculture Research Station for allowing me the user of their laboratory facilities and the ICP for my samples analysis. Thanks to Miguel Santiago and the Department of Geology of UPRM for their support with the XRD analysis of clays minerals. Special thanks to Dr. Alejandro Segarra for helping in the sand microscopy evaluation.

I am very grateful to the Department of Agroenvironmental Sciences for the financial support and a wonderful educational experience.

To my family and friends, your support has been essential to me.

Table of Contents

Abstract	i
Resumen	iii
Acknowledgements	vi
List of Tables	viii
List of Figures	ix
1. Introduction	1
2. Literature Review	3
3. Methodology	14
3.1 Site Description	14
3.2 Soil Sampling and Analysis	15
4. Results and Discussion	21
4.1 Evaluation and Characterization of a Rio Piedras – Bajura Toposequence	21
4.2 Evaluation and Characterization of a Rio Piedras Vertically Stratified Profile	45
4.3 Geologic Aspects and Evolution of the Rio Piedras-Bajura Soil Toposequence	65
5. Conclusions	76
References	79
Appendix	84

List of Tables

Table 4.1: Field description of Rio Piedras backslope profile	22
Table 4.2: Field description of Rio Piedras footslope profile	24
Table 4.3: Field description of Bajura profile	26
Table 4.4: Chemical properties of Rio Piedras and Bajura soil profiles	29
Table 4.5: Exchangeable manganese of Rio Piedras and Bajura Toposequence	32
Table 4.6: Physical properties of Rio Piedras and Bajura soil profiles	33
Table 4.7: Crystalline and amorphous oxides content of Rio Piedras and Bajura profiles	37
Table 4.8: Crystalline and amorphous oxides content and weathering index	41
Table 4.9: Rio Piedras vertically stratified field description	47
Table 4.10: Chemical properties of Rio Piedras vertically stratified profile	50
Table 4.11: Aluminum content of Rio Piedras vertically stratified profile	51
Table 4.12: Average values for chemical properties of the strata	52
Table 4.13: Average values for aluminum content of the strata	53
Table 4.14: Physical properties of Rio Piedras vertically stratified profile	54
Table 4.15: Average values for physical properties of the strata	55
Table 4.16: Crystalline and amorphous oxides in Rio Piedras vertically stratified profile	59
Table 4.17: Average values for crystalline and amorphous oxides	60
Table 4.18: Crystalline and amorphous oxides and weathering index	61
Table 4.19: Average values for amorphous and crystalline oxides and weathering index	62
Table 4.20: Clay fraction mineralogical composition of Rio Piedras vertically stratified	64

List of Figures

Figure 2.1: Soil map of study site showing location of Rio Piedras and Bajura soil series and other soil series in the Coloso Valley	5
Figure 2.2: General geologic map of Puerto Rico showing the study site (red star) located over Eocene Cerrillos Belt	10
Figure 2.3: Geologic map of the Aguadilla Quadrangle, Puerto Rico	13
Figure 3.1: Aerial view of study site showing location of soil profiles	14
Figure 3.2: Landscape positions sampled for the Rio Piedras-Bajura soil toposequence	15
Figure 4.1: Rio Piedras backslope profile	23
Figure 4.2: Manganese nodules on soil surface of Rio Piedras footslope	24
Figure 4.3: Rio Piedras footslope profile.....	25
Figure 4.4: Manganese masses (a) and manganese concretions (b) in Bajura soil	26
Figure 4.5: Bajura profile	27
Figure 4.6: Sand sample 8x of RP BS Bt ₁	35
Figure 4.7: Sand sample 8x RP FT Bt ₁	35
Figure 4.8: Sand sample 1x RP FT Bt ₁	35
Figure 4.9: Sand sample 8x Bajura Bwg ₁	35
Figure 4.10: Sand sample 1x Bajura Bwg ₁	36
Figure 4.11: X-ray diffraction pattern of the clay fraction of Rio Piedras Backslope A _p horizon. 42	
Figure 4.12: X-ray diffraction pattern of the clay fraction of Rio Piedras Backslope B _{t1} horizon 42	
Figure 4.13: X-ray diffraction pattern of the clay fraction of Rio Piedras Footslope A _p horizon.. 43	
Figure 4.14: X-ray diffraction pattern of the clay fraction of Rio Piedras Footslope AB horizon 43	
Figure 4.15: X-ray diffraction pattern of the clay fraction of Bajura A _p horizon	44
Figure 4.16: X-ray diffraction pattern of the clay fraction of Bajura B _w horizon	44

Figure 4.17: Vertical strata designation for the Rio Piedras profile	46
Figure 4.18: Soil clod from B, C, E and F strata (a) and saprolite fragment from A, D and G strata (b)	46
Figure 4.19: Microscope images of sand grains from selected strata. (a) sample A3, (b) sample B3, (c) sample C3, (d) sample D3, (e) sample E3, (f) sample F3, (g) sample G3 and (h) sample Ctop	57
Figure 4.20: X-ray diffraction pattern of Rio Piedras vertically stratified B1	62
Figure 4.21: X-ray diffraction pattern of Rio Piedras vertically stratified C2	63
Figure 4.22: X-ray diffraction pattern of Rio Piedras vertically stratified D3	63
Figure 4.22: Central and southwestern blocks of Puerto Rico before collision	65
Figure 4.23: Compression in sedimentary rocks	66
Figure 4.24: Anticlines and synclines in sedimentary rocks	67
Figure 4.25: Block diagram of the Rio Piedras-Bajura-Coloso soil toposequence	68
Figure 4.26: Model showing the stratification and deformation of Rio Piedras parent material ..	68
Figure 4.27: Profiles of Rio Piedras and Bajura soil toposequence	69

1. Introduction

A toposequence is formed by adjacent soils that show different profile characteristics influenced by local topography. The comprehensive analysis of toposequences allows the characterization and assessment of environmental and biotic elements of a region. It can provide information on the diversity of soil degradation processes and trends in the landscape evolution (López-Galindo et al., 2003). Soils on hill slopes differ from those at summits or valleys in terms of moisture distribution, soil depth, cations distribution, pH and organic matter contents (Oku et al., 2010; Lawal et al., 2013; Dessalegn et al., 2014).

The soil toposequence at Coloso Valley Agricultural Reserve shows very interesting features. A soil profile with no defined typical horizons was found at a site corresponding to the Rio Piedras Soil Series (Soil Survey Staff, 2015). This soil profile shows a pattern of vertical layers that is not normally seen in soils. Another profile of the Rio Piedras series located at approximately 100 meters distance, showed typical horizonation characteristic of the soil series. An abundance of manganese nodules was observed on the surface and surface horizons of Rio Piedras soil series (Pérez, 2010). The presence of manganese nodules, probably of marine origin, confirms that the geological activity in the area has been a key factor in the evolution of the topography and development of the soil series in the valley.

Considering that soil formation is the product of the interaction between parent material, topography, biodiversity and climate over time, the vertical orientation of layers in the first soil profile might be explained as a regional geological event. The soils closely associated to Rio Piedras soil series are of significant importance to understand the evolution of the Coloso Valley, like the Bajura soil series. Bajura occurs under an aquic moisture regime and shows redox features in the profile. Rio Piedras and Bajura can be related as a soil toposequence at Coloso

Valley. The present conditions of both soil series developed a special interest in the evolution of these soils. The relationship of the toposequence with its parent material could be explained from the regional geology of Coloso Valley. Tectonical events and sea level changes shaped current topography and landscape formation. We have to look for similarities or differences between soil series in spite of being of different orders and being located in different landscape position.

In Puerto Rico, research projects relating soil science and geology are not very common. There are no previous reports in Puerto Rico on soils profiles showing vertical layers in such non-typical orientation. Little is known about the formation and behavior, and if there is a direct relation to the topography and geological formations.

The research herein presented integrates soil science and geology concepts to study detailed aspects of a soil toposequence in the Coloso Valley, with special interest in the Río Piedras soil series. Theories on the Caribbean and Western Puerto Rico geology will be used to explain and theorize about the occurrence of the Rio Piedras soil profile showing vertical strata (Laó-Davila, 2014; McIntyre et al., 1970; Monroe, 1969; Pindell, 1994). The Rio Piedras soil profile with vertical strata will be compared with a Rio Piedras soil profile in a nearby pit presenting typical horizons.

The Coloso Valley is of great importance for agricultural production. Sugarcane was for many decades the most important crop in the valley. At present, some sugarcane has been planted at the Coloso Valley by the Department of Agriculture, in an attempt to reborn the sugarcane industry. Also, several farmers are producing yams, tanniers, cassava, plantains and ornamental crops. A thorough knowledge on the formation of these soils, their pedological age, physical and chemical properties, and fertility will provide valuable information to implement

optimum management practices, preserve the soil quality and foresee future evolution and transformation of the soils in the toposequence.

2. Literature Review

Soils are the product of the interactions of climate, geologic formations, chemical reactions, physical work, vegetation and fauna (Van Wambeke, 1992). The regional contrast between climate and topography for a specific location results in different soil properties created by slope orientation, differences in vegetation, soil erosion and organic matter content. Soil slope and relief controls deposition of material by erosion, contributing to soil diversity in a specific area, similar to soils developed in the Coloso Valley (Encina-Rojas, 1998).

Topography controls most surface processes taking place on earth and as a soil forming factor, influences soil chemical and physical properties, and the pattern of soil distribution over landscape (Lawal et al., 2013). Dessalegn et al. (2014) mentioned topography as the dominant factor influencing soil property variation due to its influence on runoff, drainage, microclimate and soil erosion. In a sloping landscape, runoff and erosion will be more severe. Both processes remove the topsoil affecting chemical and physical properties in up slope and foot slope positions (Lawal et al., 2013).

Topography will also influence regional weathering due to its effect on slope aspect, soil microclimate and biological activity. Weathering is a predominant soil-forming process. During chemical weathering, mineral cleavage planes are weakened; primary minerals decompose and grains break apart and joined smaller particle size fractions producing sand and silt. The presence of fine silt is an indicator of actively weathering horizons. When all weatherable minerals are

decomposed, the silt fraction remains constant or decrease by dissolution, forming clay (Van Wambeke, 1992).

Sand, silt and clay are the main components of soil texture. The texture of highly weathered soils, developed in situ, is well correlated with their parent rock and regional geology (Van Wambeke, 1992). Residual soils formed in situ from solid rock are predominant in Puerto Rico, but in Quaternary areas extensive development of transported soils occur (Mitchell, 1954). Transportation of soils is possible due to relief variation. Topography controls erosion patterns and transportation of material downslope, altering soil texture. Silt and clay fractions will be abundant downslope while sand will prevail from middle slope to up slope positions. Clays and silts are very important to soil fertility due its cation exchange capacity and water holding capacity. Thus, movement and accumulation of clay and silt particles downslope increase down slope fertility (Dessalegn et al., 2014; López-Galindo et al., 2003; Lawal et al., 2013).

Oku et al. (2010) studied an Alfisols toposequence in Nigeria and found significant variability in soil physical and chemical properties due to topography. Upper slope and middle slope soils show comparable pH values, cation exchange capacity, electric conductivity, base saturation and organic carbon content, while foot slope shows more variability in bulk density, porosity, gravimetric moisture content, organic carbon and cations concentration. The variability in soil properties at the series level was explained by small changes in topography that affect the transport and storage of water across and within the soil profile (Oku et al., 2010).

Dessalegn et al. (2014) worked with a soil toposequence at Ele Watershed in Southern Ethiopia. The results also showed variability in soil structure, organic carbon (OC), total nitrogen (TN), C:N ratio, available P (P) and cation exchange capacity (CEC) due to differences in local topography. The organic carbon, total nitrogen, available P and CEC increased from upper to

lower slope positions. Pedons at upper and middle slopes were found to be well drained. The one on lower position was poorly drained. The authors determined that topography also influences soil color. Soil color results showed that hue was redder and the value and chroma increased with soil depth due to illuviation and accumulation of sesquioxides. Upland soils were dark red and coarse textured, lowland soils were dark grayish due to imperfect drainage and clayey texture. A darker color in the surface layer was attributed to higher organic matter content (Dessaegn et al., 2014).

At the Coloso Valley Agricultural Reserve four soil series predominate: Rio Piedras (Ultisol), Bajura (Mollisol), Coloso (Inceptisol) and Toa (Mollisol) (Fig. 2.1). Rio Piedras soil series is classified as *Fine, kaolinitic, isohyperthermic Typic Hapludults*; Bajuras clay as *Fine, mixed, superactive, nonacid, isohyperthermic Vertic Endoaquolls*; Coloso clays as *Very fine, kaolinitic, acid, isohyperthermic Vertic Endoaquepts* and Toa as *Fine, mixed, active, isohyperthermic Fluvaquentic Hapludolls* (Gierbolini, 1975).

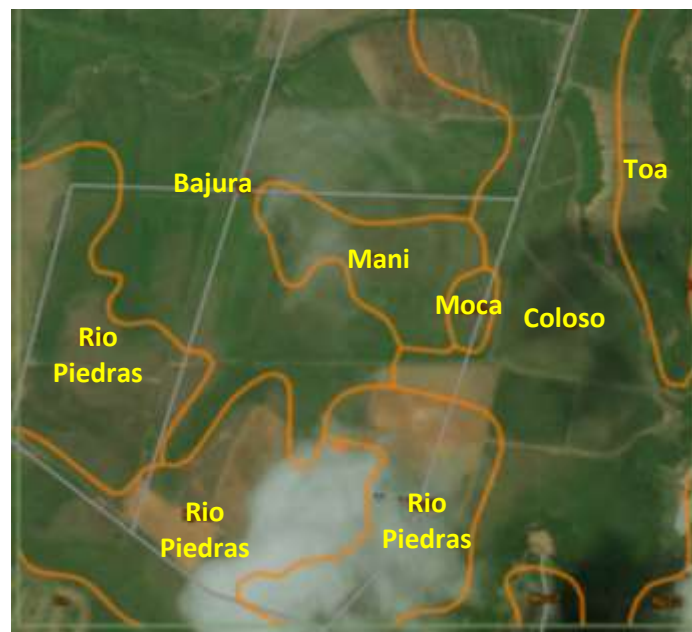


Figure 2.1: Soil map of study site showing location of Rio Piedras and Bajura soil series and other soil series in the Coloso Valle (Web Soil Survev. 2015)

An Ultisol is characterized by the presence of an argillic horizon or a kandic horizon and a base saturation less than 35%, by sum of cations, at a depth of 125 cm below the upper limit of the argillic or kandic horizon, or to a depth of 180 cm from the soil surface (Soil Survey Staff, 1999). Ultisols can be formed in temperate and tropical regions, but need warm temperatures and humidity with a period of precipitation. They can form from a variety of parent materials with little content of primary minerals, with exception of mica minerals and are deficient in basic cations. The clay fraction of these soils is mainly composed of kaolinite, gibbsite and hydroxy interlayered aluminum silicates. The most important process in the formation of Ultisols is the migration of clay from the surface, forming an illuvial horizon that is designated as Bt horizon (Soil Survey Staff, 1999).

The Rio Piedras soil series has been described in the Mayagüez Soil Survey (Gierbolini, 1975) as moderately deep Ultisol, well drained, extremely acid and of slow permeability. This soil has formed from weathered material from thin-bedded siltstone and shales. The slope ranges from 5% to 20%. In a representative profile the surface layer is reddish-brown and extremely acid. The reddish subsoil is extremely acid, slightly sticky and plastic clay with few small rock fragments. The substratum begins at a depth of 27 inches and is highly weathered thin-bedded siltstone with reddish, yellowish and grayish colors (Gierbolini, 1975).

A typical profile of the Rio Piedras series (*Fine, kaolinitic, isohyperthermic Typic Hapludults*) (NRCS, 1975) is as follows:

Ap: 0 - 7 inches. Reddish Brown (5YR 4/4) moist color. Light reddish Brown (5YR 6/4) dry color, moderate medium granular structure, hard, firm, slightly sticky, slightly plastic, many fine roots, extremely acid, clear smooth boundary, 6 to 8 inches thick.

Bt₁: 7 - 11 inches. Yellowish red (5YR 4/8), weak medium subangular blocky structure, firm, slightly sticky, slightly plastic, few faint clay films, few fine roots, extremely acid, clear smooth boundary, 4 to 6 inches thick.

Bt₂: 11 – 21 inches. Red (2.5YR 4/8) and pale brown (10YR 6/3) mottles, moderate medium subangular blocky structure; firm, slightly sticky, slightly plastic, few fine roots, few small siltstone fragments, extremely acid, clear smooth boundary, 8 to 12 inches thick.

Bt₃: 21 – 27 inches. Red (2.5YR 5/6), weak medium subangular blocky structure, firm, slightly sticky, slightly plastic, few faint clay films, many weathered and partially weathered shale fragments giving a yellow (10YR 7/6) mottled appearance; extremely acid, gradual smooth boundary, 6 to 8 inches thick.

C: 27 – 42 inches plus. Highly weathered thin bedded siltstone, original platy structure clearly visible; variegated colors consisting of red, gray and yellow.

Mollisols are mineral soils that have a mollic epipedon described as a dark-colored surface horizon with a base saturation greater than 50 percent as determined by the ammonium-acetate method (Wilding et al., 1983b). These soils have formed mostly in Quaternary materials on gentle to moderate slopes, and on alluvial plains from residuum weathered from sedimentary rocks (Wilding et al., 1983b). Mollisols are distinguished from other soil orders because they have a high organic carbon content, high fertility and good water holding capacity (Encina-Rojas, 1998). These soils are considered the best and most productive agricultural soils.

The Bajura soil series has been described as a poorly drained Mollisol with slow permeability and medium acidity (Gierboini, 1975). These soils are found in the lower areas of the flood plains along rivers and drainage channels, are subjected to frequent flooding and the

water table is seasonally high. These soils were formed in the recent deposits of silt and clay washed from the volcanic and limestone hills. In a representative profile, the surface layer is very dark grayish-brown clay with a medium acidity. The subsoil is very dark grayish brown and gray, medium acid, very firm, sticky and plastic. The substratum is dark gray or greenish-gray, very firm, sticky, plastic and medium acid (Gierbolini, 1975).

A typical profile of Bajura soil series as classified by the Natural Resources Conservation Service (Gierbolini, 1975) is as follows:

Ap: 0 – 4". Very dark grayish brown (2.5YR 3/2). Strong fine and medium subangular blocky structure, slightly hard, firm, slightly sticky, slightly plastic, many fine and medium roots; neutral pH and clear smooth boundary.

Bw: 4 - 16". Very dark grayish brown (2.5YR 3/2). Strong medium prismatic structure; very hard, very firm, slightly sticky, slightly plastic, many fine and medium roots. Iron accumulation on ped surfaces and along root channels with colors dark reddish brown (5YR 3/2) and very dark gray (7.5YR 3/1) neutral; clear wavy boundary.

Bwg: 16 - 42". Very dark gray (N 3/0); strong medium and coarse prismatic structure; very hard, very firm; slightly sticky, slightly plastic; few fine roots; common fine and medium masses of iron accumulation along root channels very dark gray (5YR 3/1) and dark brown (7.5YR 3/3); neutral; clear smooth boundary.

Cg₁: 42 - 47". Dark greenish gray (10Y 3/1); massive; hard, firm; slightly sticky, slightly plastic; few fine roots; many fine yellowish red (5YR 4/6) masses of iron accumulation along root channels; neutral.

Cg₂: 47 - 60". Black (N 2.5/); massive; hard, firm; slightly sticky and plastic; few fine roots; common fine and medium yellowish red (5YR 4/6) masses of iron accumulation on surfaces along root channels; many distinct dark greenish gray (10Y 4/1) areas having less iron and manganese than the matrix; moderately alkaline.

Cg₃: 60 – 80". Black (N 2.5/); massive; few fine roots; common fine and medium dark red (2.5YR 3/6) masses of iron accumulation on surfaces along root channels; moderately alkaline.

Pérez (2010) reported on the occurrence of manganese nodules in a toposequence formed by Coloso series, Rio Piedras series and Bajura series in the Coloso Valley Agricultural Reserve. Manganese is one of the most common elements in soil and it can be found in four different forms: water soluble, exchangeable, reducible and residual (Wilding et al., 1983b). Manganese can be present in soils as oxide mineral like pyrolusite, the most stable form, birnesite, todorokite or hollandite (Wilding et al., 1983a). Manganese oxides show a greater tendency to occur in concretions or nodules in soils than iron oxides (Wilding et al., 1983a). Pérez (2010) suggested ground uplift as an explanation for hydrologic fluctuations in the region that affect the occurrence of manganese nodules in the Rio Piedras soil, the higher soil in the toposequence. The largest manganese nodules were found in the Ap horizon of Rio Piedras soils, while a higher incidence of manganese masses, was observed in the Bw horizon of Bajura soil. The redoximorphic conditions in Bajura soil favor the formation of manganese nodules and masses (Pérez, 2010). The presence of hardpans, flakes and nodules, containing high concentrations of iron and manganese in tropical highlands and at lower elevations was also reported by Eze et al. (2014).

Geology of Western Puerto Rico

The island of Puerto Rico has undergone a series of geological processes since its formation that have influenced the development of its topography. Tectonic reconstructions in the Caribbean and the Gulf of Mexico show how the island of Puerto Rico was forming and moving through the Caribbean until reaching the geographical position that it is today (Pindell, 1994). From the Paleocene to the Eocene, Puerto Rico and the Caribbean islands collided with the Bahamas platform (Laó-Dávila, 2014). In the Middle Eocene, subduction of the Proto-Caribbean plate in the area of the Lesser Antilles was still ongoing, where there was magmatism associated with plates subduction (Laó-Dávila, 2014).

Because of the Eocene subduction, a fault system was developed in the Caribbean that separated The Hispaniola and Puerto Rico. This separation caused a collision occurred in the southwest area of Puerto Rico, between the Bermeja Complex with the Eocene Belt (Pindell, 1994), or Cerrillos Belt (Laó-Dávila, 2014), creating a fault system and deforming rocks along the west side of the island (Pindell, 1994) (Fig.2.2).

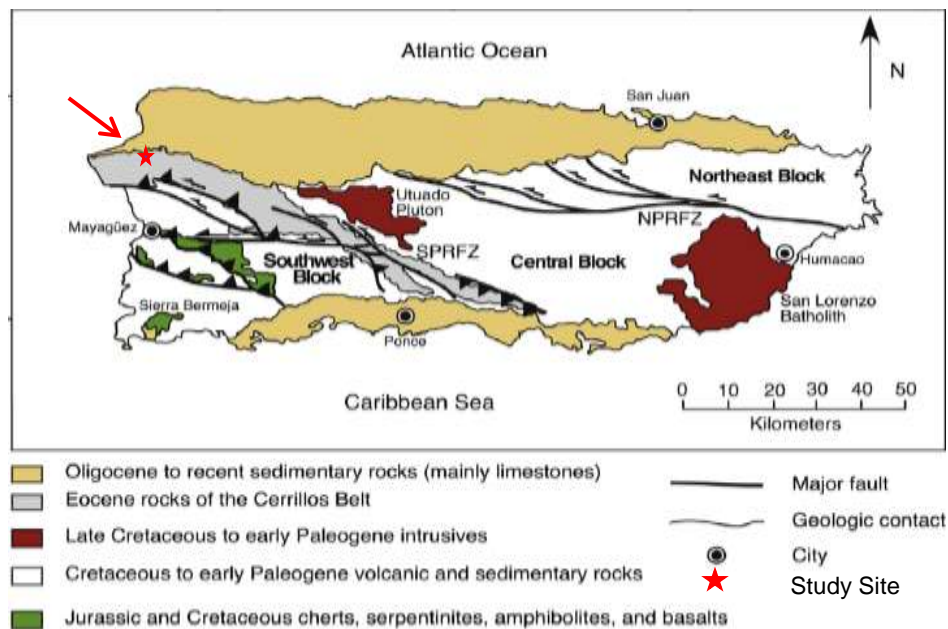


Figure 2.2 General geologic map of Puerto Rico showing the study site (red star) located over Eocene rocks of Cerrillos Belt. (Laó-Dávila, 2014)

Tectonic and sea level changes continued to shape the geology of Puerto Rico in the next fifty million years (Pindell, 1994; Laó-Dávila, 1994). This added to the climate and biological activity, affected erosion and the sedimentation processes of the island. The combination of these factors formed the soils and the landscapes in the western part of the island. The Eocene rocks of the Cerrillos Belt formed the parental material of many soils in western Puerto Rico (Monroe, 1969; Gierbolini, 1975).

Geology of Study Site

The Coloso Valley Agricultural Reserve is located in northwest Puerto Rico in the municipalities of Aguada, Aguadilla and Moca, comprising 2,985 acres of land (LexJuris, 2015). The climate is humid tropical with average annual precipitation of 80 inches and mean annual air temperature of 78°F. The Coloso, Bajura, Rio Piedras, Moca and Maní soil series are topographically associated in the Coloso Valley. This association was developed in the last two million years by geological, pedological and biological activity influenced by topography and regional climatic conditions (Gierbolini, 1975) (Fig. 2.1).

Coloso is an Inceptisol found on river flood plains and low terraces. Moca is an Ultisol located on foot slopes and side slopes of low hills with gradients of 5 to 40 percent. Maní is an Inceptisol on flood plains and terraces of the Humid Coastal Plains. Bajura is a Mollisol formed on river flood plains. The Rio Piedras soil is an Ultisol that occurs on gently to strongly slopes of dissected uplands, with gradients from 2 to 20 percent (Gierbolini, 1975).

The study site comprising the Rio Piedras and Bajura soils, is surrounded by Quaternary Alluvial Deposits and stratified tuffaceous sandstone from Eocene (Monroe, 1969). The Eocene Cerrillos Belt, surrounding the valley, shows high deformation features including large anticlines and

synclines at the northwest, product of the Caribbean tectonic activity during the Eocene (Monroe, 1969; Laó-Dávila, 2014) (Fig. 2.3). At the northern part of study site, the Valley is in contact with Late Cretaceous rocks. The Eocene Cerrillos Belt and Late Cretaceous rocks are separated by a fault system (Laó-Dávila, 2014). These volcanic and calcareous rocks contribute to the parental material of the soils of the study site.

The alluvial deposits in this valley are formed by clayey sand and sandy clay containing scattered pebbles and cobbles of volcanic rocks (Monroe, 1969) mainly eroded in the last 2.6 million years from the river basins of Río Culebrinas and Río Cañas; and volcanic and calcareous hills in the island (Beinroth, 1972). The stratified tuffaceous sandstone consists of grained sandstone and siltstone composed of particles of volcanic ash; locally weathered to thin bedded to massive clay (Monroe, 1969). These rocks are product of submarine volcanic activity (McIntyre, 1970).

The Cerrillos Belt is composed by thin - to massive - bedded turbidite, volcanoclastic and volcanic rocks (Laó-Dávila, 1994). Lavas are more abundant in the center, while volcanoclastic rocks are more abundant in the northwest and southeast limits of the belt. Laó-Dávila (2014) suggests these turbidite rocks were formed by eruption and sedimentation of volcanic material in a narrow basin during the Eocene. When the ejected volcanic material fell into the sea, and reached the bottom, perfect bedding resulted (Mitchell, 1954). Foraminifera and nanofossils present in the layered rocks of the Cerillos Belt indicate a mid-Eocene age (Laó-Dávila, 2014).



Figure 2.3: Geologic map of the Aguadilla Quadrangle, Puerto Rico (Monroe, 1969). Study site is delimited inside red square and red circles pointing Rio Piedras soil pits and blue for Bajura

3. Materials and methods

3.1 Site Description

The Coloso Valley Agricultural Reserve is located in northwest Puerto Rico in the municipalities of Aguada, Aguadilla and Moca, comprising 2,985 acres of land (LexJuris, 2015). The climate is humid tropical with an average annual precipitation of 80 inches and mean annual air temperature of 78°F. The Río Piedras soil occurs on gently to strongly slopes of dissected uplands with gradients from 2 to 20 percent. Bajura soils are formed on river flood plains (Gierbolini, 1975). The study site comprising the Río Piedras and Bajura soils, is surrounded by Quaternary Alluvial Deposits and overlaying highly deformed stratified tuffaceous sandstone of Eocene age (Monroe, 1969; Laó-Dávila, 2014). At the northern part of study site, separated by a fault system, the Valley is in contact with Late Cretaceous rocks. The Culebrinas and Cañas rivers flow between Aguada and Aguadilla municipalities, eroding and depositing volcanic and calcareous rocks in the valley flood plains. Four study sites were selected at the toposequence, three belonging to the Río Piedras soil series and one to Bajura soil series (Figure 3.1).



Figure 3.1 Aerial view of study site showing location of soil profiles

The first site of Río Piedras is in backslope position (Figure 3.2), at coordinates 18.37939915, - 67.14995207, the second site is in footslope position, at coordinates 18.37974981, -67.14992603, and a third Río Piedras site with a soil profile showing vertical stratification was selected in shoulder position at coordinates 18.37894347, - 67.15143585. The Bajura site was selected in the flood plain, at coordinates 18.380494°, - 67.149858°.



Figure 3.2: Diagram showing landscape positions sampled for the Río Piedras-Bajura soil toposequence (Ontl and Schulte, 2012).

3.2 Soil Sampling and Analysis

A soil pit was dug at each selected site, at the Coloso Valley Agricultural Reserve, following the toposequence from backslope to flood plain position. Each soil profile was physically described using the Field Book for Describing and Sampling Soils from the Natural Resources Conservation Services and the Munsell Color Chart. Soil horizons were described taking into consideration thickness, color, structure, root presence, special features and others.

The soil samples collected were air dried, ground to pass through a 2 mm mesh sieve and analyzed for pH, organic matter percent (% OM), cation exchange capacity (CEC), iron and aluminum oxides content, texture, aggregate stability, and clay mineralogy.

A. pH

Soil pH was evaluated in a 2:1 water/soil ratio. Five grams of soil were placed into 25 ml vials, mixed with 10 ml of distilled water, agitated for five minutes and pH measured using a Sper Scientific 860031 Benchtop pH Meter.

B. Soil particles separation

Forty grams of the ground soil were treated with H_2O_2 (30 %) to remove organic matter. A stepwise 5 ml addition of H_2O_2 was performed until a significant decrease in CO_2 evolution was observed. During the process that last about 3 hours, the samples were heated at 80°C in a water bath. Samples were transferred to a centrifuge bottle using 100 ml of 0.25 M NaCl and centrifuged for 5 minutes at 2000 rpm. The solution was decanted and the soil transferred to an electric mixer using a sodium carbonate solution (Na_2CO_3). The sample was stirred for 15 minutes, transferred to a 250 ml centrifuge bottles and centrifuged for 3.5 minutes at 700 rpm for clay extraction. After each centrifugation, the sample was dispersed again in Na_2CO_3 solution and the centrifugation process repeated until a clear suspension was obtained. The clay suspension was allowed to stand for 1 to 2 weeks and the excess liquid was decanted. The clay suspension was saturated with 1N MgCl_2 , dried in an oven at 65°C and pulverized for XRD analysis (Gee and Bauder, 1986). Sand and silt fractions were separated by sieving, dried at 105°C and the weight recorded. The weight of the clay fraction was determined by subtraction and the texture of each horizon calculated based on the 40 gram weight of the sample. The size and roundness of the sand fraction was evaluated using an Olympus SZX16 Microscope and a series of photographs taken. The clay fraction was stored for further xrd analyses.

C. Organic Matter

Soil organic matter content (% OM) was determined by the Walkley and Black method as modified by Greweling & Peech (Nelson and Summers, 1996). A 0.5 g soil sample was mixed with 10 ml of 1N potassium dichromate and 20 ml of concentrated sulfuric acid in a 500-ml Erlenmeyer Flasks. The flask was manually agitated and left to rest for 30 minutes. Then, 200 ml of distilled water were added and 5 drops of ferrosin for color development. Samples were titrated with 0.5 N ferrous ammonium sulfate solution. Organic matter percent was calculated from Organic Carbon percent (% OC) as follows:

$$\%OC = \frac{\text{meq } K_2Cr_2O_7 - \text{meq } Fe (NH_4)_2(SO_4)_3}{\text{Soil weight (g)}} \times \frac{0.003 \text{ g of C}}{\text{meq}} \times 100$$

Where, 0.003 g is the weight of 1 meq of C,

$$\%OM = (\% OC) (1/0.77) (1/0.58)$$

Where, 0.77 is the %C recovered by the Walkley and Black method and 0.58 is the conversion factor from carbon to organic matter.

D. Aggregate Stability

Aggregate stability was determined by the wet sieving method (Kemper and Rosenau, 1986). Soil samples were sieved through a #4 sieve mesh (4.75 mm) and placed on top of a #10 sieve (2 mm). Two samples of 30.0 g were collected from the #10 sieve, one to determine the oven-dry weight at 105° C and the other for aggregate analysis. The 30 g sample was placed in a #10 sieve, which in turn was placed over a #20 mesh sieve and set up in the agitator. Enough water was added to cover the aggregates. The system was agitated for 30 minutes in an upward/downward motion at about 60 cycles per minute. After the 30 minutes agitation period

the samples were dried for 2 hours at 105° C and transferred to small aluminum plates and placed into oven again for 8 hours. The percentage of aggregate stability was calculated as follows:

$$\% \text{ A.S} = [(A+B)/C] \times 100$$

Where *A* is the weight of aggregates retained on sieve #10, *B* the weight of aggregates retained on sieve #20 and *C* is the oven-dry weight of the initial sample.

E. Cation Exchange Capacity

The cation exchange capacity was determined by the ammonium acetate method (pH 7.0) (Sumner and Miller, 1996). A 5 g soil sample was treated with 30 ml of 1M NH₄AOc pH 7.0. The samples were agitated for 5 minutes, centrifuged for 5 minutes at 2,500 rpm and the solution collected in a 250 ml volumetric flask. The process was repeated four times. The solution was brought to volume (250 ml) with distilled water. The exchangeable cations (Ca²⁺, K⁺, and Mg²⁺) were determined by Inductive Coupled Plasma using an *Optima 8000* model.

Exchangeable aluminum was extracted with 1M KCl (Bertsch and Bloom, 1996). A 5 g soil sample was treated with 25 mL of 1M KCl, agitated for 30 minutes and centrifuged for 10 minutes at 2,000 rpm. The decanted solution was collected and acidified to a pH <3.0 with a drop of concentrated HNO₃. Exchangeable aluminum was also determined by Inductive Coupled Plasma. The cation exchange capacity was calculated by sum of cations:

$$\text{CEC} = \Sigma (\text{Ca}^{2+} + \text{Mg}^{2+} + \text{K}^{+} + \text{Al}^{3+})$$

F. XRD analysis of the clay fraction

X-Ray diffraction was used for mineralogy identification in the clay fraction. The analysis was performed using a Siemens Diffraktometer D5000. $\text{CuK}\alpha$ radiation was used to generate the X-rays. The unit was equipped with a graphite monochromator, computer-controlled theta-compensating slit and an automated sample changer. Scans were collected from 4 to $70^\circ 2\theta$, with 2 counts per second at 0.020 degree steps.

G. Iron and Aluminum Oxides

Iron oxides content of the clay fraction were extracted by the citrate-bicarbonate-dithionate method (CBD) for crystalline, amorphous inorganic and organic complexed iron and aluminum oxides fraction (Mehra and Jackson, 1960). The amorphous fraction was extracted by the acid ammonium oxalate method (AAO) (McKeague and Day, 1966). The AAO extracts the amorphous and organic- complexed Fe and Al oxides.

1. Citrate-Bicarbonate-Dithionate Method

Clay samples of 0.5 g were transferred to a centrifuge tube, 5 ml of citrate-bicarbonate buffer and 0.2 g of sodium dithionate ($\text{Na}_2\text{S}_2\text{O}_4$) were added and the sample placed into a water bath at 80°C . After 15 minutes with periodical stirring, the samples were removed and 1 ml of a saturated sodium chlorite solution was added. The samples were centrifuged for 5 minutes at 1500 rpm and filtered into a 100 ml volumetric flask. The extraction process was repeated twice, and the solution was added to the volumetric flask and brought to volume of 100 ml with distilled water (Mehra and Jackson, 1960). The iron and aluminum extracted were determined by Inductive Coupled Plasma and calculated as % Fe, % Fe_2O_3 , % Al, and % Al_2O_3 .

2. Acid Ammonium Oxalate Method

Clay samples of 0.25 g were transferred to centrifuge tubes and 10 ml of ammonium oxalate solution were added. The tubes were wrapped with aluminum foil to avoid light contact and kept in constant shaking in the dark for 4 hours. The samples were centrifuged and the suspension filtered into 25 ml vials (McKeague and Day, 1966). The iron and aluminum extracted were determined by Inductive Coupled Plasma and calculated as % Fe, % Fe₂O₃, % Al, and % Al₂O₃.

4. Results and Discussion

4.1 Evaluation and characterization of a Rio Piedras – Bajura Soil Series

Toposequence

A. Field description

The Rio Piedras pedon at backslope position had 6 horizons (Figure 4.1). They were identified as: Ap (0 – 19.0 cm), Bt₁ (19.0 – 37.0 cm), Bt₂ (37.0 – 58.0 cm), BC (58.0 – 93.0 cm), C₁ (93.0 – 107.0 cm) and C₂ (more than 107.0 cm). Yellow to red colors of 5YR and 10YR hues were dominant through the profile with white – pinkish white mottles (Table 4.1). Manganese nodules were observed in the surface horizon of Rio Piedras footslope (Figure 4.2). The Rio Piedras pedon at footslope position had 7 horizons identified as: Ap (0 – 25.0 cm), AB (25.0 – 38.0 cm), Bt₁ (38.0 – 53.0 cm), BC (53.0 – 94.0 cm), C₁ (94.0 – 132.0 cm), C₂ (132.0 – 155 cm) and saprolite (155 – 183 cm) (Figure 4.3). Yellowish and brownish colors of 7.5YR and 2.5YR were dominant through the profile with grayish (gley hue) mottles below AB horizon (Table 4.2). The Bajura pedon had 6 horizons: Ap (0 – 15.0 cm), Bw (15.0 – 41.0 cm), Bwg₁ (40.1 – 56.0 cm), Bwg₂ (56.0 – 94.0 cm), Cg₁ (94.0 – 107.0 cm) and Cg₂ (107.0 – 145.0 cm). Brownish and yellowish color of 2.5YR and 10YR dominated the profile with grey mottles appearance occurring below Bwg₁ horizon (Table 4.3). Manganese concretions and masses were observed in this profile (Figures 4.4).

The soil profiles were at a close distance from each other, however, they looked very different in color, structure and other features such as presence of soil cracks and manganese nodules and masses. Redder colors were observed in higher elevation and gley colors at lower elevations, where redox reactions are more active. The Rio Piedras pedon at footslope position is in a transitional zone toward the Bajura pedon and it is subjected to flooding and water saturation

during the rainy season. The grayish mottles observed in this profile are indicative of more active redox reactions when compared to the Rio Piedras pedon located at backslope position.

Table 4.1: Field description of Rio Piedras backslope profile.

Rio Piedras Backslope			
Horizon	Depth (cm)	Color (moist)	Structure
Ap	0 – 19	7.5 YR 5/8 strong brown	granular
Bt ₁	19 – 37	5YR 5/8 yellowish red 5YR 8/1 white (mottled)	Subangular blocky
Bt ₂	37 – 58	10YR 6/8 brownish yellow 5 YR 5/8 yellowish red 7.5 YR 8/2 pinkish white (mottled)	Subangular blocky
BC	58 – 93	5YR 5/8 yellowish red 10YR 8/2 very pale brown (mottled)	Subangular blocky
C ₁	93 – 107	5YR 4/6 yellowish red 10YR 8/2 very pale brown (mottled)	Subangular blocky
C ₂	➤ 107	10YR 4/8 Red 7.5YR 5/8 strong brown 7.5YR 5/2 brown 7.5YR 8.2 pinkish white (mottled)	Massive

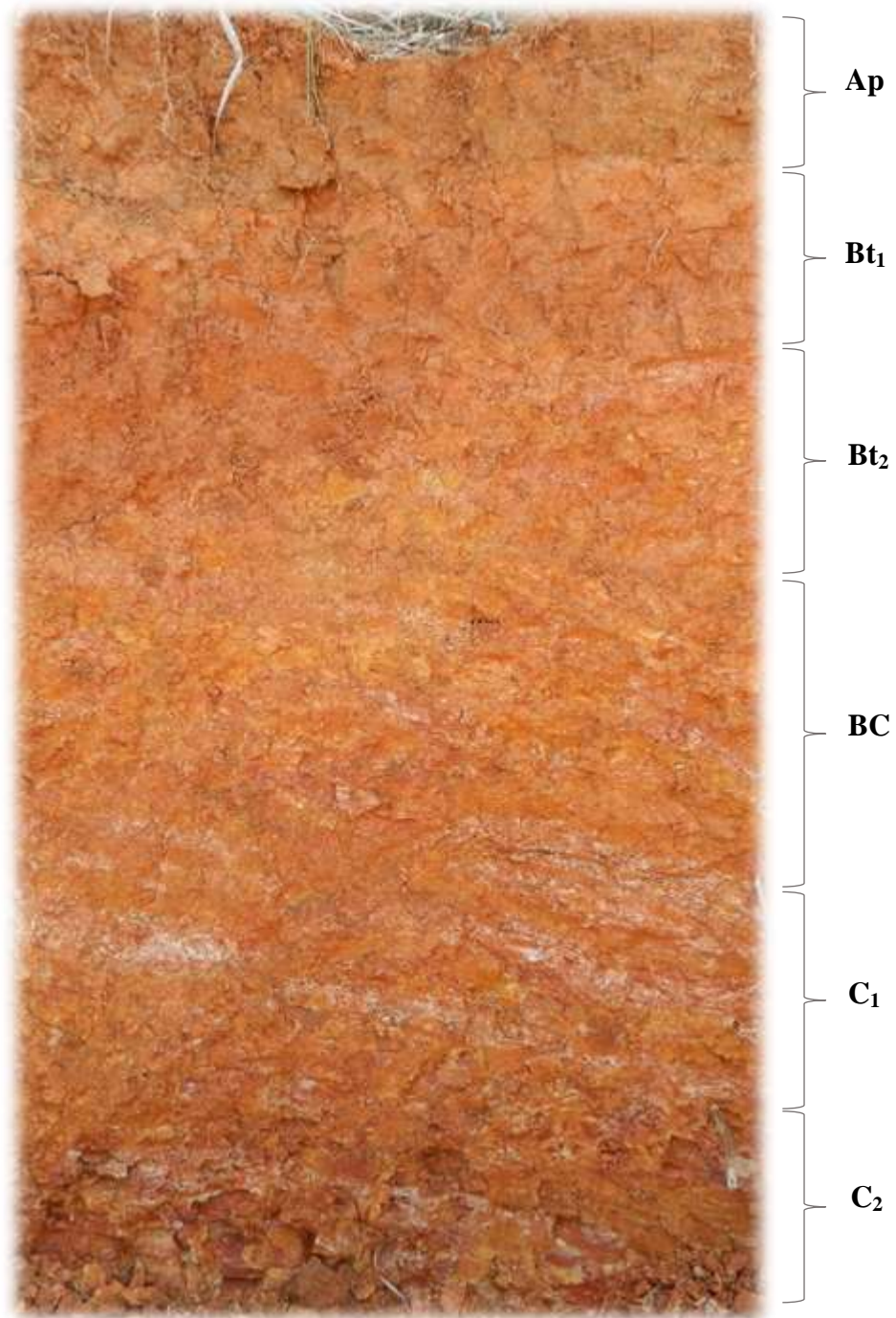


Figure 4.1: Rio Piedras backslope profile

Table 4.2: Field description of Rio Piedras footslope profile.

Rio Piedras Footslope			
Horizon	Depth (cm)	Color (moist)	Structure
Ap	0 – 25	5YR 6/4 yellowish red	Subangular blocky
AB	25 – 38	7.5YR 4/6 strong brown	Subangular blocky
Bt ₁	38 – 53	Gley 8/1 light greenish grey 7.5YR 5/6 strong brown	Subangular blocky
BC	53 – 94	7.5YR 8/1 white 7.5YR 6/8 reddish yellow	Subangular blocky
C ₁	94 – 132	7.5YR 7/1 light grey 2.5YR 4/8 dark red 10YR 6/8 brownish yellow	Subangular blocky
C ₂	132 – 155	7.5YR 7/1 light grey 2.5YR 6/8 dark red	Subangular blocky
Saprolite	155 – 183	7.5YR 7/1 light grey 2.5YR 6/8 dark red	Massive



Figure 4.2: Manganese nodules on soil surface of Rio Piedras footslope profile.

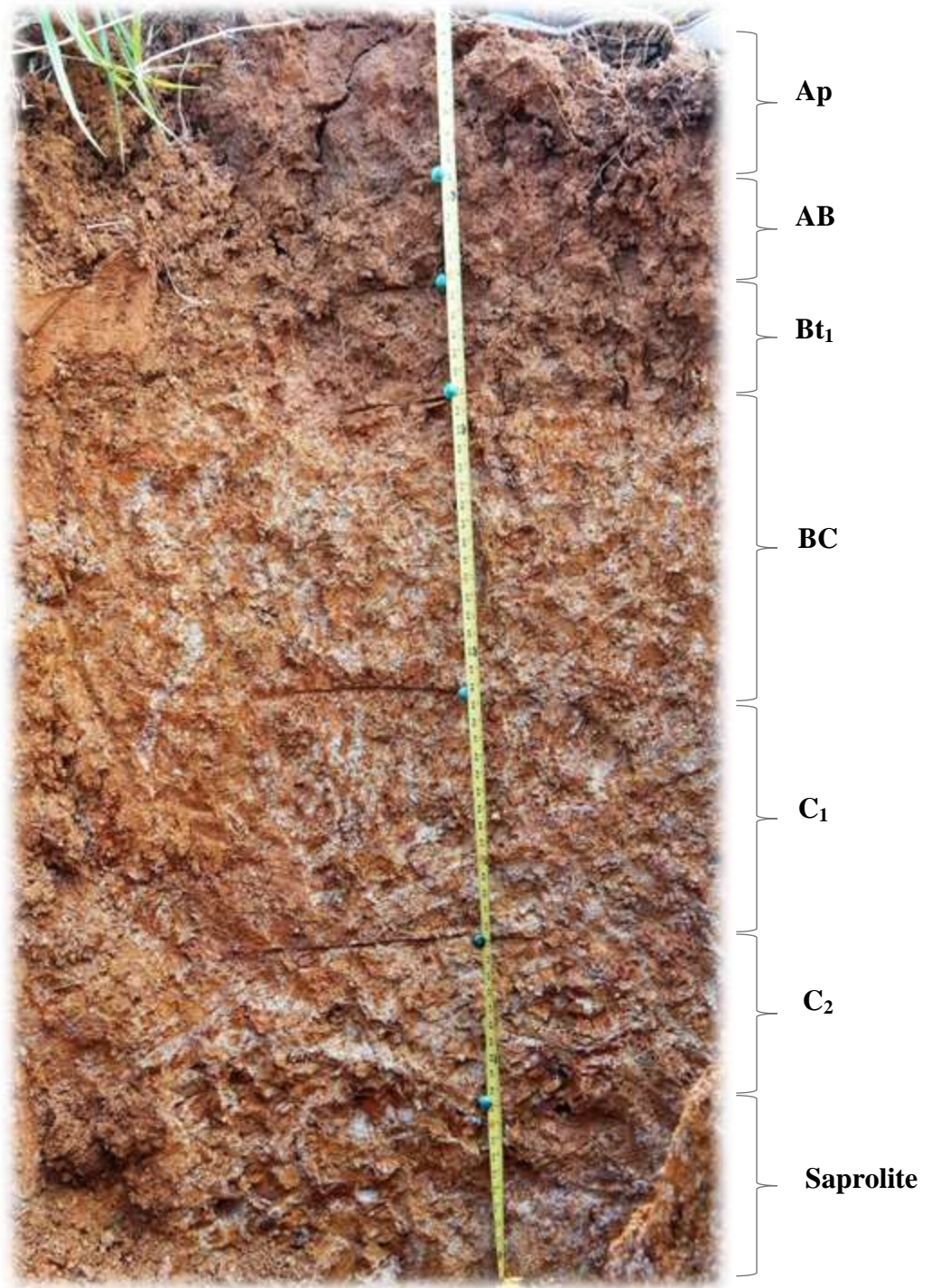


Figure 4.3: Rio Piedras footslope profile

Table 4.3: Field description of Bajura profile.

Bajura					
Horizon	Depth (cm)	Color (moist)	Structure	Mn	Others
Ap	0 – 15	2.5 Y 3/2 very dark grayish brown	Subangular blocky	Conc . < 1%	Cracks Worms Ants
Bw	15 - 41	2.5Y 3/2 very dark grayish brown 7.5 YR 5/8 strong brown	Subangular blocky	Conc. (1cm) 1-2%	Cracks Worms Ants
Bwg ₁	41 – 56	10YR 5/8 yellowish brown 2.5Y 4/2 dark grayish brown	Subangular blocky	Conc. 1% Nodules Shape	
Bwg ₂	56 – 94	10YR 4/6 dark yellowish brown 2.5Y 4/1 dark gray	Prismatic	5% Nodules & Masses	Redox Colors
Cg ₁	94 – 107	10YR 5/8 yellowish brown (80% dominant) 2.5Y 5/1 gray	Subangular blocky	1% Conc	Redox Colors
Cg ₂	107– 145	2.5Y 5/1 gray (dominant) 10YR 5/8 yellowish brown	Subangular blocky		Strong Gleyzation



Figure 4.4: Manganese masses (a) and manganese concretions (b) in Bajura soil

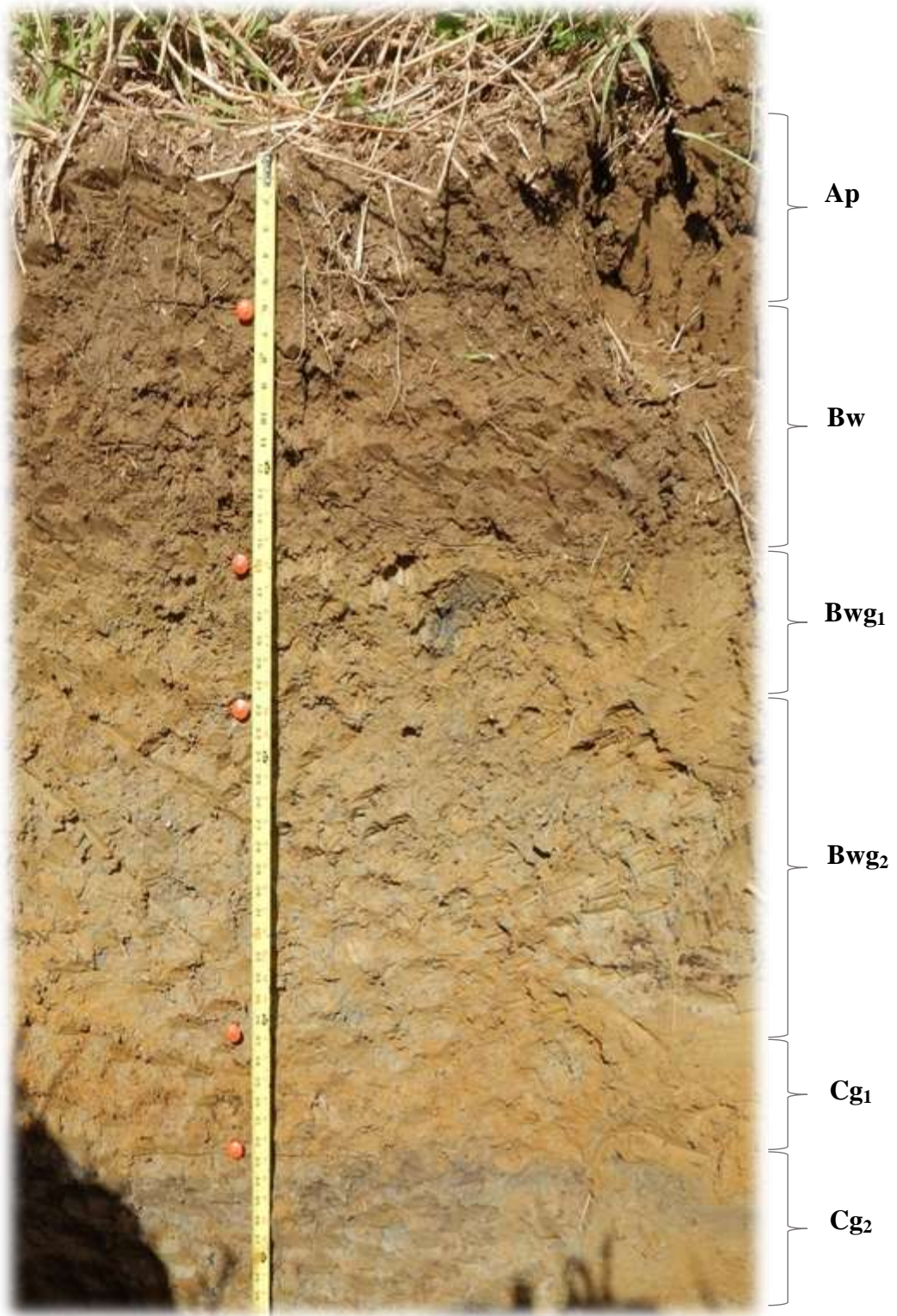


Figure 4.5: Bajura profile

B. Chemical properties

Soil pH ranged from 4.00 to 4.68 in the Rio Piedras soil profile at backslope position (Table 4.4). In the Rio Piedras profile at footslope position, pH ranged from 4.5 to 5.0 with a tendency to decrease pH levels down the soil profile (Table 4.4). However, soil pH of Rio Piedras footslope profile was higher than those observed at the backslope position. In the Bajura soil profile, the pH ranged from 4.76 to 6.85 (Table 4.4). The lowest pH value (4.76) was observed in the Ap horizon. An increase in pH is observed down to the horizon Bwg₁ where it reaches 6.85 and stayed over 6.70 in the last two horizons. The acid conditions of the Ap horizon of Bajura soil was not expected, since Mollisols usually present higher pH values. The intensive fertilization of these fields may have contributed to the acid conditions observed in the Ap horizon. Also, acid leachates moving downward from higher elevations, where very high levels of exchangeable Al³⁺ are present can be an acidity factor. Generally an increase in soil pH as we descend the landscape into the valley is observed. This effect in the pH as topography changes, can be explained by differences in soils according to their composition and parent material. Ultisols are soils predominantly acid due to a high content of exchangeable Al³⁺, while Mollisols have a more alkaline pH and are considered the most fertile soils.

The organic matter content is higher in the upper horizons for each soil profile (Table 4.4). In the Rio Piedras soil profile at backslope position, the organic matter content was 2.62 % in the topsoil horizon and decreased in horizons Bt₁ and Bt₂. No organic matter was detected in the following horizons of this profile. The Rio Piedras profile at footslope position has an organic matter content of 1.93 % in the horizon Ap. However, organic matter content in subsurface horizons was higher than in the subsurface horizons of Rio Piedras backslope profile. Bajura soil profile has an organic matter content of 3.26 % in the Ap horizon. Organic matter

Table 4.4: Chemical properties of Rio Piedras and Bajura soil profiles.

Depth cm	Horizon	pH	O.M. %	Ca ²⁺ -----	K ⁺ -----	Mg ²⁺ cmol _c kg ⁻¹	Al ³⁺ -----	CEC -----
Rio Piedras Backslope								
(0 - 19)	Ap	4.48	2.6	5.3	0.4	1.7	21.6	29.0
(19 - 37)	Bt ₁	4.26	0.5	4.0	0.2	1.1	31.4	36.6
(37 - 58)	Bt ₂	4.66	0.2	3.8	0.4	1.0	32.0	37.2
(58 - 93)	BC	4.0	0	3.1	0.2	1.2	29.3	33.9
(93 - 107)	C ₁	4.33	0	2.3	0.2	1.7	25.1	29.3
(>107)	C ₂	4.64	0	2.2	0.3	2.7	32.7	37.8
Rio Piedras Footslope								
(0 - 25)	Ap	5.0	1.9	8.5	0.2	2.3	7.1	18.06
(25 - 38)	AB	4.86	1.4	4.0	0.2	1.2	13.9	19.26
(38 - 53)	Bt ₁	4.72	1.3	2.4	0.3	0.9	17.5	21.05
(53 - 94)	BC	4.58	0.6	2.6	0.4	1.5	22	26.44
(94 - 132)	C ₁	4.58	0.3	2.4	0.3	3.7	23.5	29.87
(132 - 155)	C ₂	4.52	0.1	1.5	0.3	6.1	32.9	40.81
(155 - 183)	Sap	4.51	0.1	3.4	0.2	1	31.2	35.8
Bajura								
(0 - 15)	Ap	4.76	3.3	14.1	0.1	5.8	1.6	21.5
(15 - 41)	Bw	5.87	1.3	17.8	0	7.3	0.1	25.2
(41 - 56)	Bwg ₁	6.65	0.9	22.1	0.1	9.8	0	31.9
(56 - 94)	Bwg ₂	6.85	0.7	21.3	0.1	10.2	0	31.5
(94 - 107)	Cg ₁	6.81	0.7	19.4	0.1	9.4	0	28.9
(107 - 145)	Cg ₂	6.79	0.4	20.9	0.1	10.1	0	31.2

* Sap – saprolite

content over 3.0 % is considered excellent in soils and it is common to observe values over 3 % in most Mollisols. As expected, a decrease in organic matter is observed in the subsurface horizons.

The higher content of organic matter as we move down the toposequence could be explained by a topographic effect. Topography plays a major role in the regional microclimate because it affects the soil exposure to sun and water movement. Hills and mountains with less vegetation, usually present lower infiltration rates and lower water retention. Also, erosion from higher elevations contributes to organic matter accumulation in lower areas. The microclimate controls the humidity and evaporation rate of these soils. There will be a higher biomass production at lower areas of the toposequence due to higher moisture content. The increase in biomass is directly related to the increase in organic matter (Encina-Rojas, 1998). Also, Bajura soil is an Aquolls subjected to flooding and decomposition of organic matter slows down under reduced conditions (Gierbolini, 1975).

The cation exchange capacity (CEC) in Rio Piedras profile at backslope position ranges from 29.0 cmolc kg⁻¹ to 37.8 cmolc kg⁻¹, the profile at footslope position ranges from 18.0 cmolc kg⁻¹ to 40.8 cmolc kg⁻¹ and Bajura from 21.5 cmolc kg⁻¹ to 31.9 cmolc kg⁻¹ (Table 4.4). Cation exchange capacity is higher in Rio Piedras soil profiles than Bajura as result of the high content of exchangeable Al³⁺. The exchangeable Al³⁺ exceeds 18 cmolc kg⁻¹ in Rio Piedras, whereas the highest Al³⁺ content in Bajura was 1.6 cmolc kg⁻¹. Exchangeable calcium and magnesium content was higher in Rio Piedras footslope profile than in Rio Piedras backslope profile. A decrease in exchangeable calcium was observed at higher depths in the profiles. Exchangeable calcium and magnesium were higher in Bajura soil and their concentration increased in the lower horizons. The highest exchangeable calcium concentration observed in Bajura soil was 22.07

cmolc kg⁻¹, which is four times the exchangeable calcium observed in Rio Piedras backslope profile. Its availability, according to parameters established by the Central Analytical Laboratory of the Agricultural Experiment Station (Appendix 1), is low at the backslope, medium to low on the footslope and high in Bajura. Magnesium increases with soil depth and reach a value of 2.7 cmolc kg⁻¹ in the Rio Piedras profile at the backslope position but it reaches higher values (10.17 cmolc kg⁻¹) in Bajura. Magnesium availability is low to medium at backslope position, medium to high footslope and high at Bajura site. Potassium availability is low in all profiles but even when its level decreases downslope, a slight increase in concentration with depth is observed in Bajura.

Results show that cation exchange capacity increases with depth on each soil profile. Exchangeable Al³⁺ was the most abundant cation in Rio Piedras profiles and increased with depth. In Bajura soil it was only detected in the Ap and Bw horizons at low concentrations. At a depth of 40 cm no exchangeable Al³⁺ was detected in Bajura soil. The content of exchangeable Al³⁺ in soils is directly related to pH. Authors like Kamprath (2010), Power and Prasad (1997), Muñoz et al. (1994) and Abruña et al. (1975) have documented that exchangeable Al³⁺ decreases as the soil pH increases. When soil pH reaches values above 5.5, the exchangeable Al³⁺ decreases sharply and near pH 7.0 precipitation occurs (Kamprath, 2010; Power and Prasad, 1997 and Abruña, 1975).

The occurrence of manganese masses and nodules was observed in Rio Piedras and Bajura profiles. The exchangeable manganese fraction is of importance from a fertility perspective, since manganese is an essential nutrient, however in some instances can cause toxicity problems to certain crops. Exchangeable manganese was detected only in the Ap horizon of the Rio Piedras backslope profile, but in all horizons of the Rio Piedras footslope profile (Table

4.5). Manganese in Bajura was only detected in the upper two horizons, Ap and Bw, but in higher amounts than the upper toposequence profiles. Manganese toxicity is expected to occur in acid soils and under redox conditions (Smyth, 2011). Manganese levels as high as 50 mg/kg could be toxic to sensitive species such as beans and tomatoes (Wang et al., 2002). Manganese levels of Bajura and Rio Piedras footslope Ap horizon could be toxic to manganese sensitive species. Water table fluctuations and redox conditions at Rio Piedras footslope and Bajura profiles may be contributing to the higher levels of exchangeable manganese found in these profiles. No exchangeable manganese was detected in Bajura soil below 40 cm (Bwg₁) where soil pH was above 6.60.

Table 4.5: Exchangeable manganese of Rio Piedras and Bajura Toposequence.

Exchangeable Manganese mg/kg					
Rio Piedras Backslope		Rio Piedras Footslope		Bajura	
Ap	8.1	Ap	55.3	Ap	223.4
Bt₁	0	AB	35.85	Bw	79.51
Bt₂	0	Bt₁	31.74	Bwg₁	0
BC	0	BC	12.65	Bwg₂	0
C₁	0	C₁	12.96	Cg₁	0
C₂	0	C₂	16.75	Cg₂	0
		Sap	31.57		

C. Physical properties

A clay texture predominates throughout the three profiles but higher content of sand and silt were observed in Bajura soil (Table 4.6). The clay content ranged from 74 % to 88 % in Rio Piedras backslope profile, from 71 % to 93 % in Rio Piedras footslope profile and from 60 % to 79 % in Bajura profile. Bajura showed the largest silt content ranging from 15 % to 32 % with

the higher content at surface horizons. Silt content in Rio Piedras backslope ranged from 8.9% to 18% and decreased with depth. In the footslope profile ranged from 5.2% to 21.5% and also

Table 4.6: Physical properties of Rio Piedras and Bajura soil profiles.

(Depth cm)	Horizon	A. S. %	Sand %	Silt %	Clay %	Texture
Rio Piedras Backslope						
(0 - 19)	Ap	63.9	7.9	17.8	74.3	Clay
(19 – 37)	Bt ₁	31	9.3	11.8	79.0	Clay
(37 – 58)	Bt ₂	20.1	5.9	11.9	82.3	Clay
(58 – 93)	BC	21.0	4.3	10.4	85.3	Clay
(93 – 107)	C ₁	9.7	8.9	10.9	80.2	Clay
(>107)	C ₂	36.9	2.7	8.9	88.4	Clay
Rio Piedras Footslope						
(0 – 25)	Ap	67.7	7.4	21.5	71.1	Clay
(25 – 38)	AB	47.6	6.0	20.75	73.2	Clay
(38 – 53)	Bt ₁	54	4.3	21.2	74.5	Clay
(53 – 94)	BC	23.9	7.6	18.7	73.7	Clay
(94 – 132)	C ₁	18.8	5.5	7.0	87.5	Clay
(132 – 155)	C ₂	3.3	1.6	5.2	93.2	Clay
(155 – 183)	Sap	10.7	8.9	19.9	71.2	Clay
Bajura						
(0 – 15)	Ap	75.9	5.1	32.2	62.6	Clay
(15 – 41)	Bw	70.5	14.8	25.1	60.1	Clay
(41 – 56)	Bwg ₁	6.8	11.8	17.6	70.6	Clay
(56 – 94)	Bwg ₂	18.7	5.2	15.1	79.7	Clay
(94 – 107)	Cg ₁	32.7	7.3	19.8	72.9	Clay
(107 – 145)	Cg ₂	5.02	11.4	18.7	69.9	Clay

*A.S – aggregate stability

decreased with depth. Sand ranges from 5% to 14% in Bajura profile, from 1.6% to 8.9% in Rio Piedras footslope profile and from 2.7% to 9.3% in Rio Piedras backslope profile. Results show that a clay soil texture predominates along the toposequence although lower clay content is observed in the Bajura soil. The increment in coarse material in the lower parts of the toposequence can be caused by the alluvial sediments that form Bajura soil. Rio Piedras soil is formed from highly stratified tuffaceous sandstone that has undergone intensive weathering which results in in situ clay accumulation.

Soil aggregate stability for Rio Piedras profile at backslope position decreased from 63.9% at surface (Ap) to 9.7% in C₁ horizon, then increased to 36.9% at the C₂ horizon. This increase can be attributed to saprolite presence at C₂ and not to a real increase in stable aggregates. In the Rio Piedras profile at footslope position, soil aggregate stability decreased from 67.7% at the surface (Ap) horizon to 3.3% in the C₂ horizon. An increase to 10.7% was observed below 155 cm depth where saprolite presence was abundant. At the valley, Bajura aggregate stability ranged from 5.02% - 75.99%. The first two horizons had an aggregate stability of 76% and 71%. However, a sharp decrease in aggregate stability (6.8%) was observed at a depth of 45 cm, in the Bwg1 horizon. At this depth soil organic matter content decreased sharply and gleyzation conditions predominate down the profile.

Soil aggregate stability in the toposequence shows a general tendency to decrease as depth increase in the subsoil. The highest values for aggregate stability were observed in the surface horizons of the three profiles and increase downslope into the valley. The increment in the aggregate stability downslope could be easily explained by the organic matter content, which also increases downslope into the valley. The organic matter acts as a cementing agent, attaching sand, silt and clay particles and forming stable soil aggregates. Organic matter content over 3.0%

is desirable in surface horizons to attain good aggregate stability and other physical properties of agricultural soils. Values below 1.0% were observed in Bt₁ and Bt₂ of Rio Piedras backslope, BC of Rio Piedras footslope and Bwg₁ of Bajura soil (Table 4.4).

The sand fractions of Bt₁ of Rio Piedras and Bwg₁ of Bajura were observed under the microscope. The sand particles of Rio Piedras revealed subangular to subrounded mineral grains. Coarser particles were observed in Bt₁ horizon at backslope position (Figure 4.6) than Bt₁ at footslope position (Figure 4.7). Quartz grains dominated the sand fraction in both samples but a higher content of red and oxidized grains were found in Bt₁ at footslope. Small manganese grains (black grains) were observed in Bt₁ footslope (Figure 4.8). Bajura Bwg₁ sand had bigger grains than Rio Piedras (Figure 4.8 – 4.10). Sand grains had a more subrounded shape probably the result of alluvial deposition processes. The presence of dark sand particles, probably manganese concretions was more prevalent in Bajura sand.



Figure 4.6: Sand sample 8x of RP BS Bt₁



Figure 4.7: Sand sample 8x RP FT Bt₁



Figure 4.8: Sand sample 1x RP FT Bt₁



Figure 4.9: Sand sample 8x Bajura Bwg₁



Figure 4.10: Sand sample 1x Bajura Bwg₁

D. Clay mineralogy

The crystalline iron oxides content in the backslope profile ranges from 1.42% to 3.44% with the lowest values at the bottom horizon. Aluminum oxides ranges from 0.45% to 0.91% but values remain mostly over 0.86%. The Rio Piedras footslope profile showed an iron oxide content ranging from 1.31% to 2.52% and aluminum oxide content ranging from 0.71% to 1.14% with the lowest values at C horizon. Bajura has an iron oxide content ranging from 2.14% to 3.59% with the highest content in Bw horizon. The aluminum oxide content in Bajura ranges from 0.91% to 2.14% with the lower percentage at the deepest horizons (Table 4.7). Oxides influence soil chemical and physical properties such as phosphates adsorption, aggregate stability, structure, porosity, soil electric charge and buffering capacity (Goldberg, 1989).

Table 4.7: Crystalline and amorphous oxides content of Rio Piedras and Bajura soil profiles.

Horizon	Crystalline Oxides				Amorphous Oxides			
	Fe %	Fe % in Fe ₂ O ₃	Al %	Al % in Al ₂ O ₃	Fe %	Fe % in Fe ₂ O ₃	Al %	Al % in Al ₂ O ₃
Rio Piedras Backslope								
(0 - 19)	2.19	3.13	0.48	0.91	0.36	0.52	0.43	0.81
(19 - 37)	1.99	2.84	0.46	0.87	0.38	0.55	0.68	1.29
(37 - 58)	2.41	3.44	0.47	0.88	0.11	0.16	0.43	0.82
(58 - 93)	2.25	3.22	0.48	0.90	0.09	0.13	0.49	0.92
(93 - 107)	0.99	1.42	0.24	0.45	0.07	0.10	0.45	0.85
(107 >)	1.87	2.67	0.45	0.86	0.10	0.15	0.62	1.17
Rio Piedras Footslope								
(0 - 25)	1.47	2.10	0.56	1.05	0.33	0.47	1.74	3.29
(25 - 38)	1.76	2.52	0.58	1.09	0.30	0.44	0.64	1.20
(38 - 53)	1.61	2.30	0.60	1.14	0.20	0.28	0.94	1.78
(53 - 94)	1.67	2.38	0.58	1.09	0.10	0.15	1.16	2.18
(94 - 132)	1.17	1.68	0.47	0.89	0.07	0.11	0.81	1.52
(132 - 155)	0.92	1.31	0.38	0.71	0.15	0.21	1.79	3.39
(155 - 183)	1.05	1.50	0.57	1.08	0.06	0.09	1.79	3.39
Bajura								
(0 - 15)	1.90	2.72	0.48	0.91	1.18	1.69	0.92	1.73
(15 - 41)	2.51	3.59	0.44	0.83	1.00	1.43	0.64	1.21
(41 - 56)	1.95	2.79	0.43	0.81	0.16	0.23	0.59	1.11
(56 - 94)	1.71	2.44	0.40	0.76	0.16	0.23	0.65	1.22
(94 - 107)	2.11	3.02	0.43	0.81	0.70	1.00	0.97	1.84
(107 - 145)	1.50	2.14	0.37	0.69	0.70	1.01	1.09	2.07

The oxides content in the crystalline fraction is considerably higher than amorphous fraction, showing predominance of free and well crystallized oxide phases in the toposequence (Table 4.7). Iron crystalline oxides index are similar in Rio Piedras backslope and Bajura while Rio Piedras footslope has lower iron content but higher amount of aluminum oxides. Results are consistent with the study of Osodeke et al. (2005) that reported a predominance of crystalline oxides along a soil toposequence formed by Alfisols and Ultisols in Nigeria.

Amorphous iron oxides content decreased with depth in all profiles higher values were observed in Bajura (Table 4.7). Similar results were obtained by Osodeke et al. (2005). These authors reported that amorphous forms of iron and aluminum dominated the valley in their Nigerian soil toposequence. The amorphous iron oxides ranged from 0.03% – 1.14% with a mean of 0.28%. The amorphous aluminum oxides ranged from traces to 0.12% with a mean of 0.07%. The highest amorphous iron oxides content at the valley was attributed to poor drainage conditions. The crystalline iron oxides content ranged from 0.60% to 7.49% with a mean of 2.28% and the aluminum fraction ranged from 0.34% to 1.78% with a mean of 0.82%. The amorphous forms of oxides pre-dominate the valley bottom profile and crystalline forms pre-dominate the upper profiles in the toposequence (Osodeke et al., 2005). Almeida et al. (2017) reported amorphous iron oxides content ranging from 0.32 - 3.90 g kg⁻¹ with the higher values at the surface horizons in the valley. The authors attributed this result to the hydromorphic conditions in the valley (Almeida et al., 2017). Similar results in amorphous oxide content were observed at the Coloso Valley toposequence. The higher content in amorphous Fe and Al oxide was observed at Rio Piedras footslope and Bajura soils. Lateral movement of oxides from higher elevations must be taken place at the toposequence. Water enriched with iron oxides is commonly observed in drainage ditches at Coloso Valley. The Rio Piedras footslope profile as

well as Bajura is subjected to redox conditions due to seasonal water saturation. Thus, iron oxides will decrease their crystallinity as result of the process. The high organic matter content is also affecting the iron oxides crystallization (Almeida et al., 2017). The higher content of amorphous iron oxides was reported in the upper two horizons of each soil profile, where the organic matter content was higher (Table 4.5). The combination of the carboxyl-hydroxyl groups of the organic acids with the anions such as phosphates, sulphates and silicates adsorbed to the surface of the minerals slow the rate of transformation of ferrihydrite towards crystalline minerals like goethite. This phenomenon of crystalline retardation increases with the adsorption of calcium cations to the surface of the mineral (Cabria et al. 2005; Baltpurvins et al., 1997; Schwertmann, 1985). The pH levels in the Ap and Bw horizons of Bajura were higher than pH levels of the upper horizons of Rio Piedras backslope and footslope profiles, allowing a better calcium adsorption that retards the crystallization of iron oxides and increase the amorphous iron oxide content (Cabria et al. 2005; Baltpurvins et al., 1997; Schwertmann, 1985). Also, the amount of exchangeable Ca^{2+} is almost twice in the upper horizons of Bajura soil when compared to Rio Piedras soil and increased with soil depth.

The Feo/Fed ratio (oxalate Fe/DCB Fe), or active ratio, has been previously used as a weathering index in soils (Almeida et al, 2017; Osodeke et al, 2005; Ibia, 2001; Dolui and Mustafi, 1997; Omenihu et al, 1994; Udo, 1980). An active ratio less than one is related to an advanced stage of crystallinity or ageing of free iron and aluminum oxides and supports the soil formation due to prolonged weathering in highly weathered soils (Seal et al., 2006; Mahaney et al., 1991). Oxides crystallinity increase with soil age, decreasing the iron and aluminum active ratio, while high active ratios are related to younger soils (Seal et al., 2006; Mahaney et al., 1991; Mahaney and Fahey, 1988). Low ratios in deeper horizons indicate well drained soils and

crystalline oxides are also associated with good drainage. Weathering ratios higher than 0.50 are associated with poor drained soils (Osedeke et al, 2005; Dolui and Mustafi, 1997). The higher ratios of Fea/Fec were observed in the upper horizons of the three profiles, but only in Ap horizon of Bajura soil a ratio higher than 0.50 was observed. A higher content of organic matter and poor drainage conditions in Bajura soil may be contributing to the higher values observed in the first two horizons. The organic matter in both Rio Piedras profiles was significantly lower than in Bajura profile and drainage is excellent, especially in Rio Piedras backslope. In Bajura, the active ratio in Cg₁ and Cg₂ horizons was higher than Bwg₁ and Bwg₂. These two horizons experience saturating conditions and redox reactions are very active throughout the year, conditions that prevent crystallization of the iron oxides. (Table 4.8).

The x-ray diffraction results were very similar in all Rio Piedras and Bajura horizons (Figs. 4.11 – 4.16) (Appendix). Results indicate the presence of 2:1 clay minerals and micas in the clay fraction such as vermiculite, montmorillonite, chlorite, muscovite and biotite; but more specific techniques have to be employed to identify the specific clay or mica. More defined peaks for 2:1 minerals or interstratified 2:1 clay minerals are observed in Rio Piedras footslope and Bajura. A sharp peak of quartz was identified around 26.5° 2θ. Hematite, goethite, gibbsite, and kaolinite were also identified in the clay fraction. The stronger kaolinite peaks at 12° 2θ and 36.4° 2θ interfere with pyrolusite and birnessite peaks. A peak around 28° 2θ is indicative of the presence of manganese minerals like pyrolusite and birnessite in Rio Piedras footslope and Bajura profiles, but the peaks are more defined in Bajura where the presence of manganese masses is abundant (Figure 4.4). There was no manganese minerals identified in the Rio Piedras backslope profile. A possible reason for no detection of manganese minerals in the clay fraction

is because well-formed and stable manganese nodules prevail in the soil, and are concentrated in the sand and silt fractions (Figure 4.2).

Table 4.8: Amorphous and crystalline iron oxides content and weathering index.

Horizon	Fe Crystalline %	Fe Amorphous %	Fea/Fec
<i>Rio Piedras Backslope</i>			
Ap	2.19	0.36	0.17
Bt1	1.99	0.38	0.19
Bt2	2.41	0.11	0.05
BC	2.25	0.09	0.04
C1	0.99	0.07	0.07
C2	1.87	0.10	0.06
<i>Rio Piedras Footslope</i>			
Ap	1.47	0.33	0.23
AB	1.76	0.30	0.17
Bt1	1.61	0.20	0.12
BC	1.67	0.10	0.06
C1	1.17	0.07	0.06
C2	0.92	0.15	0.16
Saprolite	1.05	0.06	0.06
<i>Bajura</i>			
Ap	1.90	1.18	0.62
Bw	2.51	1.00	0.40
Bwg1	1.95	0.16	0.08
Bwg2	1.71	0.16	0.09
Cg1	2.11	0.70	0.33
Cg2	1.50	0.70	0.47

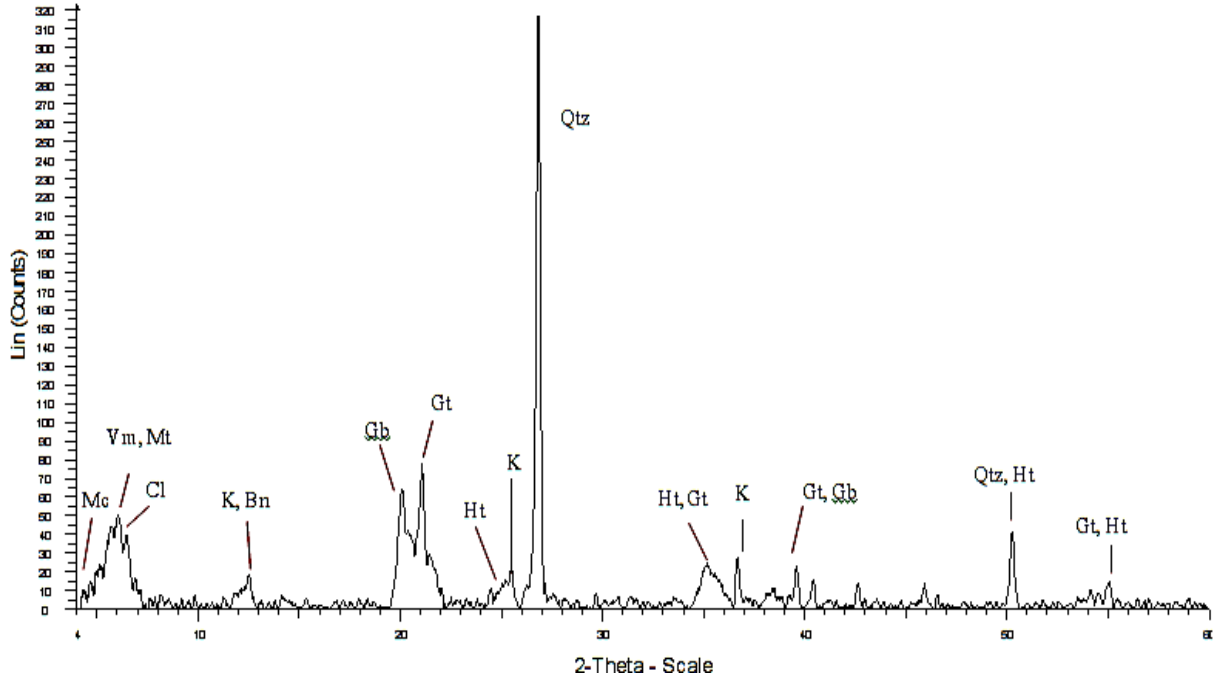


Figure 4.11: X-ray diffraction pattern of the clay fraction of Rio Piedras Backslope Ap horizon. Mc-mica; Vm-vermiculite; Mt-montmorillonite; Cl-chlorite; K-kaolinite; Bn-birnessite; Gb- gibbsite; Gt-goethite; Ht-hematite; Qtz-quartz.

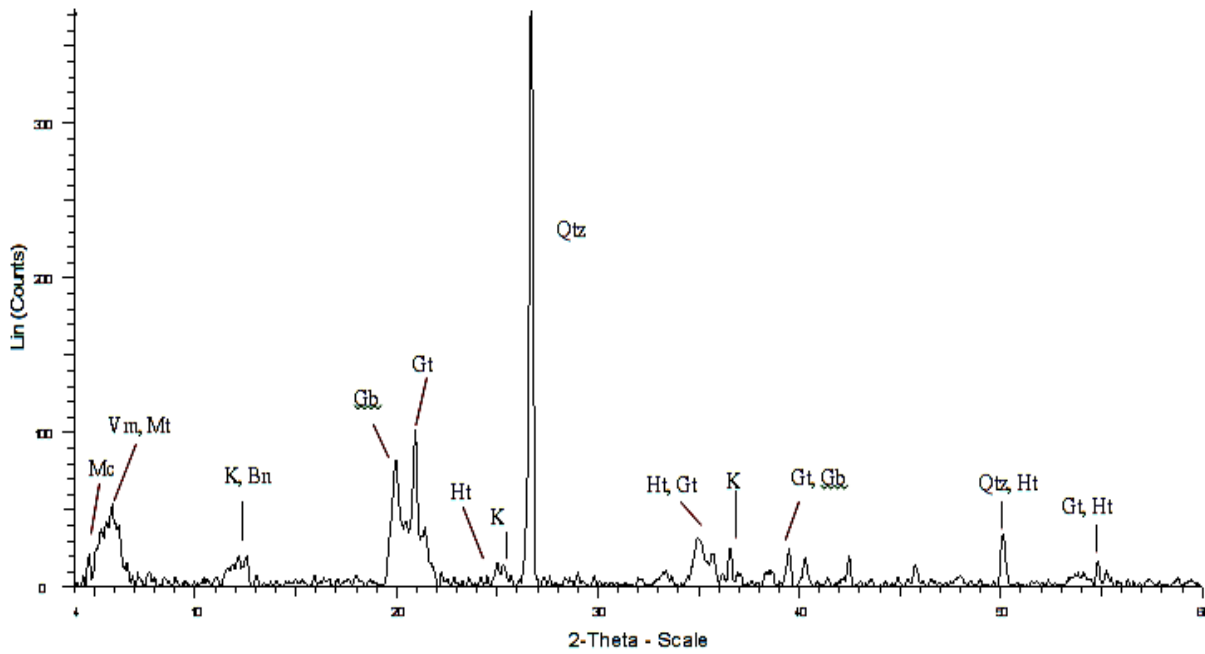


Figure 4.12: X-ray diffraction pattern of the clay fraction of Rio Piedras Backslope Bt₁ horizon. Mc-mica; Vm-vermiculite; Mt-montmorillonite; Cl-chlorite; K-kaolinite; Bn-birnessite; Gb- gibbsite; Gt-goethite; Ht-hematite; Qtz-quartz.

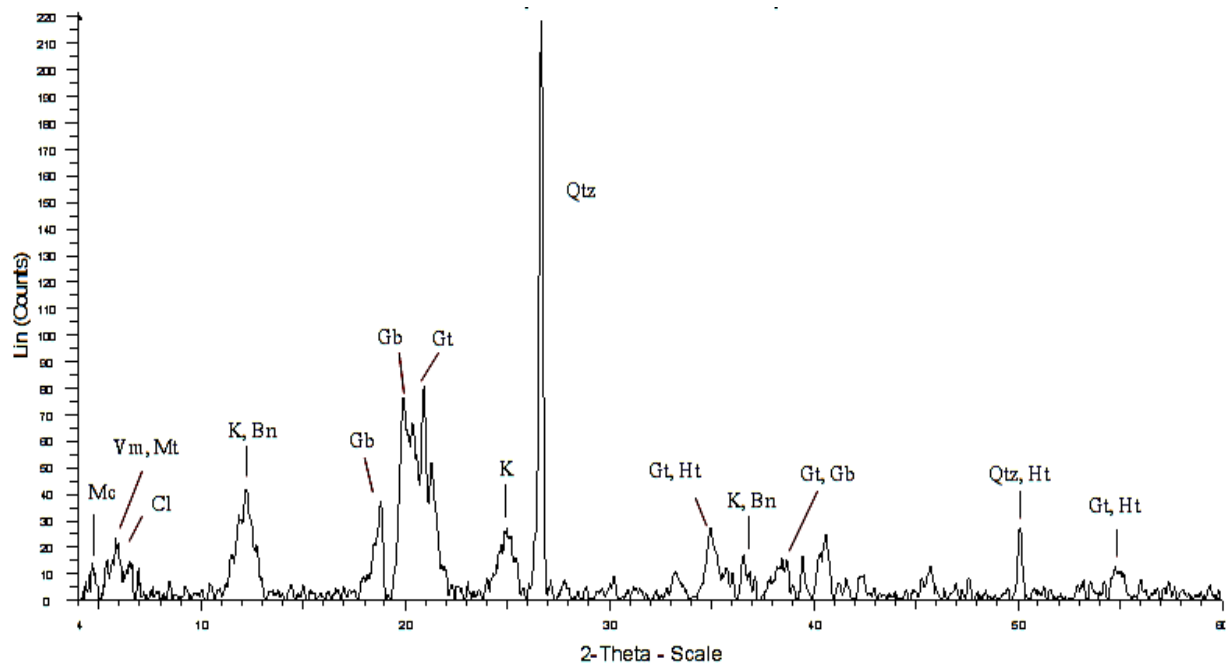


Figure 4.13: X-ray diffraction pattern of the clay fraction of Rio Piedras Footslope Ap horizon. Mc-mica; Vm-vermiculite; Mt-montmorillonite; Cl-chlorite; K-kaolinite; Bn-birnessite; Gb- gibbsite; Gt-goethite; Ht-hematite; Qtz-quartz.

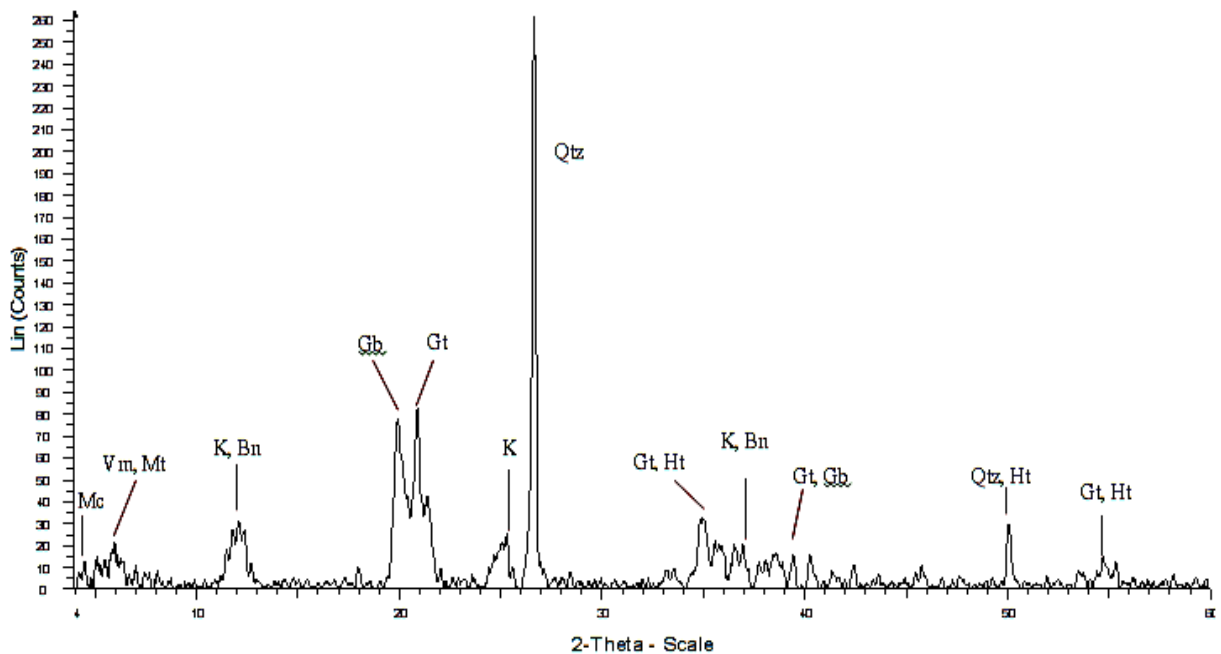


Figure 4.14: X-ray diffraction pattern of the clay fraction of Rio Piedras Footslope AB horizon. Mc-mica; Vm-vermiculite; Mt-montmorillonite; Cl-chlorite; K-kaolinite; Bn-birnessite; Gb- gibbsite; Gt-goethite; Ht-hematite; Qtz-quartz.

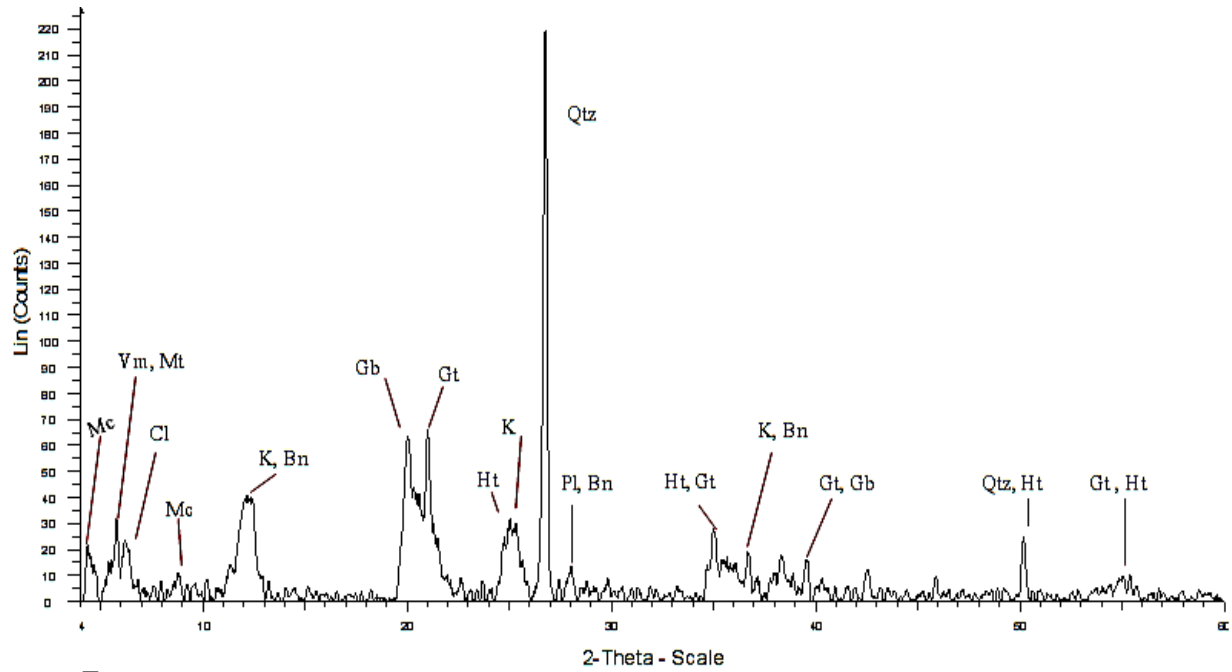


Figure 4.15: X-ray diffraction pattern of the clay fraction of Bajura Ap horizon. Mc-mica; Vm-vermiculite; Mt-montmorillonite; Cl-chlorite; K-kaolinite; Bn-birnessite; Pl-pyrolusite; Gb-gibbsite; Gt-goethite; Ht-hematite; Qtz-quartz.

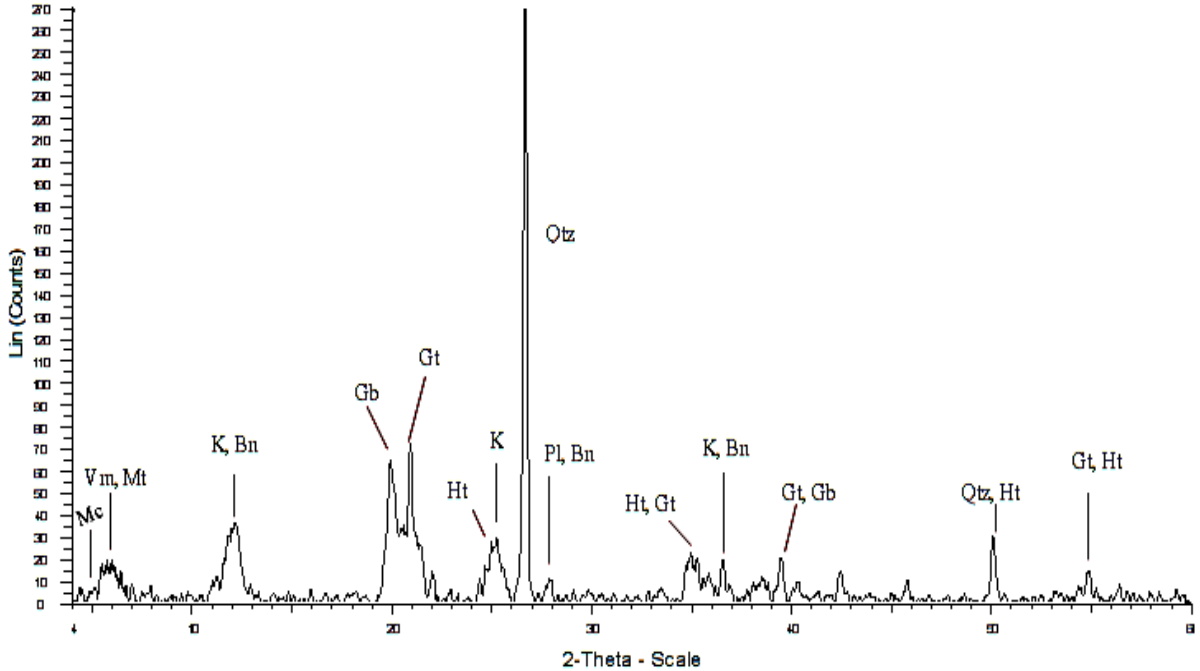


Figure 4.16: X-ray diffraction pattern of the clay fraction of Bajura Bw horizon. Mc-mica; Vm-vermiculite; Mt-montmorillonite; Cl-chlorite; K-kaolinite; Bn-birnessite; Pl-pyrolusite; Gb-gibbsite; Gt-goethite; Ht-hematite; Qtz-quartz

4.2 Evaluation and Characterization of a Rio Piedras Vertically Stratified Profile

A. Field description

Vertical strata in the atypical Rio Piedras profile were measured and designated with letters from A to G (Figure 4.17). From sections C – F, top soil was sampled from 0 – 10 cm. Strata from A to G were sampled below topsoil every 30 cm till a depth of 132 cm, having a total of 4 sections for each letter. A yellowish red color was uniform in the surface horizon above 10 cm. Strata A, D and G were similar in color and hardness or breakage resistance while strata B, C, E and F were more similar in color and texture. Strata A, D and G had a saprolitic appearance similar to C horizon of Rio Piedras Backslope profile (Figure 4.18). Dominant colors were red and yellowish brown with greyish and white mottles of hues 10R and 10YR (Table 4.9). The dominant coloration of B, C, E and F strata was red (10R), yellowish red (5YR) and brown (7.5YR). Soil peds of these strata were easily broken by hand pressure and the texture was coarser than for strata A, D and G. This profile had redder colors (10R) than profiles at backslope and footslope positions.

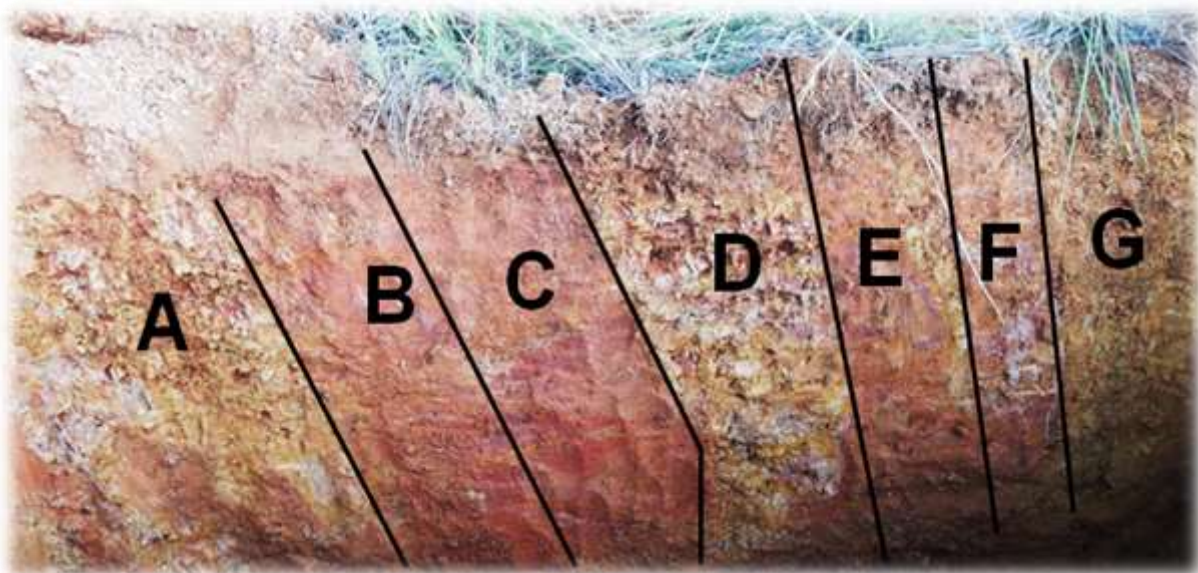


Figure 4.17: Vertical stratification designation for the profile.

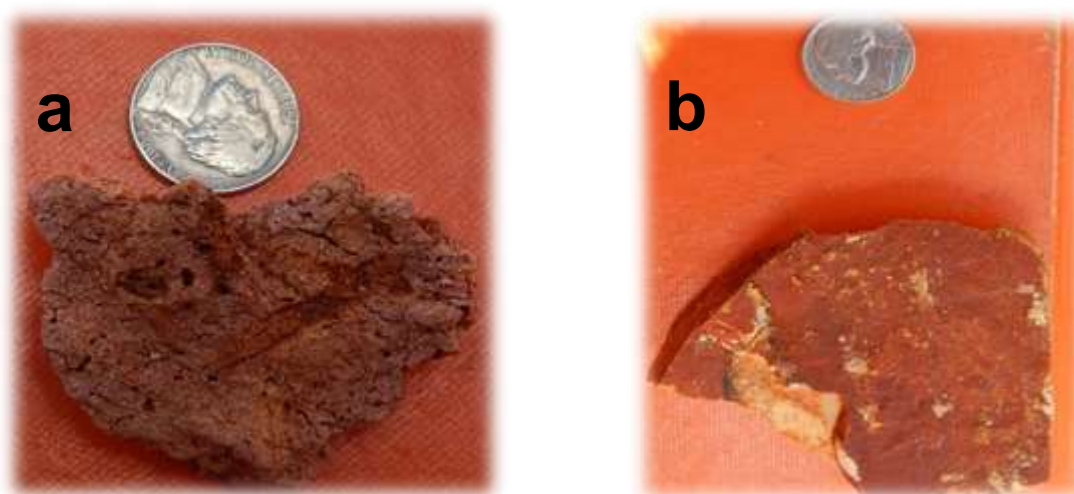


Figure 4.18: Typical soil clod from B, C, E and F strata and typical saprolite fragment from A, D and G strata.

Table 4.9: Rio Piedras vertically stratified field description.

Sample	Depth (cm)	Color (moist)	Structure
A1	10 - 41	10YR 5/8 yellowish brown 10YR 7/2 light gray 10R ¾ dusky red	Angular blocky
A2	41 - 71	10YR 5/8 yellowish brown 10YR 7/2 light gray 10R ¾ dusky red	Angular blocky
A3	71 – 102	10YR 5/8 yellowish brown 10YR 7/2 light gray 10R ¾ dusky red	Angular blocky
A4	102 – 132	10YR 5/8 yellowish brown 10YR 7/2 light gray 10R ¾ dusky red	Angular blocky
B1	10 - 41	7.5YR 5/6 strong brown	Subangular blocky
B2	41 - 71	7.5YR 5/6 strong brown 10R 4/8 red	Subangular blocky
B3	71 – 102	5YR 5/8 yellowish red	Angular blocky
B4	102 – 132	10R 4/6 red 10R 5/6 red	Angular Blocky
Ctop	0 - 10	5YR 4/6 yellowish red	Subangular blocky
C1	10 - 41	5YR 5/8 yellowish red	Subangular blocky
C2	41 - 71	2.5YR 5/8 red	Subangular blocky
C3	71 – 102	10R 5/8 red	Subangular blocky
C4	102 – 132	10R 4/8 red 7.5YR 5/8 strong brown	Subangular blocky
Dtop	0 - 10	5YR 4/6 yellowish red 10R 4/6 red	Subangular blocky
D1	10 - 41	10YR 5/8 yellowish brown 10YR 7/2 light gray 10R 4/6 red	Angular blocky
D2	41 - 71	10YR 5/8 yellowish brown 10YR 7/2 light gray 10R 4/6 red	Angular blocky
D3	71 – 102	10YR 5/8 yellowish brown 10YR 7/2 light gray	Angular blocky

D4	102 – 132	10R 4/6 red 10YR 5/8 yellowish brown 10YR 7/2 light gray	Angular blocky
Etop	0 - 10	5YR 4/6 yellowish red	Subangular blocky
E1	10 - 41	5YR 5/8 yellowish red 10R 4/6 red	Subangular blocky
E2	41 - 71	10R 4/6 red 10R 5/6 red	Subangular blocky
E3	71 – 102	7.5YR 5/8 strong brown 5YR 5/6 yellowish red	Subangular blocky
E4	102 – 132	5YR 5/8 yellowish red 10R 4/8 red 10R 5/6 red	Subangular blocky
Ftop	0 - 10	5YR 4/6 yellowish red	Subangular blocky
F1	10 - 41	5YR 5/8 yellowish red 10R 4/6 red	Subangular blocky
F2	41 - 71	7.5YR 5/8 strong brown 5YR 5/8 yellowish red 5YR 8/2 pinkish white	Subangular blocky
F3	71 – 102	10R 5/6 red 5YR 5/8 yellowish red	Subangular blocky
F4	102 – 132	10R 5/6 red 5YR 5/8 yellowish red	Subangular blocky
G1	10 - 41	10YR 6/8 brownish yellow	Angular blocky
G2	41 - 71	10YR 8/1 white	Angular blocky
G3	71 – 102	10R 4/6 red	Angular blocky
G4	102 – 132	10R 4/6 red	Angular blocky

B. Chemical properties

Soil pH was extremely acid, ranging from 3.85 to 4.36 and decrease with depth on each stratum (Table 4.10). The pH of this profile is significantly lower than the pH of Rio Piedras backslope and footslope. The weathering process has been intensive although the mixing of the soil strata is minimum. The extremely acid conditions of this profile as well as for the Rio Piedras backslope and footslope positions are related to the also extremely high content of exchangeable aluminum.

Organic matter content is higher in the topsoil or first ten centimeters of the profile. Strata C and D had organic matter content above 1% while E and F topsoil had 0.73%. This value decreased with depth for each soil section from A to G, where the highest result is 0.66% in B1 (Table 4.10). The soil at this location has been subjected to intensive erosion, evidenced by the absence of topsoil on most strata. Low fertility levels and extremely acid conditions restrict vegetation to few acid tolerant species such as ferns and grasses. There is not enough biomass or biological activity at this elevation to produce significant organic matter content.

The cation exchange capacity of the profile, was in the range 20 – 45 $\text{cmol}_c \text{kg}^{-1}$. Most of the CEC is occupied by exchangeable aluminum (Table 4.10). Calcium levels were low and decreased with soil depth. Magnesium levels were medium to high and increased with profile depth ranging between 0.45 - 3.25 $\text{cmol}_c \text{kg}^{-1}$. Potassium content was low reaching levels of 0.39 $\text{cmol}_c \text{kg}^{-1}$. Exchangeable aluminum content was very high exceeding 20 $\text{cmol}_c \text{kg}^{-1}$. The percentage of Al^{3+} saturation ranged from 83.3 to 90.9%. Most plant species will face toxicity problems when exchangeable Al^{3+} exceeds 0.05 $\text{cmol}_c \text{kg}^{-1}$. The exchangeable Al^{3+} content increased with depth in all strata except F. There are similarities in the aluminum content of

Table 4.10: Chemical properties of Rio Piedras vertically stratified profile.

Rio Piedras Vertically Stratified							
Sample	pH	O.M. %	Ca ²⁺ -----	K ⁺ -----	Mg ²⁺ Cmolc kg ⁻¹	Al ³⁺ -----	CEC -----
A1	4.36	0.07	3.55	0.25	1.02	37	41.81
A2	4.24	0.07	2.99	0.14	1.45	35.3	39.87
A3	4.09	0.14	2.10	0.40	2.57	36.7	41.77
A4	3.9	0.01	1.60	0.38	3.25	39.7	44.92
B1	4.14	0.66	2.39	0.04	0.45	17.2	20.07
B2	4.17	0.20	2.32	0.12	0.69	27	30.14
B3	4.13	0.14	1.58	0.15	1.53	27.6	30.86
B4	4.1	0.14	1.91	0.03	1.02	29.5	32.47
Ctop	4.22	1.26	2.73	0.30	0.90	33.7	37.63
C1	4.23	0.40	2.25	0.10	0.53	27.1	29.98
C2	3.99	0.27	2.38	0.12	0.93	28.1	31.54
C3	3.89	0.27	1.54	0.05	1.30	28.9	31.79
C4	3.85	0.27	1.34	0.10	1.89	28.4	31.74
Dtop	4.07	1.59	3.05	0.36	1.19	23.8	28.40
D1	3.99	0.20	3.57	0.24	1.06	24.4	29.28
D2	3.98	0.14	2.68	0.31	1.71	35.7	40.40
D3	3.92	0.14	2.03	0.36	2.59	37.7	42.68
D4	3.86	0.14	1.44	0.34	2.80	31	35.57
Etop	4.06	0.73	2.37	0.29	0.93	28.3	31.90
E1	3.95	0.27	2.18	0.12	0.48	23.7	26.47
E2	3.98	0.14	2.43	0.14	0.79	23.9	27.26
E3	3.91	0.14	1.91	0.03	1.23	24.3	27.47
E4	3.87	0.01	1.80	0.12	1.79	28.3	32.00
Ftop	4.14	0.73	3.02	0.28	1.14	32.4	36.84
F1	4.09	0.27	2.69	0.12	0.78	29.4	32.98
F2	3.99	0.60	2.61	0.21	1.37	29.8	33.98
F3	3.92	0.07	1.77	0.15	1.47	23	26.39
F4	3.9	0.07	1.39	0.01	1.38	20.2	22.96
G1	3.88	0.27	2.78	0.15	1.02	28.9	32.85
G2	4.05	0.27	2.78	0.39	2.09	29.2	34.45
G3	3.95	0.14	1.87	0.17	2.81	29.3	34.14
G4	3.86	0.14	1.71	0.30	3.23	32.8	38.04

Table 4.11: Aluminum content of Rio Piedras vertically stratified profile.

Sample	Al³⁺ Cmolc kg⁻¹	CEC	% Al³⁺ Sat
A1	37	41.81	88.5
A2	35.3	39.87	88.5
A3	36.7	41.77	87.9
A4	39.7	44.92	88.4
B1	17.2	20.07	85.7
B2	27	30.14	89.6
B3	27.6	30.86	89.4
B4	29.5	32.47	90.9
Ctop	33.7	37.63	89.6
C1	27.1	29.98	90.4
C2	28.1	31.54	89.1
C3	28.9	31.79	90.9
C4	28.4	31.74	89.5
Dtop	23.8	28.4	83.8
D1	24.4	29.28	83.3
D2	35.7	40.4	88.4
D3	37.7	42.68	88.3
D4	31	35.57	87.2
Etop	28.3	31.9	88.7
E1	23.7	26.47	89.5
E2	23.9	27.26	87.7
E3	24.3	27.47	88.5
E4	28.3	32	88.4
Ftop	32.4	36.84	87.9
F1	29.4	32.98	89.1
F2	29.8	33.98	87.7
F3	23	26.39	87.2
F4	20.2	22.96	88.0
G1	28.9	32.85	88.0
G2	29.2	34.45	84.8
G3	29.3	34.14	85.8
G4	32.8	38.04	86.2

strata A, D and G with a range of 23 - 40 $\text{cmol}_c \text{kg}^{-1}$. Average values for each strata are presented in table 4.12. The average exchangeable Al^{3+} for strata A was $37.2 \text{ cmol}_c \text{kg}^{-1}$, for strata D $32.2 \text{ cmol}_c \text{kg}^{-1}$ and for strata G $30.1 \text{ cmol}_c \text{kg}^{-1}$. The average exchangeable Al^{3+} for strata B was $25.3 \text{ cmol}_c \text{kg}^{-1}$, for strata C $28.1 \text{ cmol}_c \text{kg}^{-1}$, for strata E $25.1 \text{ cmol}_c \text{kg}^{-1}$ and for strata F $25.6 \text{ cmol}_c \text{kg}^{-1}$.

Strata A, D and G showed similar pH values in the range of 3.9 – 4.1 (Table 4.12-4.13). Organic matter content ranged 0.1 - 0.2%, exchangeable calcium ranged from 2.3-2.6 $\text{cmol}_c \text{kg}^{-1}$, potassium 0.3 $\text{cmol}_c \text{kg}^{-1}$, magnesium 2.0 - 2.3 $\text{cmol}_c \text{kg}^{-1}$ and the high aluminum content over 30 $\text{cmol}_c \text{kg}^{-1}$. A, D and G strata also had the higher mean cation exchange capacity of the profile. The mean values for B, C, E and F strata were similar in pH with a range of 3.9 - 4.1, organic matter content ranged from 0.1 - 0.3%, exchangeable calcium ranged from 1.9 to 2.1 $\text{cmol}_c \text{kg}^{-1}$, exchangeable potassium from 0.1 to 0.03 $\text{cmol}_c \text{kg}^{-1}$, exchangeable magnesium from 0.9 to 1.3 $\text{cmol}_c \text{kg}^{-1}$, and exchangeable aluminum ranged 25 - 28 $\text{cmol}_c \text{kg}^{-1}$ (Table 4.12-4.13).

Table 4.12: Average values for chemical properties of the strata.

Rio Piedras Vertically Stratified							
Sample	pH	O.M. %	Ca²⁺ -----	K⁺ -----	Mg²⁺ cmol_c kg⁻¹	Al³⁺ -----	CEC -----
A	4.1	0.1	2.6	0.3	2.1	37.2	42.1
B	4.1	0.3	2.1	0.1	0.9	25.3	28.4
C	4.0	0.3	1.9	0.1	1.2	28.1	31.3
D	3.9	0.2	2.4	0.3	2.0	32.2	37.0
E	3.9	0.1	2.1	0.1	1.1	25.1	28.3
F	4.0	0.3	2.1	0.1	1.3	25.6	29.1
G	3.9	0.2	2.3	0.3	2.3	30.1	34.9

Table 4.13: Average values for aluminum content of the strata.

Rio Piedras Vertically Stratified			
Sample	Al³⁺ cmol_c kg⁻¹	CEC	% Al³⁺ Sat
A	37.2	42.1	88.4
B	25.3	28.4	88.9
C	28.1	31.3	90.0
D	32.2	37.0	86.8
E	25.1	28.3	88.5
F	25.6	29.1	88.0
G	30.1	34.9	86.2

C. Physical properties

A clayey texture predominated in all strata and at all depths (Table 4.14). Strata A, D and G had less sand (1.8 to 2.5%) than strata B, C, E and F (11.3 to 21.0 %) (Table 4.15). Strata B had the highest sand content with an average value of 21.0% (Table 4.15). Sand fraction in C strata, not considering the surface layer, ranged from 15.5% - 23.5%. The surface layer of the C strata was the exception with 4.5%. Sand content in E and F horizons ranged between 6% - 15.4%. There was no particular pattern in sand content within depth per strata. Silt content varied from 15% - 32% in strata A-G. Strata A, D and F had a silt content of 20% - 25% while in B, C and E ranged from 21% - 32%. G has the lower silt content ranging from 15% - 18%. There was no particular pattern in silt within depth per strata. Clay content ranged from 40% - 83% in the soil profile.

Strata A and D had a similar clay range of 70 - 78%. The G strata had the higher clay percentage of the profile with a range of 80 - 82%. The clay content in strata B and C ranged

Table 4.14: Physical properties of Rio Piedras vertically stratified profile.

Rio Piedras vertically stratified					
Sample	A.S. %	Sand %	Silt %	Clay %	Texture
A1	34.7	2	23.1	74.9	Clay
A2	47.8	1.9	22.3	75.8	Clay
A3	38.3	1.8	22.7	75.6	Clay
A4	40.1	4.3	24.9	70.8	Clay
B1	19.5	22.0	27.4	50.6	Clay
B2	13.7	18.9	28.6	52.5	Clay
B3	43.8	15.3	23.9	60.8	Clay
B4	27.4	27.7	32.6	39.7	Clay Loam
Ctop	66.4	4.5	21.6	73.9	Clay
C1	5.6	19.6	28.5	51.9	Clay
C2	5.9	15.4	29.3	55.4	Clay
C3	21.9	23.5	28.2	48.3	Clay
C4	2.9	15.5	25.3	59.3	Clay
Dtop	66.5	5.5	23.4	71.1	Clay
D1	35.6	2.5	22.2	75.4	Clay
D2	39.6	1.7	22.3	76.0	Clay
D3	29.2	2.7	24.0	73.3	Clay
D4	29.0	1.9	19.9	78.2	Clay
Etop	52.5	6.4	23.3	70.3	Clay
E1	8.3	10.0	29.6	60.5	Clay
E2	8.3	15.4	32.0	52.7	Clay
E3	11.8	10.5	24.7	64.8	Clay
E4	3.3	12.5	26.5	61.1	Clay
Ftop	62.1	5.9	23.5	70.6	Clay
F1	10.1	8.6	18.9	72.6	Clay
F2	5	9.5	20.8	69.8	Clay
F3	2.1	12.8	23.7	63.6	Clay
F4	6.1	14.1	22.4	63.5	Clay
G1	35.9	1.5	17.9	80.7	Clay
G2	37	1.6	16.6	81.8	Clay
G3	52.1	2.1	15.1	82.9	Clay
G4	38.4	2.1	17.3	80.7	Clay

Table 4.15: Average values of physical properties.

Rio Piedras Vertically Stratified				
Sample	A.S. %	Sand %	Silt %	Clay %
A	40.2	2.5	23.3	74.3
B	26.1	21.0	28.1	50.9
C	9.1	18.5	27.8	53.7
D	33.4	2.2	22.1	75.7
E	7.9	12.1	28.2	59.8
F	5.8	11.3	21.5	67.4
G	40.9	1.8	16.7	81.5

from 40 to 60%, with exception of C top that has a clay content of 74%. Clay content in strata E and F was over 60%. There was no particular pattern in clay within depth per horizon. The average values of aggregate stability, sand, silt and clay content were similar in A, D and G strata (Table 4.15). Sand, silt and clay were similar in A and D while G had less silt but a higher clay content. B and C strata had similar sand, silt and clay content but different aggregate stability. There were no major differences between E and F average values but E had similar silt content with B and C while silt was lower in F strata. G stratum had higher clay content than B, C and E. Differences and similarities in the different strata of this profile could be attributed to the stratified nature of parent material.

The topsoil samples for strata C, D, E and F had the highest aggregate stability percent for each soil section (Table 4.14). This can be attributed to the higher organic matter, plant roots and organic acids present in the surface layers of the soil (Brady and Weil, 1996). Strata A, D and G had similar aggregate stability with a range of 30-52%. Strata B, C, E and F had a lower

aggregate stability, in most cases below 10%. These strata contain more sand and less clay content than strata A, D and G. Aggregate stability increases with clay content and soil aggregates having more sand particles may be less stable. The higher sand content and the saprolitic nature of these strata, where root penetration is restricted are determinant factors for the low percent of stable aggregates.

Sand samples at a depth from 71 – 101 cm depth for all strata were observed under the microscope to see shape and size of sand granule. Samples A3, D3 and G3 had the smaller sand grains. However, G3 also had the largest grains observed in 1x and 8x magnifications. Yellowish colors were dominant in sand A3, D3 and G3 while reddish color dominated sands B3, C3, E3 and F3 (Figure 3.19). Samples D, F and G had subangular to subrounded grains. Subrounded to rounded grains were observed in A, B, C and E. C top had a light coloration with dominance of quartz grains. Sand grain variation in shape and size may be the result of different deposition events that formed this parent material. The dominance of quartz grains in the surface soil could be influenced by the Cibao formation (Monroe, 1969). The Cibao formation has been eroded in the study site but the base of this deposit is characterized by the presence of quartz sands that could remain on top of the Eocene rocks.

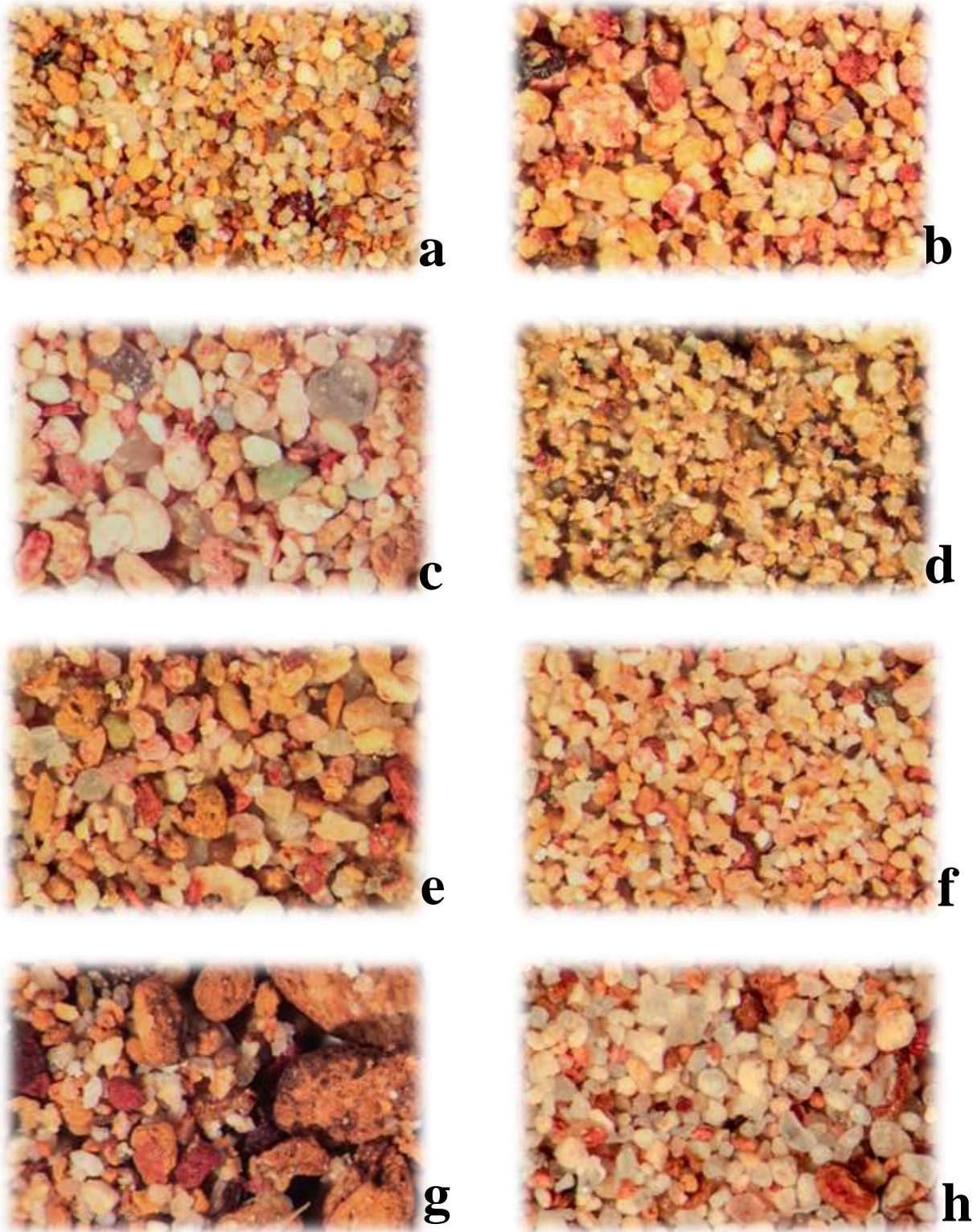


Figure 4.19: Sand grains at 8x magnification. a) sample A3, b) sample B3, c) sample C3, d) sample d3, e) sample E3, f) sample F3, g) sample G3 and h) sample Ctop.

D. Clay Mineralogy:

The iron oxides content in the Rio Piedras vertically stratified profile ranged from 0.10% to 3.92% (Table 4.16). Aluminum oxides range from 0.47% to 1.34%. The oxides content in the crystalline fraction were considerably higher than amorphous fraction, showing predominance of free and well crystallized oxide phases in this profile. Iron crystalline oxides indexes were similar in sections A, B, D and G while higher values were reached in sections C, E and F. Sections E and F had the highest iron content. Aluminum crystalline oxides ranged from 0.47 - 1.06%. Sections A, D, E and G have a similar range between 0.73 - 0.85%. Sections B, C and F have a wide range from 0.47 – 1.06%. No defined pattern was observed in crystalline oxides within depth. The highest mean values were observed in C, E and F strata with a range of 2.08-2.30%. A, B, D and G strata had a similar crystalline iron content with a range of 1.61-1.65% (Table 4.17).

The amorphous iron oxides fraction ranged from 0.07 - 1.11% (Table 4.16). Sections A and G had a similar rate 0.11 - 0.13%. Sections B and E had a rate of 0.12 – 0.19 % while C, D and F had a wide range from 0.07% to 1.11%. Aluminum amorphous oxides ranged from 0.63% to 1.34% but most values were in in range 0.70 – 1.00%. Similar values were found in sections B and G with 0.71 – 0.98%. No defined pattern was observed in amorphous oxides with depth. Strata B, D, E, F, and G had similar mean values with a range of 0.11 - 0.18% while A and C had the highest mean values with 0.25% and 0.35%.

The Fea/Fec ratio or weathering index resulted in less than 0.41 in the seven strata of this Rio Piedras profile (Table 4.18 - 4.19). The active ratio was in the range of 0.03 – 0.41, but most samples had values less than 0.16. According to Seal et al. (2006), Mahaney et al. (1991) and Mahaney and Fahey (1988), a decrease in iron and aluminum active ratio is related to an increase

Table 4.16: Crystalline and amorphous oxides in Rio Piedras vertically stratified.

<i>Horizon</i>	Crystalline Oxides				Amorphous Oxides			
	Fe %	Fe % in Fe₂O₃	Al %	Al % in Al₂O₃	Fe %	Fe % in Fe₂O₃	Al %	Al % in Al₂O₃
A1	1.88	2.69	0.42	0.79	0.77	1.11	0.71	1.34
A2	1.52	2.18	0.43	0.81	0.07	0.1	0.43	0.82
A3	1.55	2.22	0.41	0.77	0.07	0.1	0.47	0.89
A4	1.65	2.36	0.39	0.73	0.08	0.11	0.54	1.03
B1	1.58	2.26	0.37	0.69	0.13	0.19	0.52	0.98
B2	2.02	2.88	0.38	0.71	0.12	0.17	0.41	0.78
B3	0.98	1.41	0.25	0.47	0.11	0.16	0.39	0.74
B4	1.91	2.74	0.29	0.55	0.12	0.17	0.44	0.83
Ctop	2.45	3.5	0.43	0.8	0.57	0.82	0.41	0.78
C1	2.09	2.99	0.41	0.77	0.22	0.32	0.41	0.77
C2	1.87	2.67	0.33	0.61	0.53	0.76	0.6	1.13
C3	2.27	3.24	0.38	0.71	0.13	0.19	0.36	0.69
C4	2.2	3.15	0.34	0.64	0.34	0.49	0.35	0.66
Dtop	1.99	2.85	0.45	0.85	0.66	0.95	0.53	1.01
D1	1.91	2.73	0.4	0.75	0.25	0.36	0.46	0.88
D2	1.75	2.51	0.41	0.78	0.18	0.26	0.65	1.23
D3	1.66	2.38	0.43	0.81	0.05	0.07	0.38	0.71
D4	1.13	1.62	0.36	0.67	0.16	0.22	0.48	0.91
Etop	2.19	3.13	0.39	0.73	0.53	0.76	0.52	0.98
E1	2.74	3.92	0.44	0.84	0.11	0.16	0.42	0.79
E2	1.97	2.81	0.42	0.79	0.11	0.15	0.43	0.81
E3	2.17	3.10	0.43	0.81	0.09	0.12	0.6	1.13
E4	2.32	3.31	0.39	0.74	0.12	0.18	0.43	0.8
Ftop	2.17	3.1	0.56	1.06	0.22	0.32	0.52	0.98
F1	2.16	3.09	0.46	0.86	0.10	0.14	0.4	0.76
F2	2.43	3.47	0.52	0.98	0.31	0.44	0.49	0.92
F3	2.23	3.19	0.43	0.82	0.09	0.12	0.33	0.63
F4	1.5	2.15	0.28	0.54	0.2	0.29	0.39	0.74
G1	1.69	2.42	0.42	0.8	0.25	0.35	0.43	0.81
G2	1.87	2.68	0.45	0.85	0.07	0.11	0.37	0.71
G3	1.3	1.86	0.38	0.72	0.08	0.12	0.4	0.75
G4	1.73	2.48	0.44	0.83	0.09	0.13	0.38	0.71

Table 4.17: Average values for crystalline and amorphous oxides.

<i>Horizon</i>	Fe %	Fe % in Fe₂O₃	Al %	Al % in Al₂O₃	Fe %	Fe % in Fe₂O₃	Al %	Al % in Al₂O₃
A	1.65	2.36	0.41	0.78	0.25	0.36	0.54	1.02
B	1.62	2.32	0.32	0.61	0.12	0.17	0.44	0.83
C	2.11	3.01	0.37	0.68	0.31	0.44	0.43	0.81
D	1.61	2.31	0.40	0.75	0.16	0.23	0.49	0.93
E	2.30	3.29	0.42	0.80	0.11	0.15	0.47	0.88
F	2.08	2.98	0.42	0.80	0.18	0.25	0.40	0.76
G	1.65	2.36	0.42	0.80	0.12	0.18	0.40	0.75

in oxide crystallinity with soil age. The active ratio of this soil also indicates well drainage conditions that favor oxidation conditions and crystallinity (Osedeke et al, 2005; Dolui and Mustafi, 1997).

The x-ray diffraction results were very similar in all Rio Piedras strata. Results indicate the presence of 2:1 clay minerals and probably micas in the clay fraction. Probable clay minerals present are vermiculite, montmorillonite, chlorite, muscovite and biotite. This group of minerals show peaks around 4 and 6° 2θ (Figures 4.20 - 4.22). A sharp and intense peak corresponding to quartz was identified around 26.5° 2θ. Hematite, goethite, gibbsite, and kaolinite were also observed in the profile. The diagnostic peak for kaolinite is observed around 12.2° 2θ. Gibbsite, goethite and hematite peaks are observed at 20 to 22 and 35 to 40° 2θ. A peak around 28° 2θ is indicative of the presence of manganese minerals like pyrolusite and birnessite in strata A and C (Table 4.20). Some birnesite peaks could be confused with those of kaolinite at 11-13° 2θ and 36-37.5° 2θ.

Table 4.18: Amorphous and crystalline oxides and weathering index.

<i>Horizon</i>	Fe Crystalline %	Fe Amorphous %	Fea/Fec
A1	1.88	0.77	0.41
A2	1.52	0.07	0.04
A3	1.55	0.07	0.04
A4	1.65	0.08	0.05
B1	1.58	0.13	0.08
B2	2.02	0.12	0.06
B3	0.98	0.11	0.11
B4	1.91	0.12	0.06
Ctop	2.45	0.57	0.23
C1	2.09	0.22	0.11
C2	1.87	0.53	0.28
C3	2.27	0.13	0.06
C4	2.20	0.34	0.16
Dtop	1.99	0.66	0.33
D1	1.91	0.25	0.13
D2	1.75	0.18	0.10
D3	1.66	0.05	0.03
D4	1.13	0.16	0.14
Etop	2.19	0.53	0.24
E1	2.74	0.11	0.04
E2	1.97	0.11	0.05
E3	2.17	0.09	0.04
E4	2.32	0.12	0.05
Ftop	2.17	0.22	0.10
F1	2.16	0.10	0.04
F2	2.43	0.31	0.13
F3	2.23	0.09	0.04
F4	1.50	0.20	0.13
G1	1.69	0.25	0.15
G2	1.87	0.07	0.04
G3	1.30	0.08	0.06
G4	1.73	0.09	0.05

Table 4.19: Average values for amorphous and crystalline oxides with weathering index.

<i>Horizon</i>	Fe Crystalline %	Fe Amorphous %	Fea/Fec
A	1.65	0.25	0.14
B	1.62	0.12	0.08
C	2.11	0.31	0.15
D	1.61	0.16	0.10
E	2.30	0.11	0.05
F	2.08	0.18	0.09
G	1.65	0.12	0.08

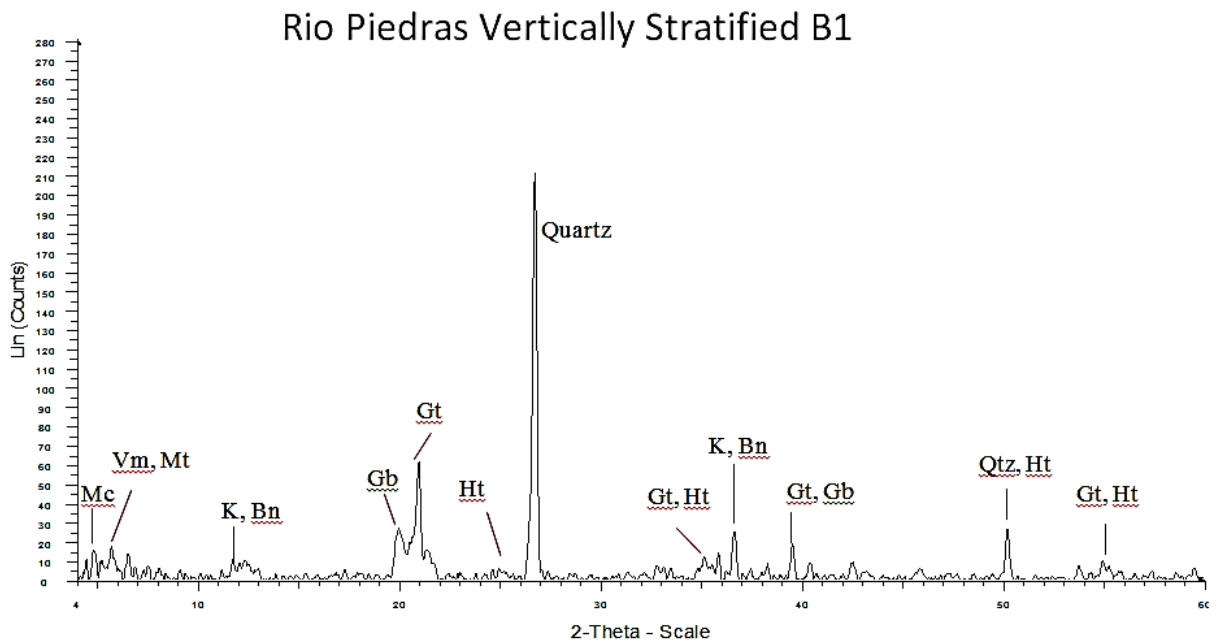


Figure 4.20: X-ray diffraction pattern of Rio Piedras vertically stratified B1

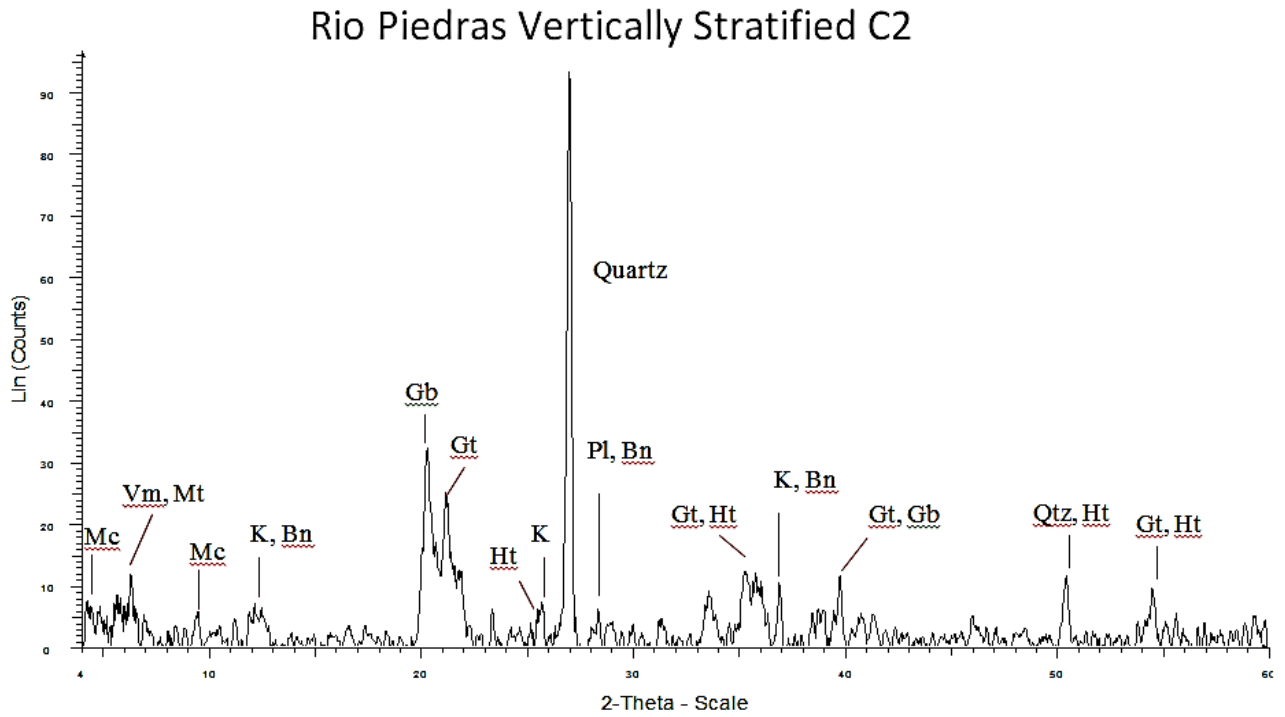


Figure 4.21: X-ray diffraction pattern of Rio Piedras vertically stratified C2

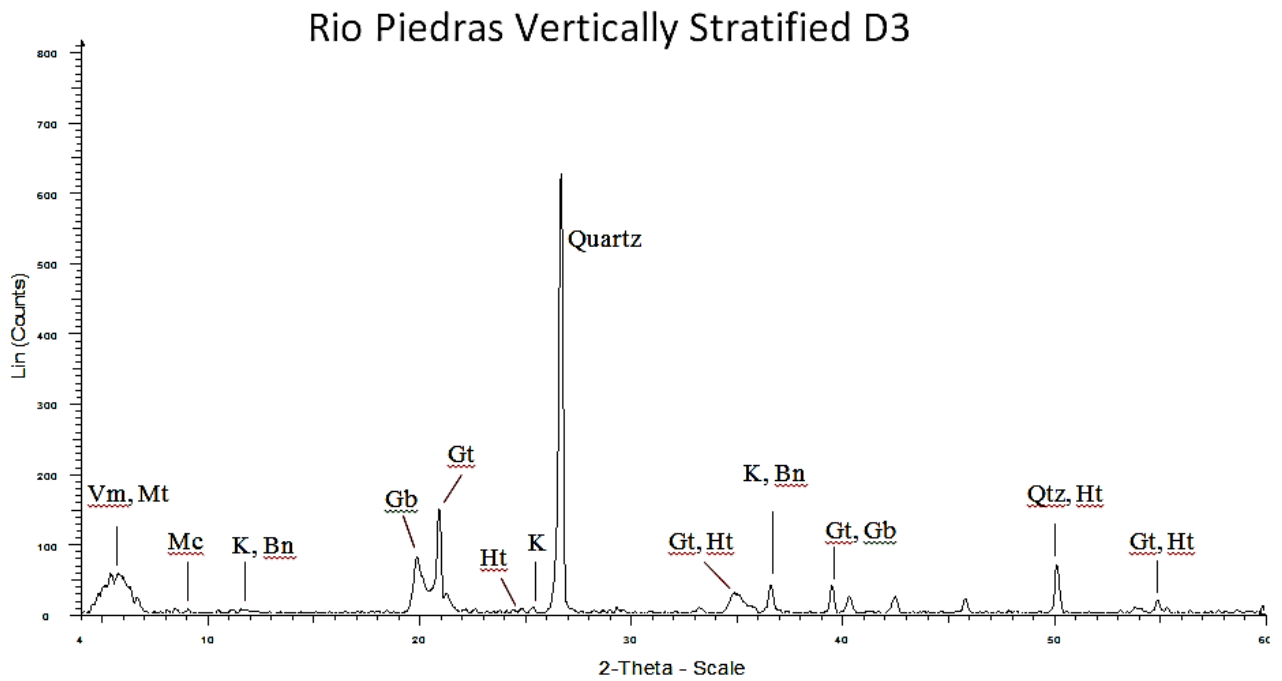


Figure 4.22: X-ray diffraction pattern of Rio Piedras vertically stratified D3

Table 4.20: Clay fraction mineralogical composition of Rio Piedras vertically stratified

Soil Strata	Minerals
A and C	Micas, expansive clays, chlorite, kaolinite , pyrolusite or birnesite, gibbsite, goethite, hematite and quartz
B, D, E, F and G	Micas, expansive clays, chlorite, kaolinite , gibbsite, goethite, hematite and quartz

4.3. Geologic Aspects and Evolution of the Rio Piedras-Bajura Soil Toposequence

The origin of Coloso Valley possibly started about 49-50 million years ago when the southwestern block of Puerto Rico containing the Bermeja Complex was separated of the main igneous and sedimentary central block by a narrow basin (Figure 4.21). The main block forming the island of Puerto Rico consists of volcanic and sedimentary rocks from Late Cretaceous (~ 100.5 - 66 Ma) and early Paleogene (~ 66 - 56 Ma)(Laó-Dávila, 2014; Pindell, 1994). During the Eocene, turbidites and volcanic rocks were deposited in this narrow basin due to submarine volcanic activity associated with the Proto-Caribbean plate subduction and aerial erosion and deposition of exposed basement rocks. The subduction occurred at the Proto-Caribbean plate in the Middle Eocene (~ 49 Ma), and generated a fault system that affected the island with a compressive movement between the central and southwestern blocks, folding and uplifting the volcanoclastic-sedimentary rock system deposited under water in this basin. Folds are wavelike bends in layered or stratified rocks formed by compressional movements in rocks (Figure 4.22). The rocks along the fault system, including the actual Cerrillos Belt rocks, were folded into a series of large anticlines and synclines. Anticlines are upward arching fold and synclines are downward arching folds (Figure. 4.23). The compression that last approximately 10-20 million

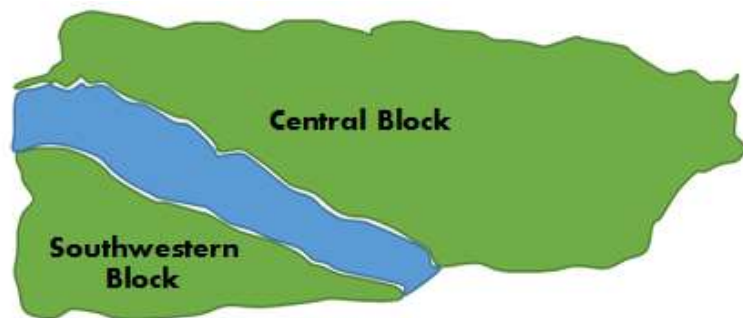


Figure 4.21: Central and southwestern blocks of Puerto Rico before collision.

years, caused a ground uplifting of the basin rocks, today the Eocene Cerrillos Belt, next to the Cretaceous and Paleogene volcanic and sedimentary rocks (Laó-Dávila, 2014; MacFee et al., 2003; Pindell, 1994; McIntyre, 1970; Monroe, 1969; Mitchel, 1954). The Cerrillos Belt remains exposed over sea level until Middle Oligocene (~ 30 Ma) when sea level began to rise and covered the rocks that had risen during the Eocene (MacFee et al., 2003; Vail et al., 1977). The rocks were covered by carbonates and sedimentary deposits under marine conditions that later resulted in more recent geologic formations such as Cibao, dated from Early Miocene (~12.17 Ma)(Ortega-Ariza et. al., 2015; Monroe, 1969). A later sea level fall (22-19 Ma) exposed the Eocene - Miocene deposits into another erosion-weathering cycle. MacFee et al. (2003) establish that Puerto Rico has been emerging or uplifting since Middle Miocene (~16 Ma) exposing the Eocene rocks to an intense tropical weathering and erosion-deposition cycles.



Figure 4:22: Compression in sedimentary rocks (Schott, 2006).

According to Monroe (1969), Eocene and Oligocene (39 Ma) deposits have been eroding in high lands and these materials have been covering low lands for the last 2.6 million years, forming an alluvial valley that is actually dissected by the Culebrinas and Cañas rivers. The rocks exposed to

the surface have served as parent material for different soil orders in the Coloso Valley. These soils have been developed with different physical and chemical properties due to the nature of their parent material and topographic position.

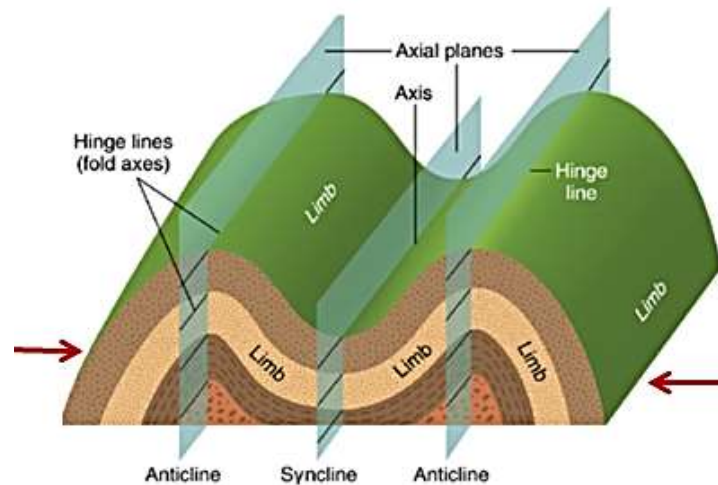


Figure 4.23: Anticlines and synclines in sedimentary rocks. Arrows indicate compression. (Edited from Carlson et al., 2006).

The relationship of the soils with their geologic formation was modeled in a block diagram presented in Figure. 4.24. The block diagram show the Rio Piedras-Bajura-Coloso soil toposequence and relationship with parent material. The model was developed following the guide of Eikleberry (1960). Coloso is an Inceptisol found in the river flood plains and low terraces. Bajura is a Mollisol formed in river flood plains. The Rio Piedras soil is an Ultisol that occurs on gently to strongly slopes of dissected uplands, with gradients from 2 to 20 percent (Gierbolini, 1975). Rio Piedras soil parent material consists of stratified sedimentary rocks that have been deformed due to Caribbean and Western Puerto Rico Eocene tectonic activity. Strike and dip measurements from geologic map show an anticlinal structure in the hill, close to the site where the Rio Piedras vertically stratified profile was sampled. The strata inclination reaches 84°, giving a vertical appearance (Monroe, 1969). The strike and dip measurements were used to

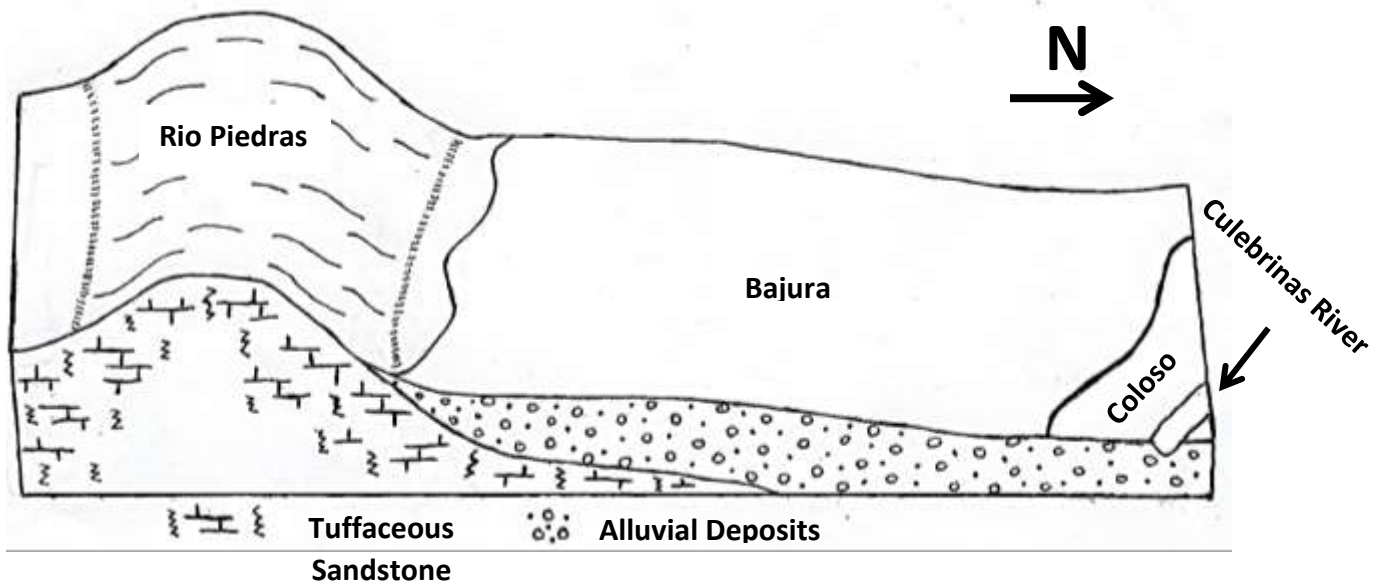


Figure 4.24: Block diagram of the Rio Piedras – Bajura – Coloso soil toposequence. The model was developed following the guide Eikleberry (1960).

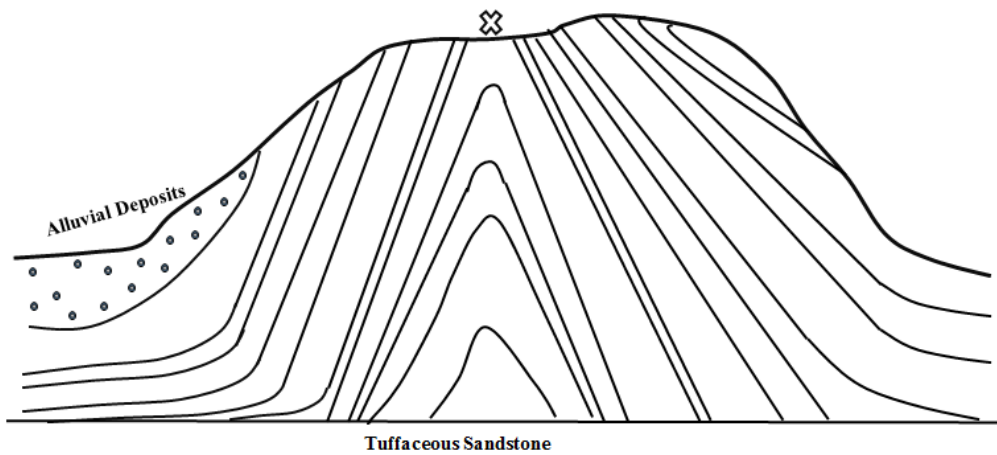


Figure 4.25: Model showing the stratification and deformation of Rio Piedras parent material. (Data used from Monroe, 1969).

developed a model showing structural deformation of Rio Piedras parent material at the site where the vertically stratified profile was sampled (Fig. 4.25). The weathering process in the vertically stratified profile is not happening at the same rate as in the typical Rio Piedras profiles. Well-developed soil horizons with depth are expected to occur in a typical soil profile like Rio Piedras backslope or footslope. The almost vertical stratification prevents and retards the mixing of the soil by pedogenic processes such as clay movement and accumulation, leaching and dissolution processes that form soil horizons. The strata operate as a lateral discontinuity in the profile. This profile will acquire properties and appearance similar to the typical Rio Piedras soil series with time, but the pedogenesis of the profile will be slower (Fig. 4.26).

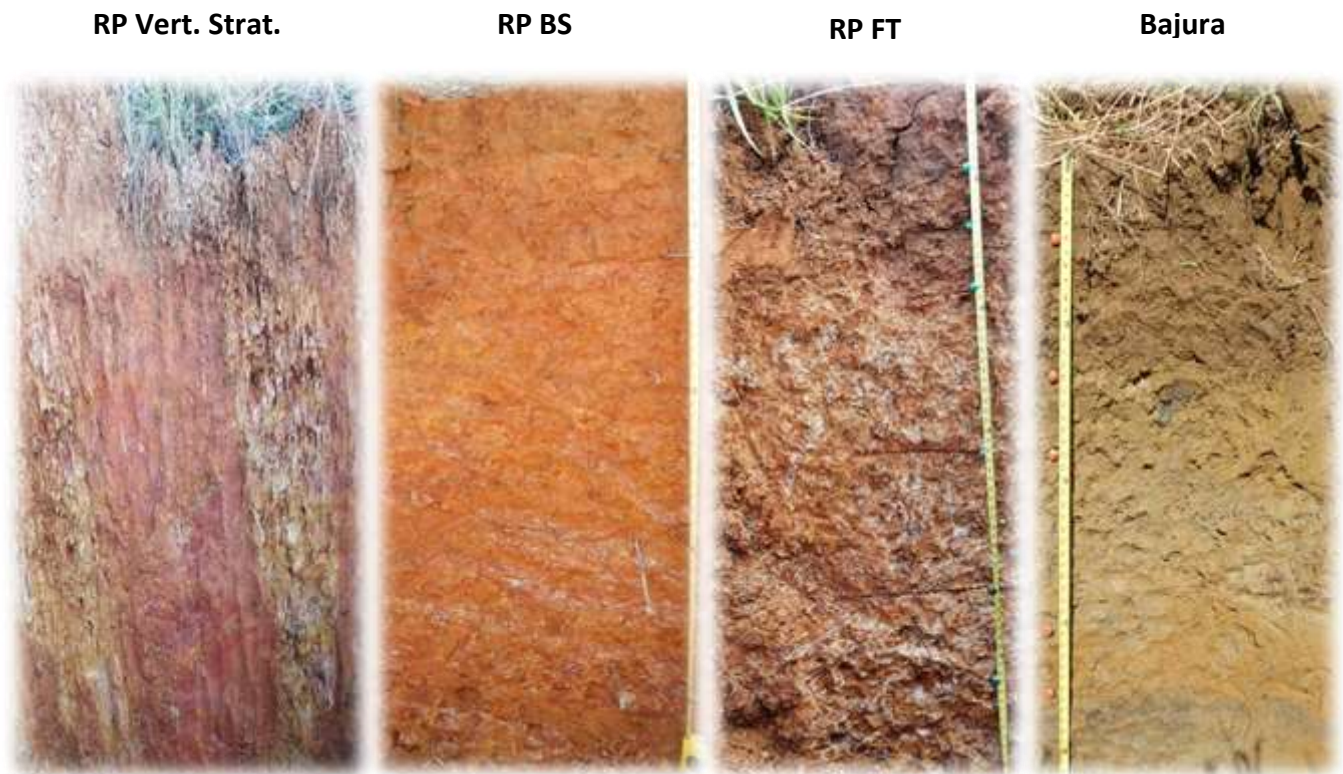


Figure 4.26: Rio Piedras – Bajura soil toposequence.

The position of the soil series in the toposequence at Coloso Valley results in differences in sun exposure, water movement and infiltration, vegetation density and diversity, biomass production, runoff, erosion and soil deposition, soil structure, water retention and drainage, biological activity and soil fertility. All these factors influence the pedological processes and soils chemical and physical properties. Chemical and physical properties evaluated in the toposequence showed differences that can be attributed partially to landscape relief. An increase in pH was observed as we move downslope to Bajura soil. However, the pH of the Ap horizon of Bajura soil was lower than expected for a Mollisol. Intensive fertilization in Coloso Valley may contribute to the acidification process, but runoff from Rio Piedras, where extremely acid conditions prevail may also contribute to the acidification of the Ap horizon.

The texture of Rio Piedras and Bajura soils is directly related to their parent materials. Sand, silt and clay in soils have also been related to their position in the toposequence (Dessalegn et al., 2014; López-Galindo et al., 2003; Lawal et al., 2013). Even when the removal of surface material could occur, sand fraction in both profiles remains constant but silt content increases downslope, as expected by slope influence in soils toposequences. The differences in texture between Bajura and Rio Piedras profiles should be evaluated considering the differences in parent material for the two soil series. The alluvial deposits forming Bajura soils have been previously described as silt and clay derived from calcareous and volcanic adjacent rocks, while tuffaceous sandstones and siltstones formed the bedded turbidite rocks forming Rio Piedras soil (Gierbolini, 1975; Monroe, 1969). Some strata of the Rio Piedras vertically stratified soil profile contains higher amount of sand particles than any other soil profile of the toposequence, which is expected for a soil forming from tuffaceous sandstones and siltstones and experiencing a less intense weathering process.

Organic matter content increased downslope, as expected, in the soil toposequence due to higher soil moisture content and a more intense vegetation growth. The darkening in surface horizons downslope is the effect of higher soil organic matter content, presence of manganese masses and prevailing reducing conditions most of the year. At the soil surface (Ap horizon), the Rio Piedras vertically stratified profile had a 1.08% organic matter. The backslope profile had 2.6% organic matter, in the footslope profile 1.9%, and Bajura profile 3.3%. The increase in soil organic matter content as we move down the toposequence can be observed clearer when we consider the first 50 cm depth of the soil profile. At a depth of 50 cm three horizons were identified and the average soil organic matter content was 1.10% for the backslope profile, 1.53 for the footslope and 1.83 for Bajura. An increase in slope favors soil erosion, decrease organic matter content, fertility level and the capacity of the soil to sustain abundant plant growth. Soils at valley floors or lower elevations are expected to have less erosion and better biologic development (Brady and Weil, 1996). The higher organic matter content, 3.3%, was reported in the valley, as expected for a Mollisol, a soil that exhibits a mollic epipedon with organic matter content of 3% or more (Gierbolini, 1975).

Aggregate stability also increased as we move down the toposequence, influenced mostly by the higher organic matter content. The organic matter acts as a cementing agent for sand, silt and clay particles forming stable soil aggregates. The highest value for aggregate stability was reached at the surface horizon (Ap) for each soil profile in the toposequence. Aggregate stability was lower in the vertically stratified profile. Higher values were reached at the first 10 cm, or top soil in a range from 52-66%. The Ap horizon of Bajura soil showed a 76% aggregate stability.

Results show a high cation exchange capacity for this soil toposequence, most of it occupied by exchangeable aluminum content. The exchangeable Al^{3+} content was extremely

high in the Rio Piedras profiles, at levels considered toxic for most crops. The Ap horizon of Bajura soil showed higher levels of exchangeable Al^{3+} also, but decreased sharply in the subsoil. Parent material and pH levels are the principal factors affecting exchangeable Al^{3+} content. The high exchangeable Al^{3+} content in Rio Piedras is the result of the intense weathering process since the first Eocene rocks were exposed over sea level that resulted in the formation of the Ultisol. Highly weathered soils, such as Ultisols may contain high levels of exchangeable aluminum and the presence of Al-hydroxy interlayered clays (Lepsch and Buol, 1974). The presence of Al-hydroxy interlayered clays in Rio Piedras is indicated by xrd peaks around $6^\circ 2\theta$. These peaks are often precluded by the presence of 2:1 clays like vermiculite and montmorillonite and the clay has to be pre-treated with treatments other than magnesium chloride saturation for specific identification. Rio Piedras soil is also very low in organic matter and chelation mechanisms that reduce exchangeable Al^{3+} are not happening at a significant rate.

Due to the presence of manganese nodules or concretions and masses described in the Rio Piedras and Bajura soil series, exchangeable manganese was expected in the soils of this toposequence. Manganese toxicity occurs in acid soils under redox conditions with levels as high as 50 ppm (Smyth, 2011; Wang et al., 2002). Manganese levels described in Bajura and Rio Piedras Footslope Ap horizon could be toxic to manganese sensitive species. However, manganese concretions and masses do not cause plant toxicity problems, toxicity problems arise when manganese solubilizes and enters the soil solution and occupies exchangeable sites in soil minerals and organic matter.

Toxicity of exchangeable aluminum and manganese can be corrected by liming, the planting of tolerant species and with phosphorus applications. Aluminum and manganese tolerance varies among plant species and cultivars. Cassava, pineapple, citrus, coffee, tea and

rice are aluminum tolerant species. Cassava is one of the most tolerant crops to Al^{3+} toxicity and acid soil conditions. This crop performs well at Al^{3+} saturation levels over 75%. Cotton, sorghum, onion, peppers lettuce, banana and wheat are sensitive species (Kamprath, 2010, Osmond et al., 2007; Abruña, 1975). Rice, sugarcane and corn are manganese tolerant but bean plants are sensitive.

Manganese nodules exposed in Rio Piedras soils were formed under marine conditions and could be related to manganese deposits previously described in Aguada, Puerto Rico. Authors like Bawiec et al. (1999), Koski (1986) and Cox and Briggs (1973) previously described volcanogenic manganese deposits in lenses and stratiform bodies occurring in Eocene volcanic-sedimentary rock sequences. Bawiec et al. (1999) explained that the manganese deposits in Aguada ore occurs as pyrolusite and psilomelane minerals with deeply weathered clay. According to Bawiec et al. (1999) and Cox and Briggs, (1973) the manganese deposits occur as discontinuously veins inside fractures and faults. This manganese deposit may be classified as a sedimentary-hydrothermal deposit (Rodríguez-Díaz et al., 2005). Sedimentary deposits refer to manganese accumulations in sedimentary basins. Hydrothermal deposits refer to manganese deposited as veins and other bodies formed from manganese rich hydrothermal solutions in hot springs, ocean ridges, island arches and oceanic intraplates (Rodríguez-Díaz et al., 2005).

Geological evidence supports the theory that Eocene Cerrillos Belt was enriched with manganese oxides under water when the west zone of Puerto Rico was still separated by the narrow basin. The manganese oxides precipitated into rock and nodules that can be found in localized deeply weathered soils of Aguada. Pérez (2010) proposed that manganese nodules formed when the Rio Piedras soil was at lower elevation under continuous water table fluctuations and precipitated in a nodular appearance with ground uplift. This theory may explain

the formation of current manganese masses of Bajura. These manganese masses, of recent origin, are the weathering product of the Eocene manganese enriched rocks. Weathering of the manganese enriched rocks in the alluvial deposits at the valley provides metallic elements like iron and manganese into soil solution. Seasonal water table fluctuations facilitate movement and concentrations of these elements in soil profile. Manganese and iron have been precipitating into irregular masses and small concretions close to the soil surface. X –rays diffraction analysis suggest the presence of birnesite and pyrolusite, the most stable form of manganese oxide minerals. These masses and small concretions may easily turn into iron and manganese nodules if future soil uplift occurs. Therefore, the statement of Pérez (2010) may be a possible explanation of how the manganese nodules were formed in the Rio Piedras soil since it is still an active process in Bajura soil. On the other hand, the Rio Piedras manganese nodules could be formed by the mechanical weathering of the manganese enriched veins deposited in the rocks. Manganese tends to occur in concretions and nodules and when it breaks, it will keep the nodular appearance but a smaller size (Wilding et al., 1983a).

Rio Piedras soil redness is caused by the presence of iron oxides. The vertically stratified profile shows higher iron content in strata B, C, E and F. These strata have a much redder coloration compared to sections A, D and G. The hue is more reddish with landscape elevation and value and chroma increased with soil depth. Soil age and landscape elevation play a major role in coloration. Markewich et al. (1989) suggested an increase in hematite, crystalline oxides and soil redness with age. Weathering of parent material contributes to oxides formation and soil ageing promotes an advance stage of oxides crystallinity. The Rio Piedras-Bajura soil toposequence shows a predominance of free and well crystallized phases of iron and aluminum oxides. The high content of amorphous oxides described in Bajura can be attributed to

redoximorphic conditions in the valley and poor drainage conditions, confirmed with grayish colors in subsoil horizons. Soil ageing and drainage conditions may also be related to the weathering index or active ratio. A ratio less than one resulted in the four profiles studied confirming a prolonged weathering stage. The formation of clay secondary minerals also supports an advanced weathering stage for these soils.

The weathering processes that result in the formation of soil horizons favors the formation and accumulation of clay minerals through time. However, the accumulation of clay by geological processes not necessarily implies an advanced weathering stage, because rocks may form from the accumulation of clays that solidify over time like mudstone and shale rocks. In the Rio Piedras vertically stratified profile, color and texture were the major criteria to identify the strata. A more reddish coloration was observed in strata B, C, E and F and the texture was sandier. Strata A, D and G had a saprolitic appearance and more clay content. But this may reflect the stratified nature of parent material and not an advanced state of weathering in the more clayey strata. Clay mineral components were similar in all strata, showing the presence of 2:1 clays, kaolinite, micas and iron and aluminum oxides. However, a higher content of crystalline and amorphous iron and aluminum oxides was observed in strata C, E and F, which is indicative of a more advanced weathering stage.

5. Conclusion

The Coloso Valley formation resulted from sea level changes and the tectonic activity associated to the Eocene Cerrillos Belt. The origin of the valley began in the Eocene when the southwestern block of Puerto Rico was separated of the main igneous and sedimentary block by a narrow basin. The subduction that occurred at the Proto-Caribbean plate in the Middle Eocene generated a fault system that folded the basin rocks (Eocene Cerillos Belt) into a series of large anticlines in synclines. The compression caused a ground uplift of the basin rocks that remained exposed over sea level until Middle Oligocene. The sea level covered these rocks until Middle Miocene, when a sea level fall exposed them into another weathering and erosion-deposition cycle. The high land erosion of the Eocene and Oligocene rocks is has been carrying materials that covered low lands during the last 2.6 million years, forming the alluvial valley containing the Rio Piedras and Bajura soils.

The stratified nature of the Rio Piedras parent material is affecting the pedological process taking place at the soil profile in shoulder position. The strata operate as a lateral discontinuity preventing the formation of soil horizons in the profile. Strata A, D and G had a saprolitic appearance, a higher clay content and dominance of yellowish colors. Strata B, C, E and F had a higher sand content and a dominant dark red color. Properties such as low organic matter content, low aggregate stability, extremely acid pH, high exchangeable Al^{3+} and very low exchangeable Ca^{2+} , K^{+} and Mg^{2+} were identified at this vertical stratified profile.

Regional geology and topography controls differences in chemical and physical properties of Rio Piedras-Bajura soil toposequence. The slope plays a major role in color, aggregate stability, organic matter content, exchangeable cation content, pH and mineralogy differences between Rio Piedras soil profiles at shoulder, backslope and footslope positions. As

weathering continues in this toposequence, more similarities are expected between these Rio Piedras soils profiles over time. Differences observed in properties of Bajura and Rio Piedras soil series are due to the nature of parent materials since Bajura is formed from alluvial deposits eroded from adjacent rock formations in the valley while Rio Piedras is formed from folded volcanoclastic – stratified sedimentary rocks.

The high exchangeable aluminum content in Rio Piedras soils was related to the intensive weathering history of the parent material that was uplifted and exposed in Oligocene, under sea level in Miocene and recently exposed in the last million years to another weathering cycle. Exchangeable Al^{3+} occupies over 90 percent of exchangeable sites in the clay fraction. The clay fraction is characterized by the presences of iron and aluminum oxides, kaolinite and to a lesser extent 2:1 clay minerals and probably hydroxy interlayered aluminum clays. The presence of hydroxy interlayered aluminum clays can be a major source of the high exchangeable levels of Al^{3+} observed in Río Piedras soil.

The Rio Piedras-Bajura soil toposequence shows a predominance of free and well crystallized phases of iron and aluminum oxides. The high content of amorphous oxides described in Bajura can be attributed to redoximorphic conditions in the valley and poor drainage conditions, confirmed with grayish colors in subsoil horizons. Soil ageing and drainage conditions may also be related to the weathering index or active ratio. A ratio less than one resulted in the four profiles studied confirming a prolonged weathering stage. The formation of clay secondary minerals also supports an advance weathering stage for these soils.

Manganese masses and nodules observed in Rio Piedras and Bajura soils had its origin in the manganese veins deposited between faults and fractures of the volcanoclastic-stratified sedimentary rocks under sea level. The manganese nodules could be a physical weathering

product of these veins but they also could be formed due to continuous redox conditions since it is still an active process in Bajura soil, forming the manganese masses. The manganese masses should acquire a more nodular appearance if future uplift occurs in Bajura soil.

Manganese and aluminum toxicity are occurring in the Rio Piedras-Bajura soil toposequence. The high exchangeable aluminum content observed in all Rio Piedras profiles and the Ap horizon of Bajura, is considered toxic to aluminum sensitive species. Manganese toxicity was observed in the Ap horizon of Bajura. The aluminum and manganese toxicity can be corrected by liming, the planting of tolerant species and with phosphorus applications. Even with the natural limitations of these soils, with an appropriate management, both soil series could be very productive for agricultural purposes.

Cited References

- Abruña, F., R. W. Pearson and R. Pérez-Escolar. 1975. Lime response of corn and beans in typical Ultisols and Oxisols of Puerto Rico p. 261 – 281. *In*. Bornemiza, E. and A. Alvarado (ed). Soil management in tropical America. Raleigh, North Carolina: North Carolina State Univ.
- Almeida Delarmelinda, E., V. De Souza, P. Salvador Wadt, Y. Deng, M. Costa Campo, and E. Guimarães Câmara. 2017. Soil-landscape relationship in a chronosequence of the middle Madeira River in southwestern Amazon, Brazil. *Catena*. 149:199-208.
- Baltpurvins, K.A., R.C., Burns and G.A. Lawrance. 1997. Effect of Ca^{2+} , Mg^{2+} , and anion type on the aging of iron (III) hydroxide precipitates. *Environmental Science & Technology* 31(4):1024-1032.
- Bawiec, W.J., R. Alonzo, D. P. Cox, A. Griscom, B. R. Lipin, S. P. Marsh, G. E. McKelvey, N. J. Page, and J. H. Schellekens. 1999. Mineral resource assessment of Puerto Rico. *In* Bawiec, W.J. (ed) Geology, geochemistry, geophysics, mineral occurrences and mineral resource assessment for the Commonwealth of Puerto Rico. U.S. Geological Survey. Open-File report (98-38).
- Beinroth, F.H. 1972. The natural environment of Puerto Rico. The University of Puerto Rico Mayaguez Campus.
- Bertsch, P. M. and P.R. Bloom. 1996. Aluminum. p. 517-550. In D. L. Sparks (ed.) *Methods of Soil Analysis. Part 3. Chemical Methods-SSSA Book Series no. 5*, SSSA, Madison, WI.
- Blume, H. P. and U. Schwertmann. 1969. Genetic evaluation of distribution of Al, Fe and Mn oxides. *Proceedings of Soil Science Society of America*. 33:438-444.
- Brady, N.C. and R.R. Weil. 1996. *The nature and properties of soils*. Prentice Halls. USA.
- Cabria, F.N., M.R. Bianchini and M.C. Mediavilla. 2005. Óxidos de hierro libres asociados a carbono orgánico en agregados de suelos del partido de Balcarce. *Ciencia del Suelo* 23(1): 23-29.
- Carlson, D.H., C. C. Plummer and D. McGeary. 2006. *Physical Geology: Earth Revealed*. 6 th Edition. McGraw-Hill Education. United States.
- Costa da Silva, A. 2014. Presence of the exchangeable aluminium in lowland soils collected in the Maranhão State. *Ciência e Natura. Ed. Especial II*. 36:769-774.
- Cox, D.P. and R.P. Briggs. 1973. Metallogenic map of Puerto Rico. U.S. Geological Survey. *Miscellaneous geologic investigations. (MAP I-721)*.

- Dessalegn, D., S. Beyene, N. Ram, F. Walley and T. Gala. 2014. Effects of topography and land use on soil characteristics along the toposequence of Ele watershed in southern Ethiopia. *Catena*. 115:47-54.
- Dolui, A. K. and S. C. Mustafi. 1997. Forms of extractable iron in relation to soil characteristics of some Alfisols. *Journal Indian Soil Science Society* 45(1):92-194.
- Eikleberry, R. W. Block Diagrams for soil survey interpretations. United States Department of Agriculture. Soil Conservation Service.
- Encina-Rojas, A. 1998. Influencia de la topografía en la formación de Molisoles en zonas áridas. *Investigación Agraria*. 1(2).
- Eze, P. N., T. K. Udeigwe and M. E. Meadows. 2014. Plinthite and its associated evolutionary forms in soils and landscapes: A review. *Pedosphere*. 24(2):153-166.
- Gee, G. W., and J. W. Bauder. 1986. Particle-size Analysis. p. 383-411. In A.L. Page (ed.) *Methods of Soil Analysis. Part 1. Physical and Mineralogical Methods*. 2nd Ed. Agronomy Monograph 9, Soil Science Society of America, Madison, WI.
- Gierbolini, R., 1975. Soil survey of Mayagüez area of Western Puerto Rico. United States Department of Agriculture: Soil Conservation Service.
- Goldberg, S. 1989. Interaction of aluminum and iron oxides and clay minerals and their effect on soil physical properties: A review. *Communication in Soil Science Plant Analysis*. 20 (11-12):1181-1207.
- Ibia, T. O. 2001. Forms of Fe and Al in soil particles of inland flood plains of southeastern Nigeria. *Proceeding of the 27th Annual Conference of the Soil Science Society of Nigeria*. 165-168.
- Kamprath, E. J. (2010). Soil acidity and liming. *Century of Soil Science*. North Carolina, 103-107.
- Kemper, W.D. and R.C. Resenau. 1986. Aggregate stability and size distribution. Pp. 425-442. In *Methods of Soil Análisis Part 1-Physical and Mineralogical Methods*, Second Edition. Soil Sci. Soc. Amer., Madison Wisconsin. 1188 p.
- Koski, Randolph A., 1986, Descriptive model for volcanogenic Mn. In Cox, D.P., and D. A. Singer (ed). *Mineral deposit models: U.S. Geological Survey Bulletin* 1693, p. 139.
- Laó-Dávila, D.A. 2014. Collisional zones in Puerto Rico and the northern Caribbean. *Journal of South American Earth Sciences*. 54:1-19.
- Lawal, B., A. Ojanuga, P. Tsado and A. Mohammed. 2013. Characterization, classification and agricultural potentials of soils on a toposequence in Southern Guinea Savanna of Nigeria.

International Journal of Biological, Biomolecular, Agricultural, Food and Biotechnological Engineering. 7(5): 214-218.

Lepsch, I. F. and S. W. Buol. 1974. Investigations in an Oxisol-Ultisol toposequence in Sao Paulo State, Brazil. Soil Sci. Soc. Am. Proc. 38: 491-496.

LexJuris. 1997. Ley Num. 142 del año 2000. LexJuris de Puerto Rico y Publicaciones CD. [online september 11, 2015].

López-Galindo, F., D. Muñoz-Iniestra, M. Hernández-Moreno, A. Soler-Aburto, M. Castillo-López, and I. Hernández-Arzate. 2003. Análisis integral de la toposecuencia y su influencia en la distribución de la vegetación y la degradación del suelo en la Subcuenca de Zapotitlán Salinas, Puebla. Boletín de la Sociedad Geológica Mexicana. 56 (1): 19-41.

MacFee, R.D.E., M. A. Iturralde-Vinent and E. S. Gaffney. 2003. Domo de Zaza, an Early Miocene vertebrate locality in south-central Cuba, with notes on the tectonic evolution of Puerto Rico and the Mona Passage. American Museum Novitates. (3394).

Mahaney, W.C., R. G. V. Hancock and K. Sanmugadas. 1991. Extractable Fe-Al and geochemistry of late Pleistocene paleosol in the Dalijia Shan, Western China. J. Southeast Asian Earth Sci., 6: 75-82.

Mahaney, W.C. and B. D. Fahey. 1988. Extractable Fe and Al in late Pleistocene and Holocene paleosols in Niwot Ridge, Colorado front range. Catena. 15:17-26.

Markewich, H. W., M. J. Pavich, M. J. Mausbach, R. G. Johnson, and V. M. Gonzalez. 1989. Guide for using soil and weathering profile data in chronosequence studies of the Coastal Plain of the Eastern United States. United States Geological Survey Bulletin. 1589-D.

McIntyre, D., J. Aaron, and O. Tobisch. 1970. Cretaceous and Lower Tertiary stratigraphy in Northwestern Puerto Rico. Geological Survey Bulletin. 1294-D.

McKeague, J. A. and J.H. Day. 1966. Dithionate –and oxalate- extractable Fe and Al as aids in differentiating various classes of soil. Canadian Journal of Soil Science. 46:13-22.

Mehra, O.P., and M.L. Jackson. 1960. Iron oxide removal from soils and clays by a dithionite-citrate system buffered with sodium bicarbonate. Clays Clay Miner. 7:317-327.

Mitchell, R.C. 1954. A Survey of the Geology of Puerto Rico. University of Puerto Rico Agricultural Experiment Station- Rio Piedras, PR. Technical paper (13).

Monroe, W., 1969, Geologic map of the Aguadilla Quadrangle, P.R.: Reston Virginia, USA, U.S.Geological Survey Miscellaneous Investigations Series. Map I-569.

Muñoz, M.A., L. Peña, L. and J. M. O'Hallorans. 1994. Use of an industrial by-product as a liming source. The Journal of Agriculture of the University of Puerto Rico. 78(3-4).

- Munsell, A. 2000. Munsell: Soil Color Charts. Munsell Color X-Rite.
- Nelson, D. W. and L.E. Summers. 1996. Total Carbon, Organic Carbon and Organic Matter. p. 961-1010. In D. L. Sparks (ed.) Methods of Soil Analysis. Part 3. Chemical Methods-SSSA Book Series no. 5, SSSA, Madison, WI.
- Oku, E., A. Essoka and E. Thomas. 2010. Variability in soil properties along an Udalf Toposequence in the Humid Forest Zone of Nigeria. *Natural Science*. 44:564-573.
- Omenihu, A. A., E. E. Opuwaribo and P. M. Statton. 1994. Forms and extractable Fe and Al oxides in coastal plains soils of southern Nigeria. 21th Annual Conference of Soil Science of Nigeria. University of Uyo, Nigeria.
- Ontl, T. A. and L. A. Schulte. 2012. Soil Carbon Storage. *Nature Education Knowledge* 3(10):35. Available online at <https://www.nature.com/scitable/knowledge/library/soil-carbon-storage-84223790>. Accessed [December3/2017].
- Ortega-Ariza, D., E.K. Franseen, H. Santos-Mercado, W. Ramírez-Martínez E. Core-Suárez. 2015. Strontium Isotope Stratigraphy for Oligocene-Miocene Carbonate Systems in Puerto Rico and the Dominican Republic: Implications for Caribbean Processes Affecting Depositional History. *The Journal of Geology*. 123(6): 539-560.
- Osmond, D.L., T. J. Smyth, R.S. Yost, D. L. Hoag, W. S. Reid, W. Branch, X. Wang and H. Li. 2007. Nutrient management support system (NuMaSS), v. 2.2. Soil Management Collaborative Research Support Program, North Carolina State University, Raleigh, NC.
- Osodeke, V., I. Nwotiti and B. Nuga. 2005. Sesquioxides distribution along a toposequence in Umudike area of southeastern Nigeria. *Electronic Journal of Environmental, Agricultural and Food Chemistry*. 4(61):117-124.
- Pérez, S. 2010. Occurrence and characterization of Mn nodules in a toposequence at Coloso Valley Agricultural Reserve. MS Thesis. University of Puerto Rico Mayaguez Campus.
- Pindell, J.L., 1994, Evolution of the Gulf of Mexico and the Caribbean: in Donovan S.K. and Jackson, T. A. (eds.) *Caribbean Geology: An introduction*, University of the West Indies Publishers Association/University of the West Indies Press, Kingston, Jamaica. 13-39.
- Power, J.F. and R. Prasad. 1997. *Soil Fertility Management for Sustainable Agriculture*. CRC Press. United States.
- Rodríguez-Díaz, A.A., M. G. Villaseñor-Cabral, C. Canet, R. M. Prol-Ledesma and A. Camprubí. 2005. Clasificación de los yacimientos de manganeso y ejemplos de depósitos mexicanos e internacionales. *Boletín de Mineralogía* 16:33-43.
- Schoeneberger, P.J., D. A. Wysocki, E. C. Benham and Soil Survey Staff. 2012. Field book for describing and sampling soils, Version 3.0. Natural Resource Conservation Service, National Soil Survey Center, Linln, NE.

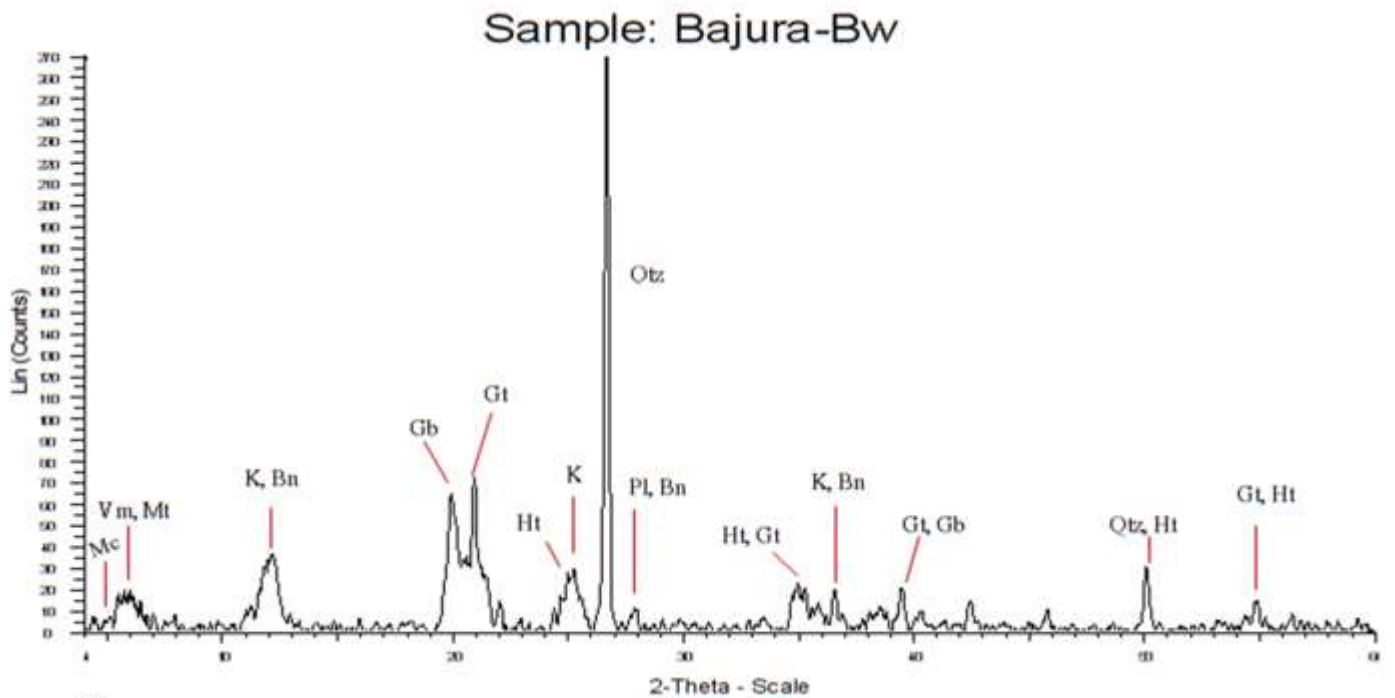
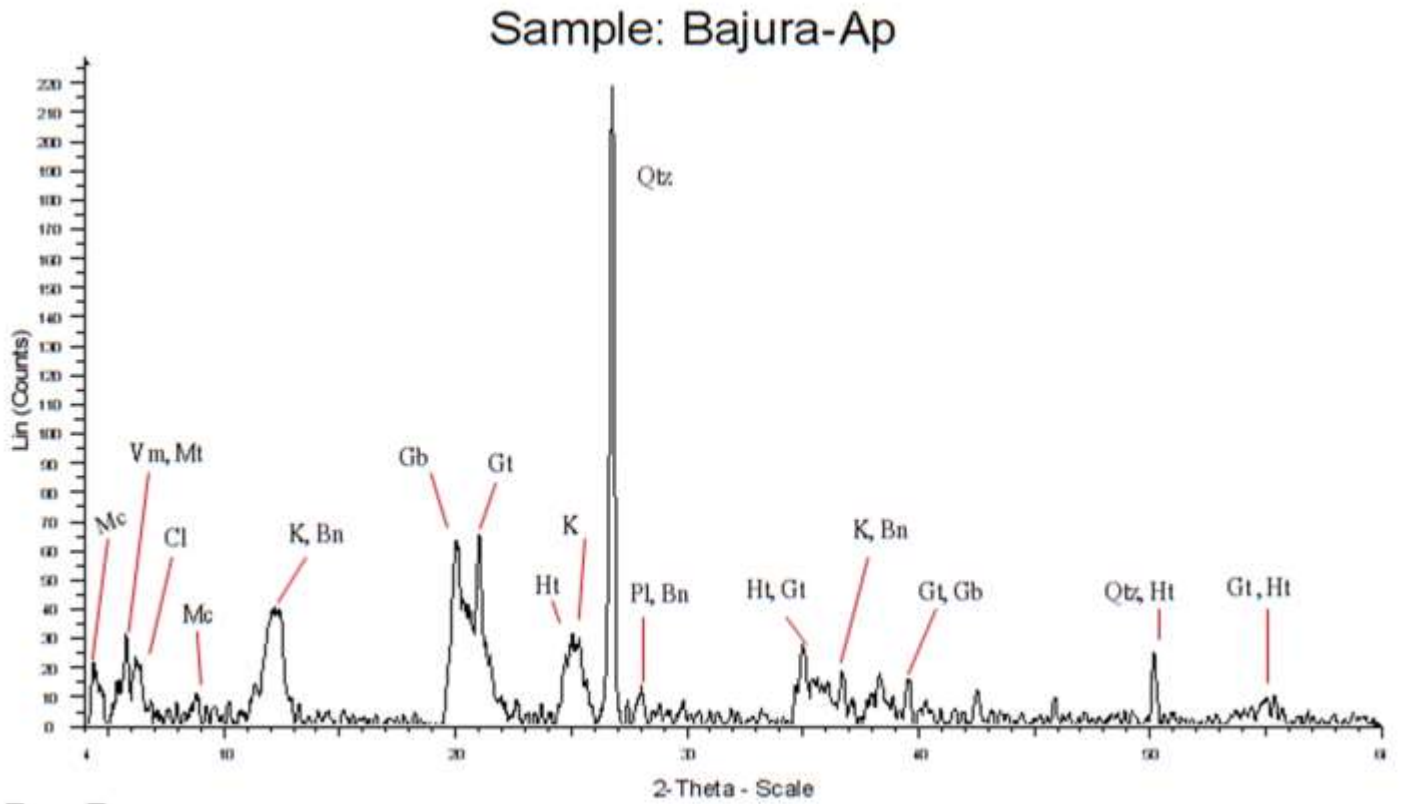
- Schott, R. 2006. Mid-Atlantic regional geology gallery. Available online at <https://www.flickr.com/photos/rschott/albums/72157623059546957>. Accessed [April2/2017].
- Schwertmann, U. 1985. The effect of pedogenetic environments on iron oxide minerals. *Advances in Soil Science*. Vol 1. p. 171-200.
- Seal, A. R. Bera, P. Bhattacharyya, K. Mukhopadhyay and R. Giri. 2006. Degree of soil development in some alfisols of subtropical India with special reference to the nature and distribution of Fe and Al. *International Journal of Agricultural Research*. 1:305-311.
- Smyth, T.J. 2011. Soil acidity and liming p. 12-1-12-7. *In* Ming Huang, P. et al. (ed.) *Handbook of soil sciences resource management and environmental impacts: Second edition*. CRC Press, United States.
- Soil Survey Staff, 1999. *Soil Taxonomy – A basic system of soil classification for making and interpreting soil surveys*, 2nd ed. USDA Natural Resources Conservation Service, Agric. Handbook 436, US Govt. 869 p.
- Soil Survey Staff, Natural Resource Conservation Service, United States Department of Agriculture. Web Soil Survey. Available online at <http://websoilsurvey.nrcs.usda.gov/>. Accessed [August30/ 2015].
- Sumner, M. E. and W. P. Miller. 1996. Cation Exchange Capacity and Exchange Coefficients. p. 1201-1229. *In* D. L. Sparks (ed.) *Methods of Soil Analysis. Part 3. Chemical Methods-SSSA Book Series no. 5*, SSSA, Madison, WI.
- Udo, E. J. 1980. Profile distribution of iron sesquioxides contents in selected Nigeria soils. *Journal Agricultural Science of Cambridge* 95:191-198.
- Vail, P.R., R. M. Mitchum Jr. and S. Thompson III. 1977. Global cycles of relative changes in sea level. *Amer. Assoc. Petrol. Geol.* (26):83-98.
- Van Wambeke, A. 1992. *Soils of the Tropics: Properties and appraisal*. McGraw-Hill, Inc. United States.
- Wang, Y.X., P. Wu, Y. R. Wu and X. L. Yan. 2002. Molecular marker analysis of manganese toxicity tolerance in rice under greenhouse conditions. *Plant and Soil* 238:227-233.
- Wilding, L.P., N. E. Smeck and G. F. Hall. 1983a. Pedogenesis and soil taxonomy: I Concepts and interactions. *Developments in Soil Science*. Elsevier. 11A.
- Wilding, L.P., N. E. Smeck and G. F. Hall. 1983b. Pedogenesis and soil taxonomy: II The Soil orders. *Developments in Soil Science*. Elsevier. 11B.

Appendix

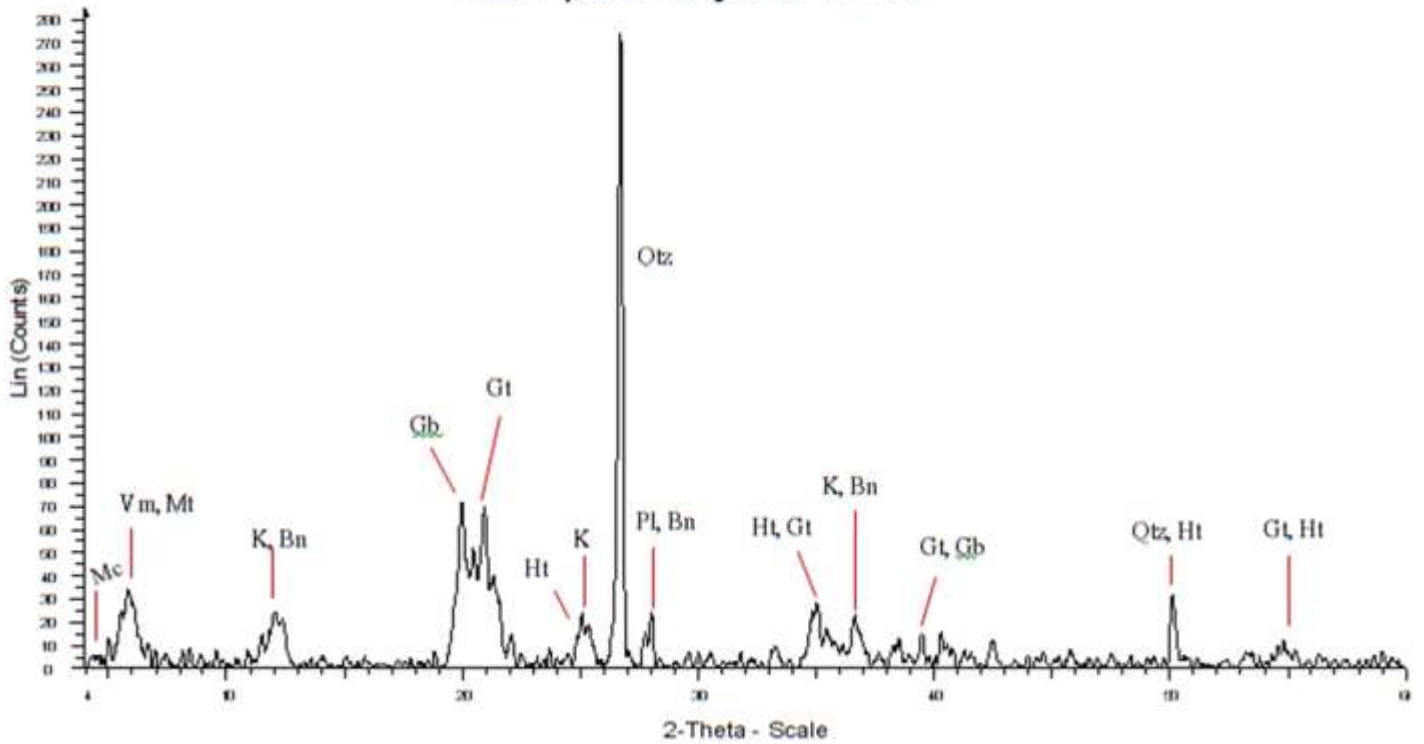
Appendix 1: Availability Index suggested for soils cations extracted by the ammonium acetate method Central Analytical Laboratory of the Agricultural Experiment Station

Availability Index for cations in ammonium acetate			
	Potassium	Calcium	Magnesium
Low	<150 ppm <0.4 cmol _c /kg	<1,000 ppm <5.0 cmol _c /kg	<60 ppm <0.5 cmol _c /kg
Medium	150 – 250 ppm 0.4 – 0.6 cmol _c /kg	1,000 – 2,000 ppm 5 – 10 cmol _c /kg	60 – 180 ppm 0.5 – 1.5 cmol _c /kg
High	250 – 800 ppm 0.6 – 2.0 cmol _c /kg	>2,000 ppm >10 cmol _c /kg	>180 ppm >1.5 cmol _c /kg
Excessive	>800 ppm >2.0 cmol _c /kg	—————	—————

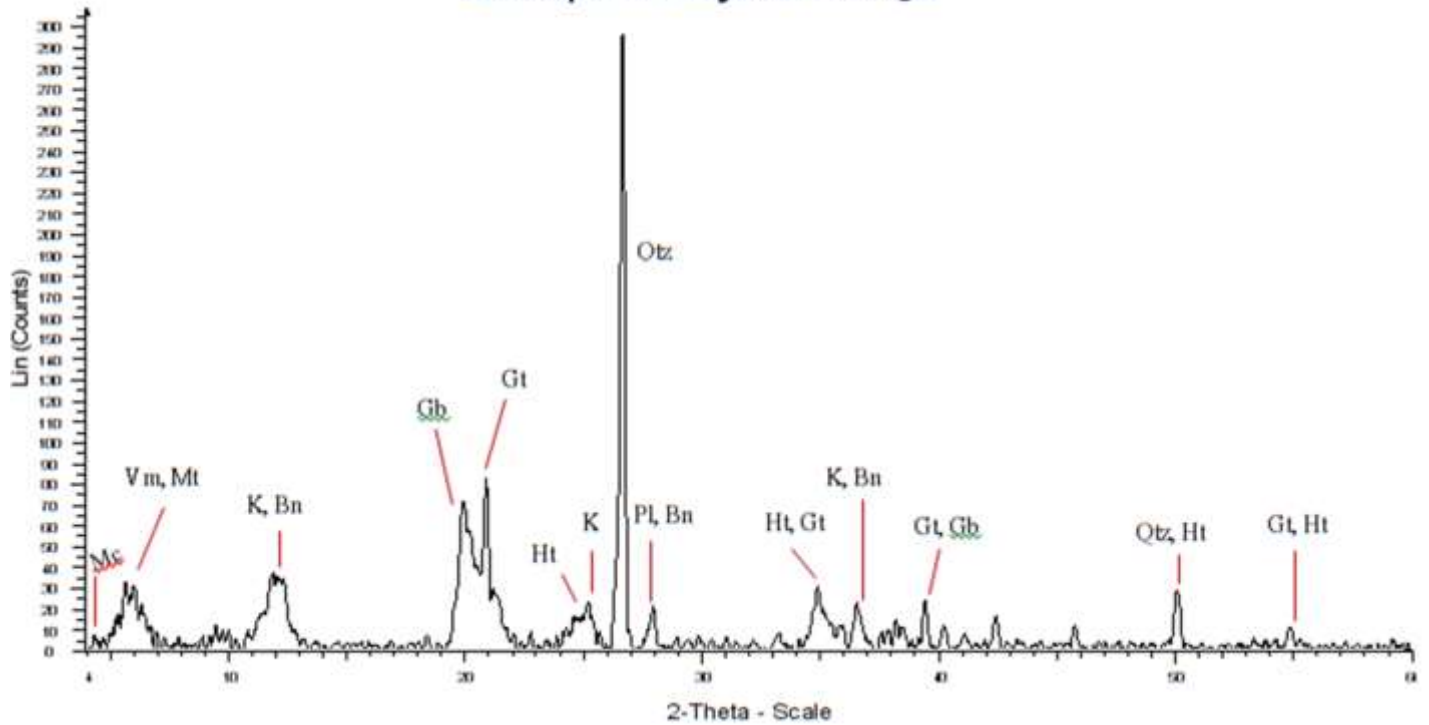
Appendix 2: X-ray diffraction results



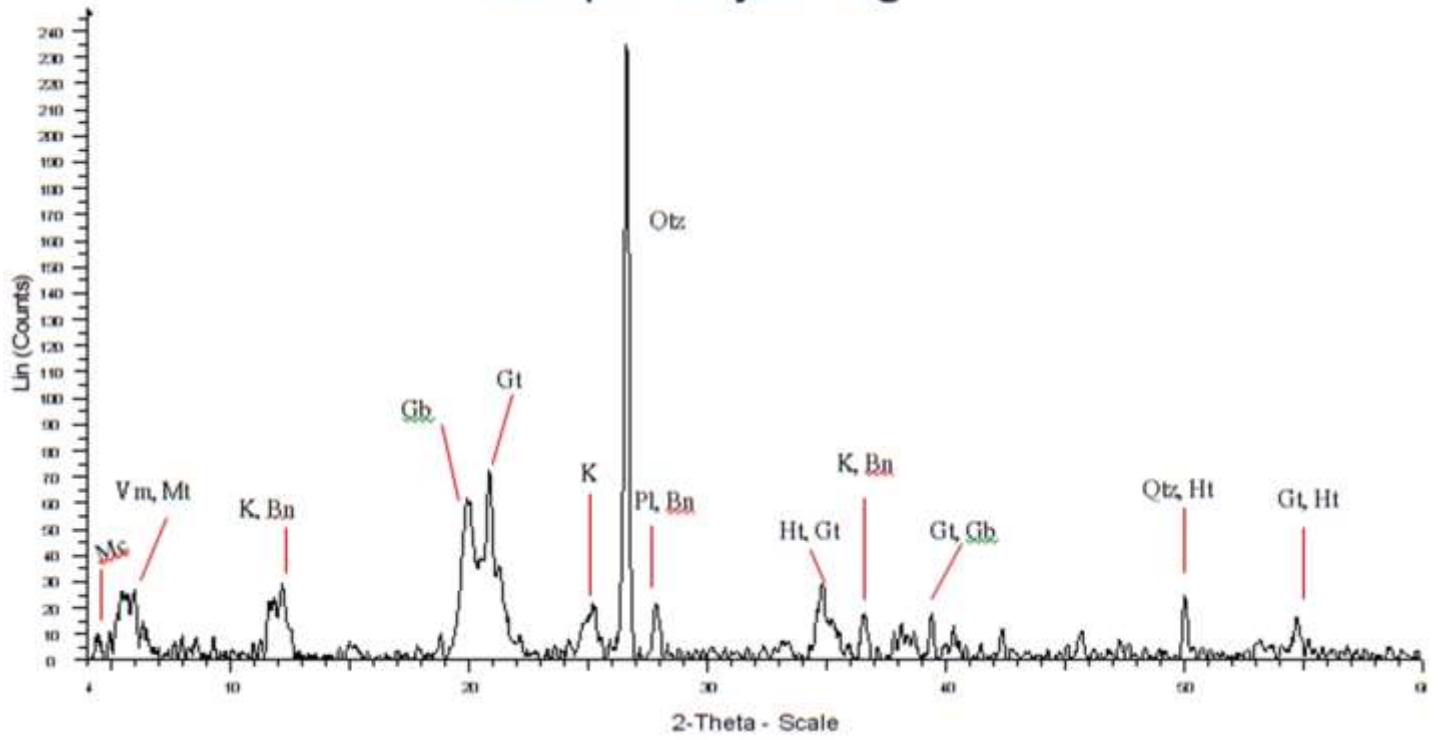
Sample: Bajura- Bwg1



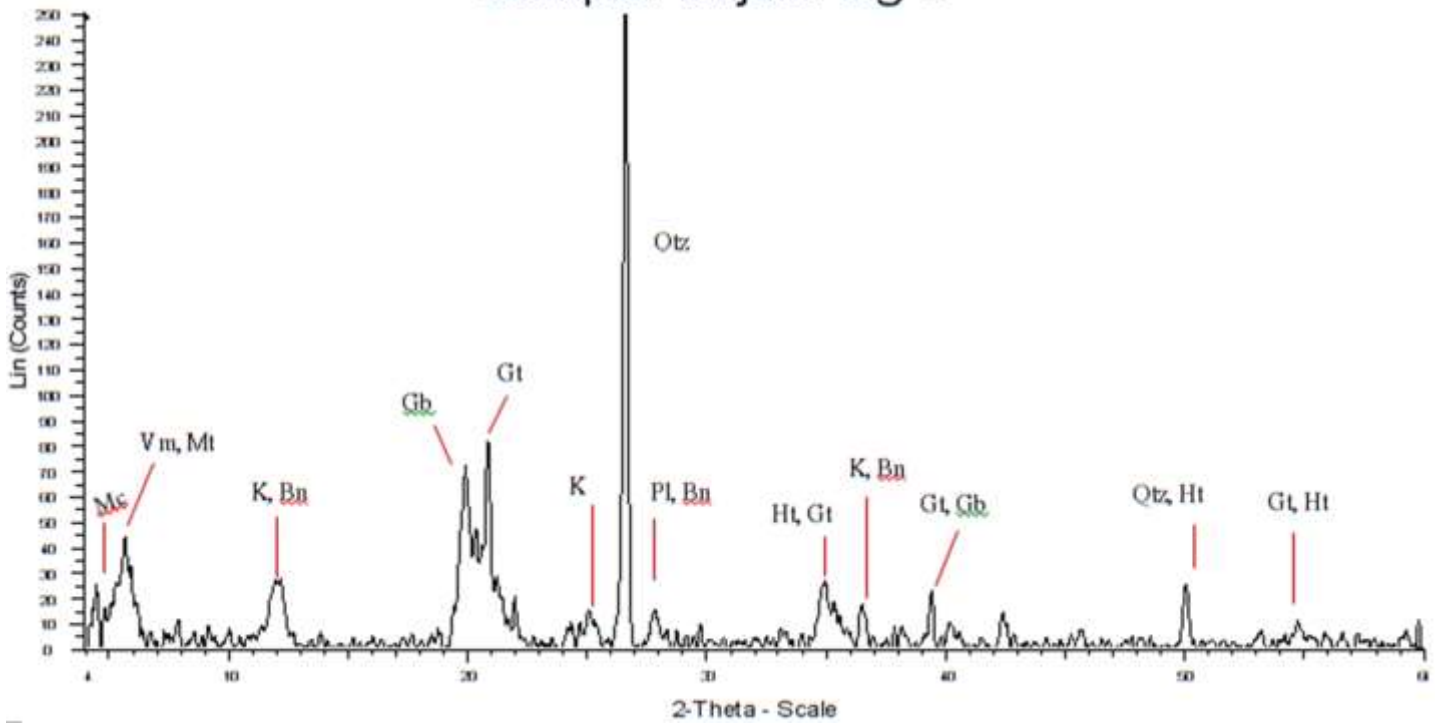
Sample: Bajura- Bwg2



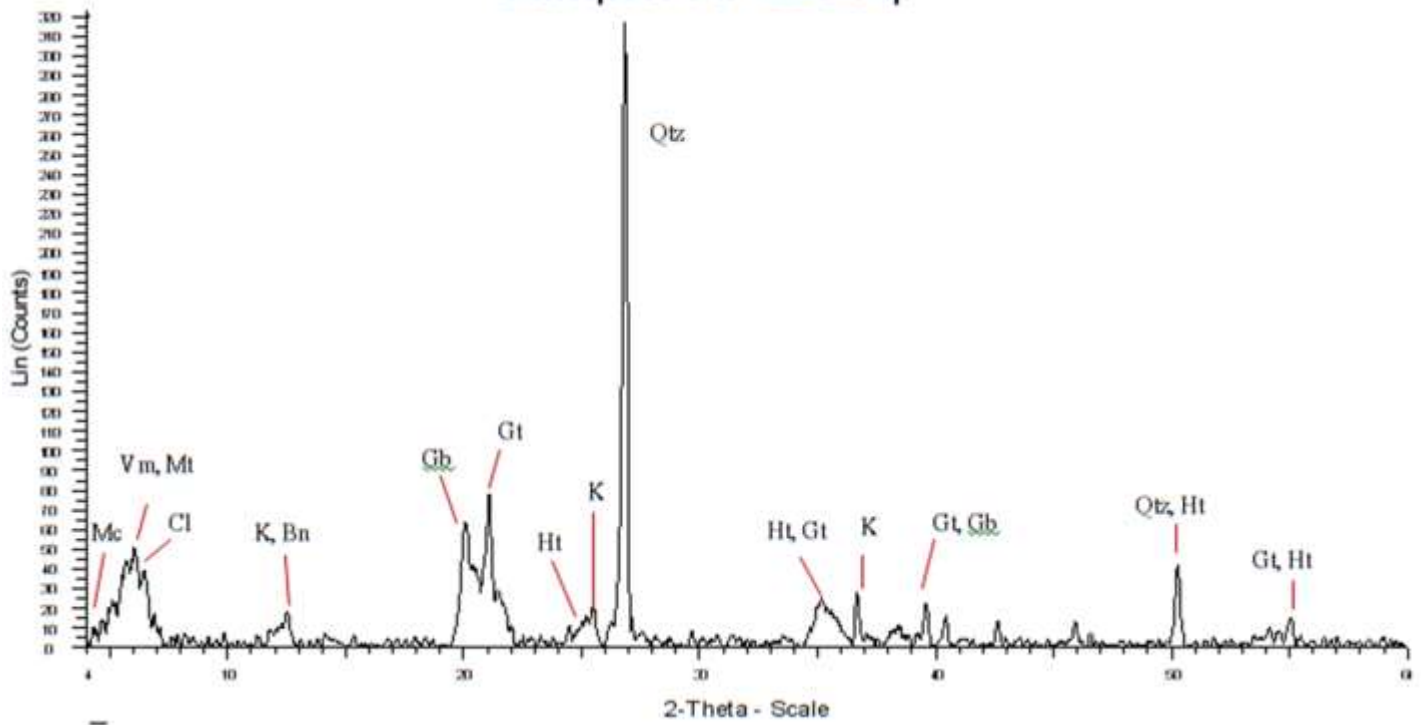
Sample: Bajura-Cg-1



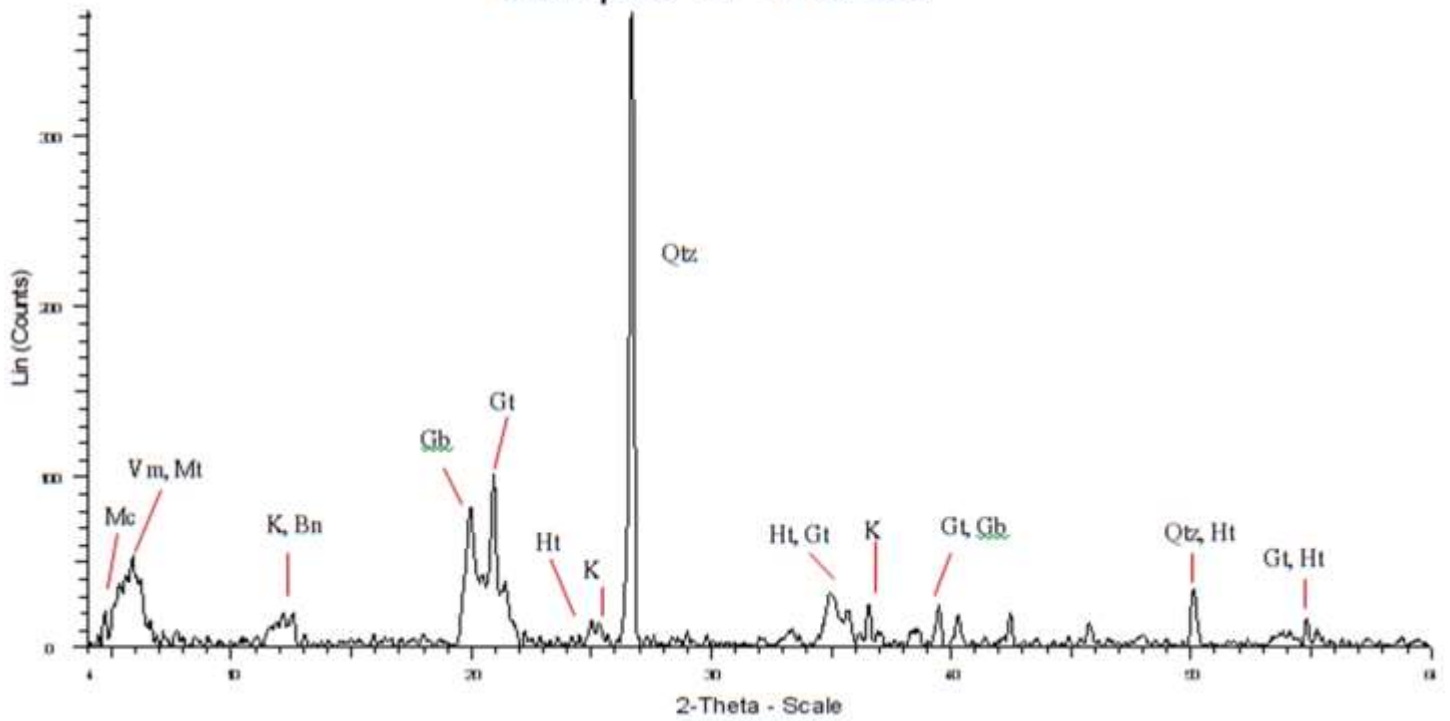
Sample: Bajura-Cg-2



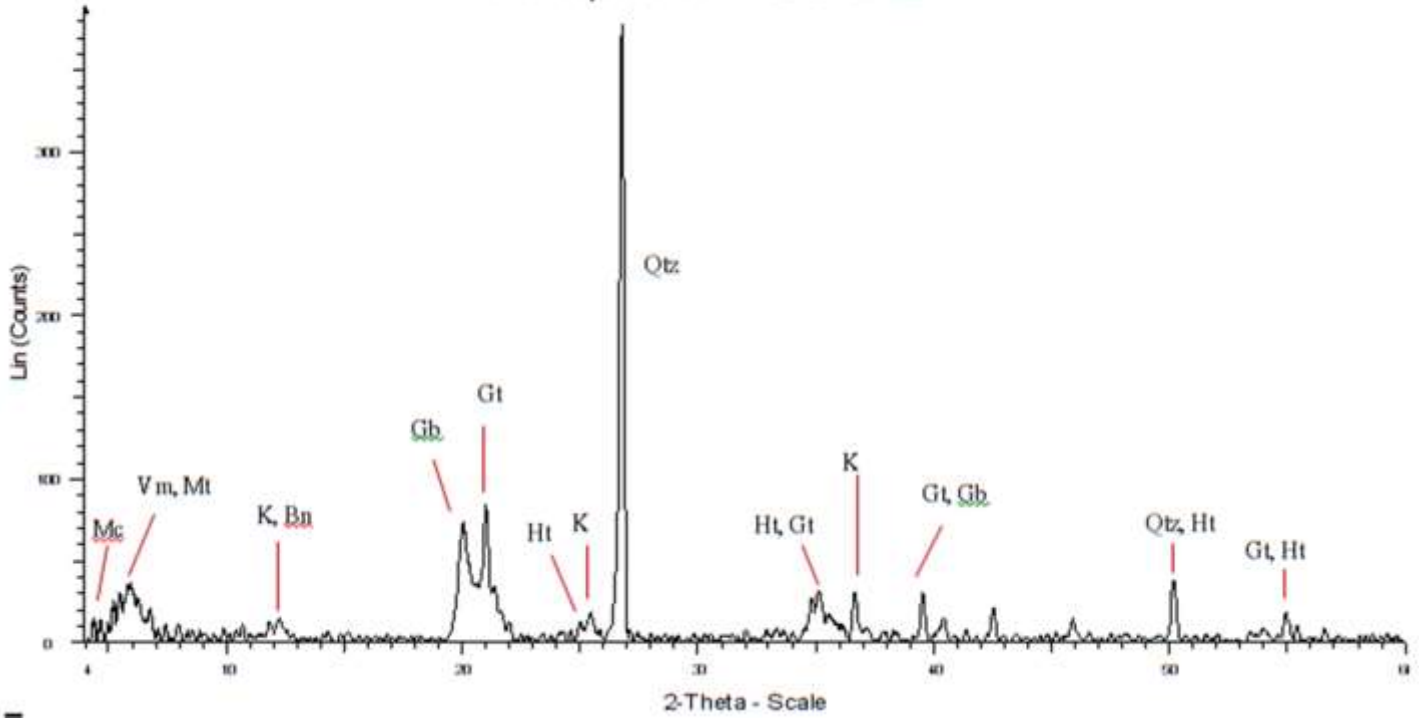
Sample: RP-BS-Ap



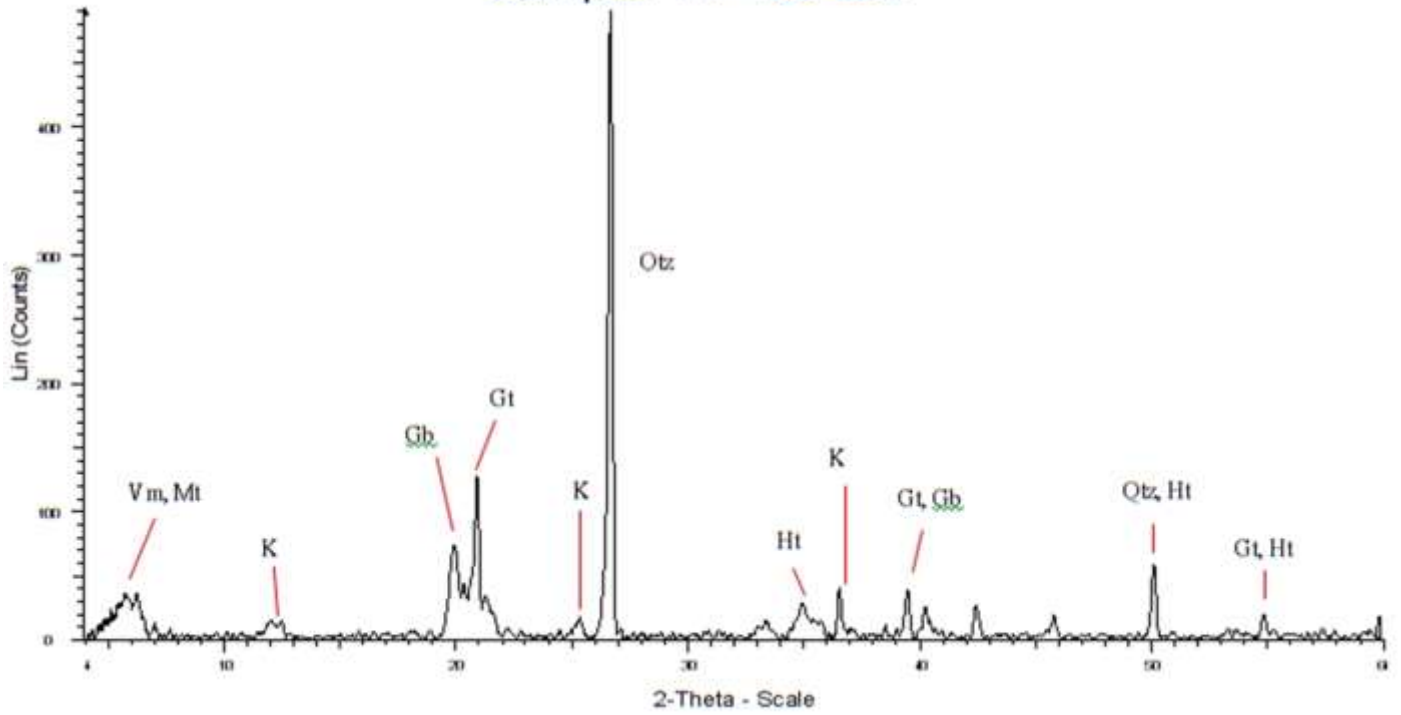
Sample: RP-BS-Bt1



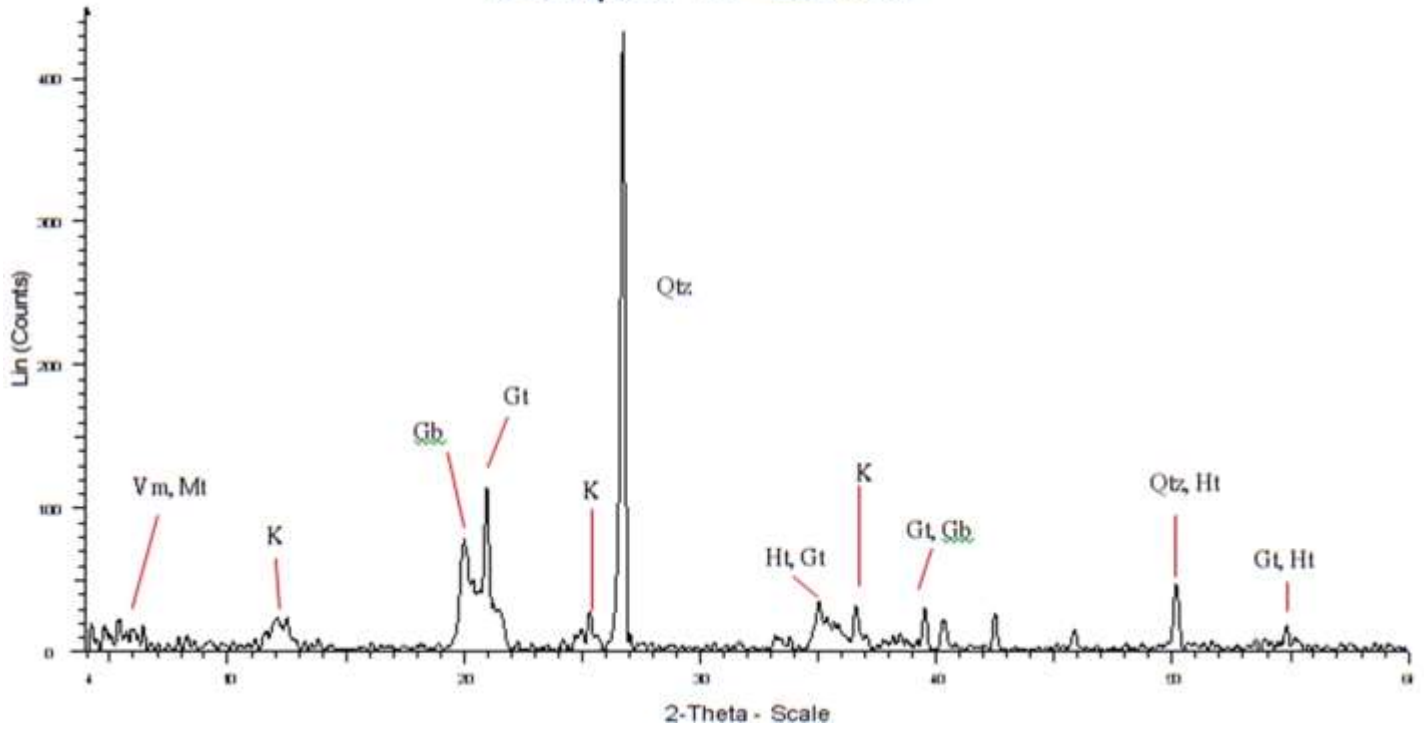
Sample: RP-BS-Bt2



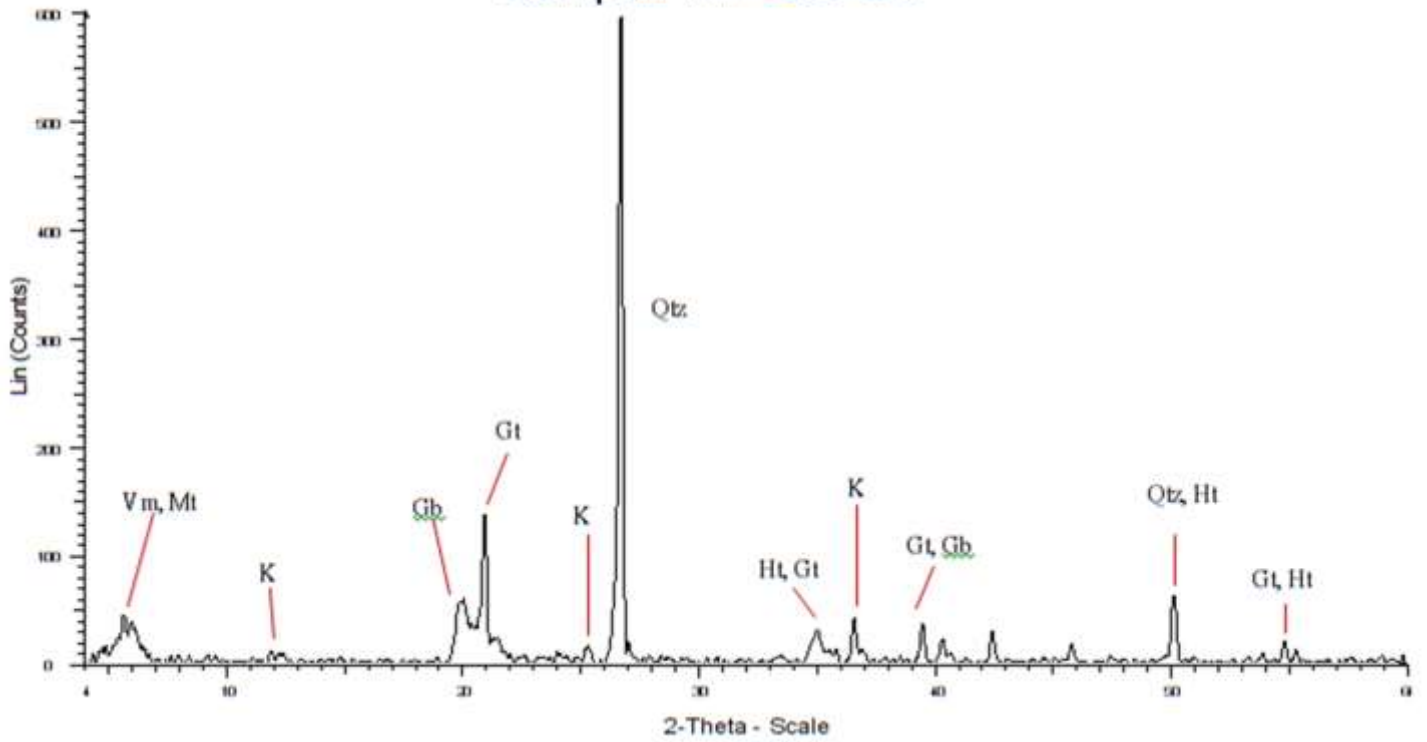
Sample: RP-BS-BC



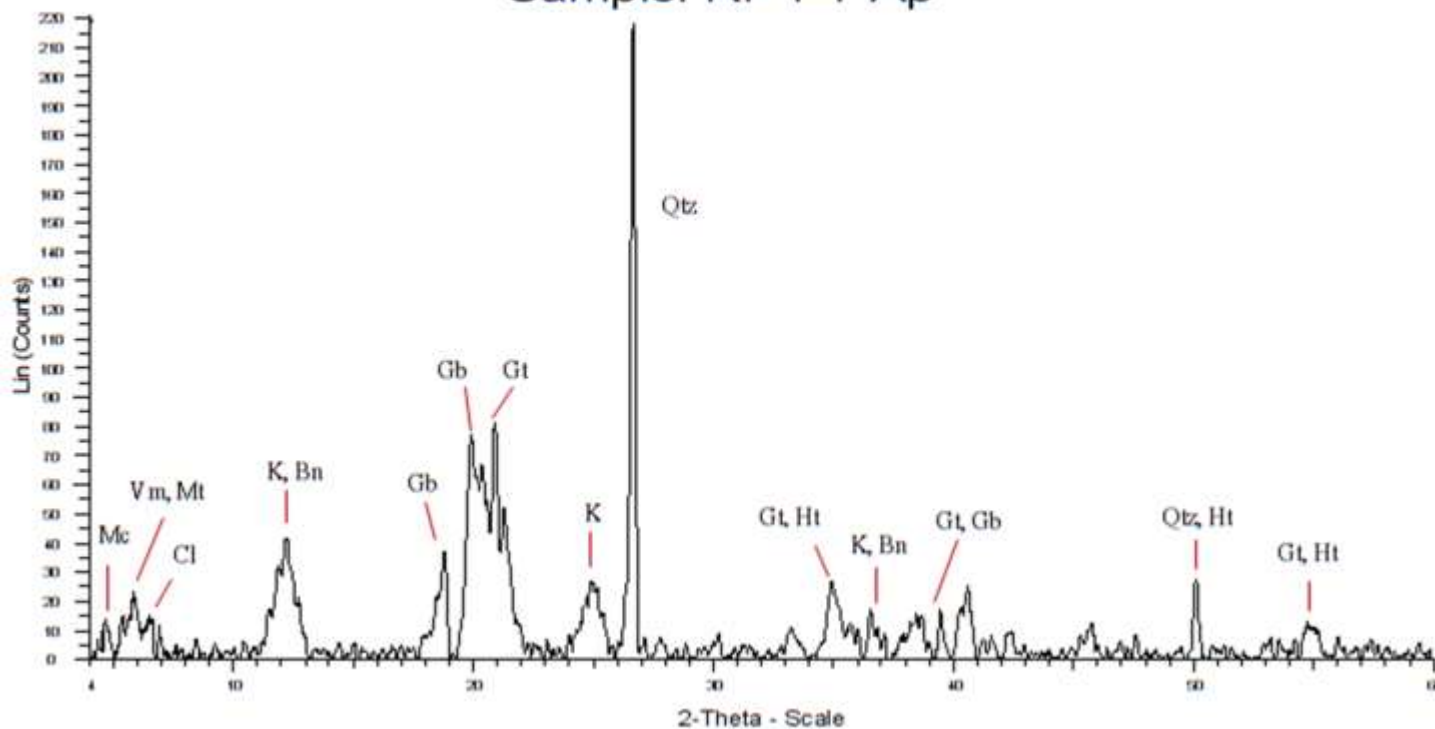
Sample: RP-BS-C1



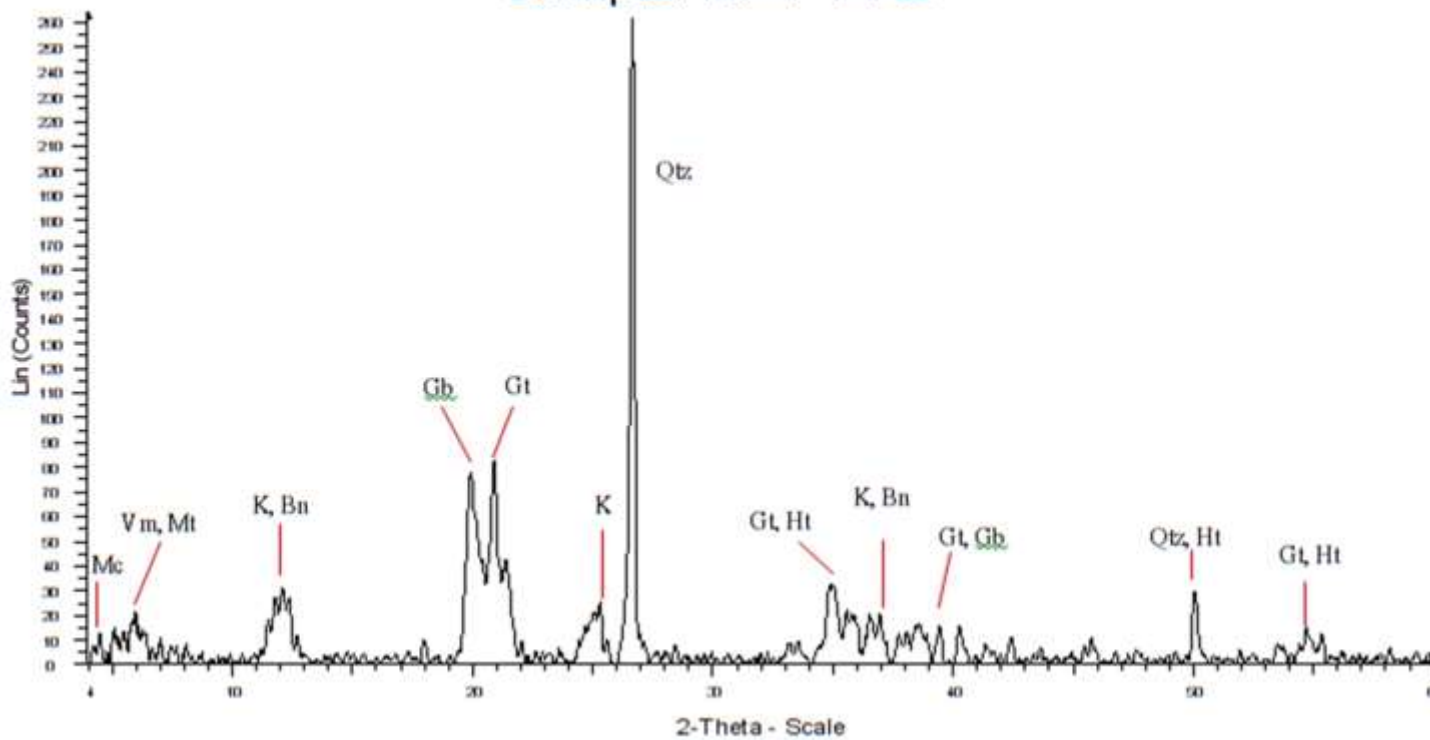
Sample: RP-BS-C2



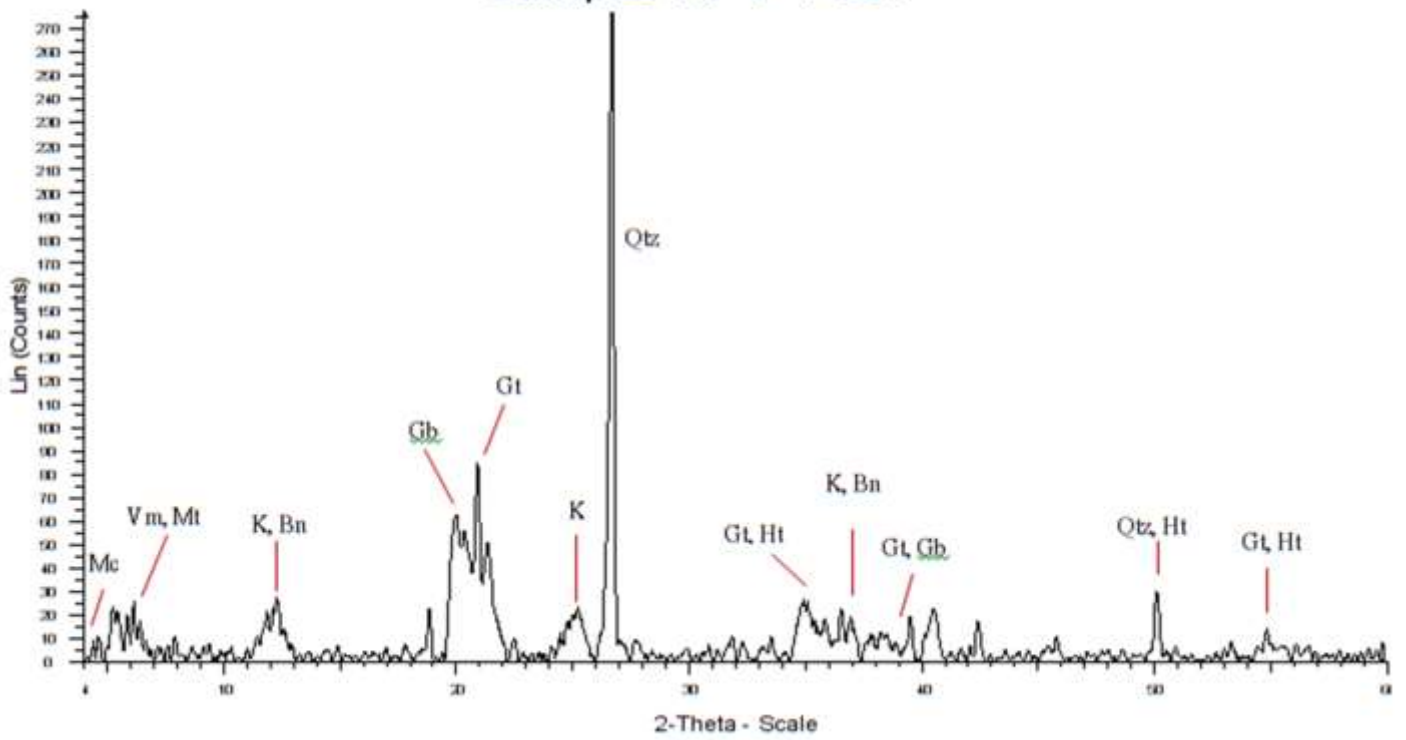
Sample: RP-FT-Ap



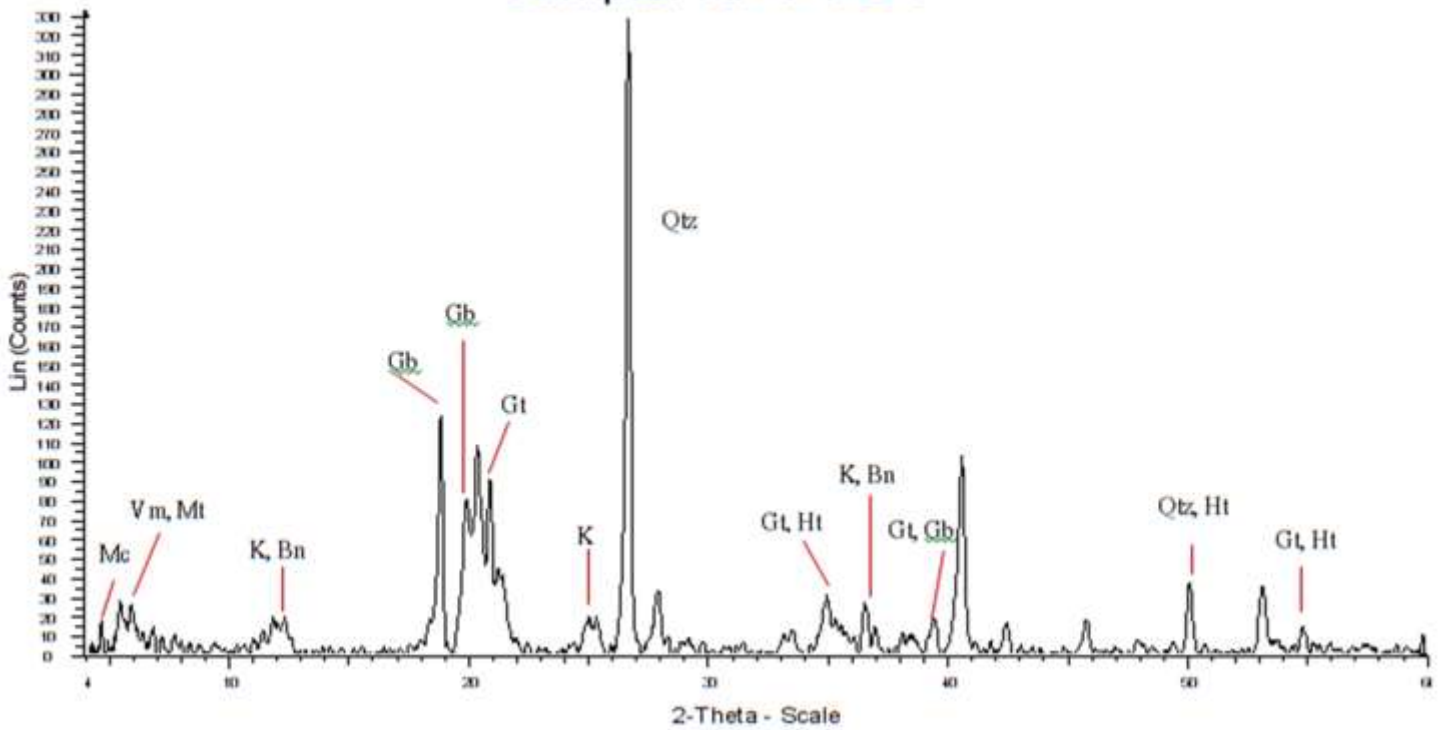
Sample: RP-FT-AB



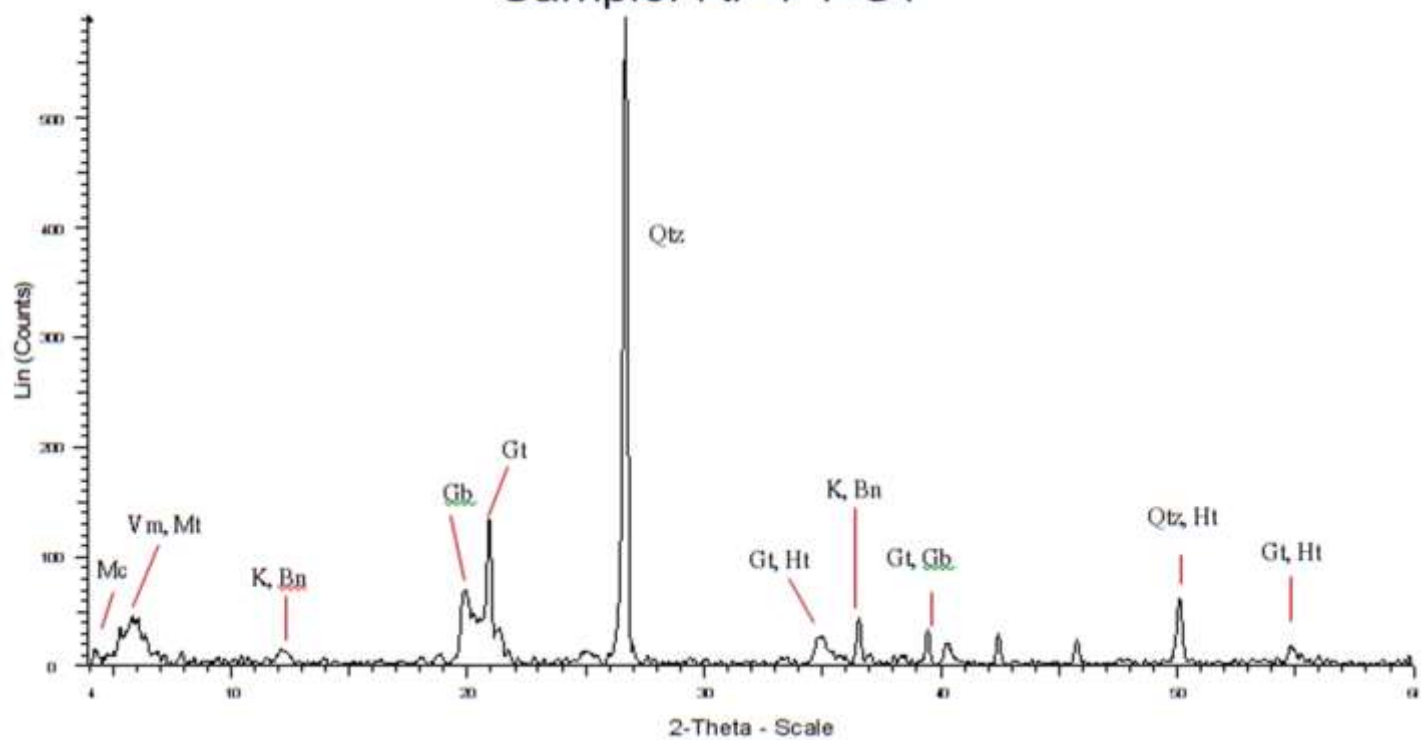
Sample: RP-FT-Bt1



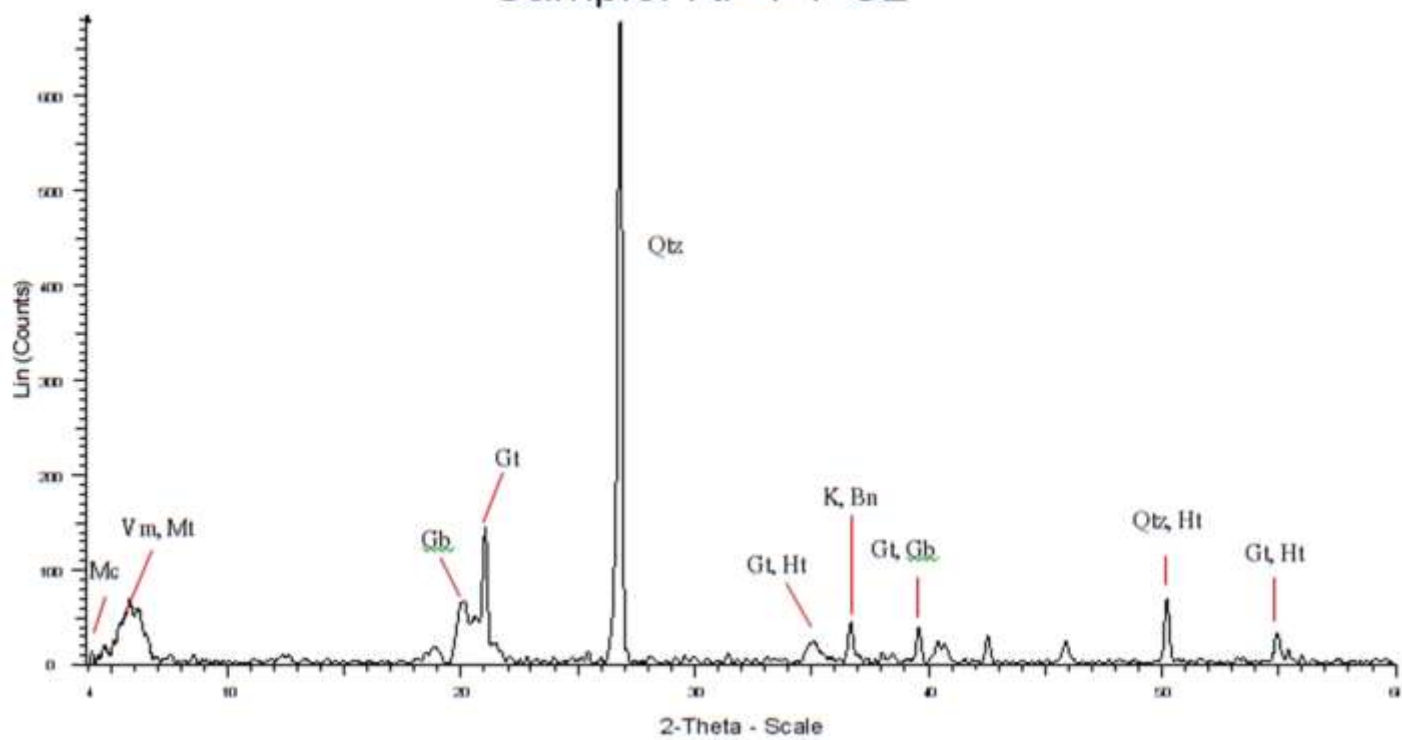
Sample: RP-FT-BC



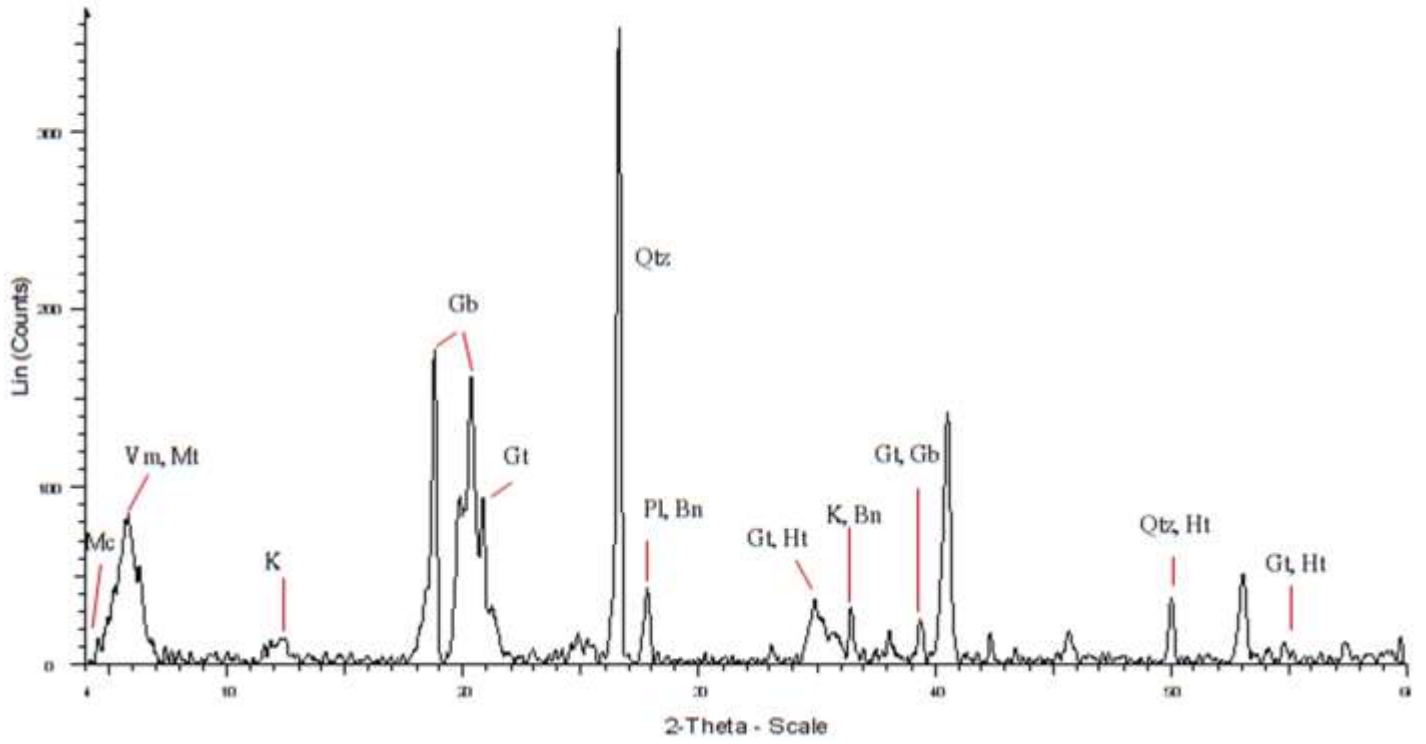
Sample: RP-FT-C1



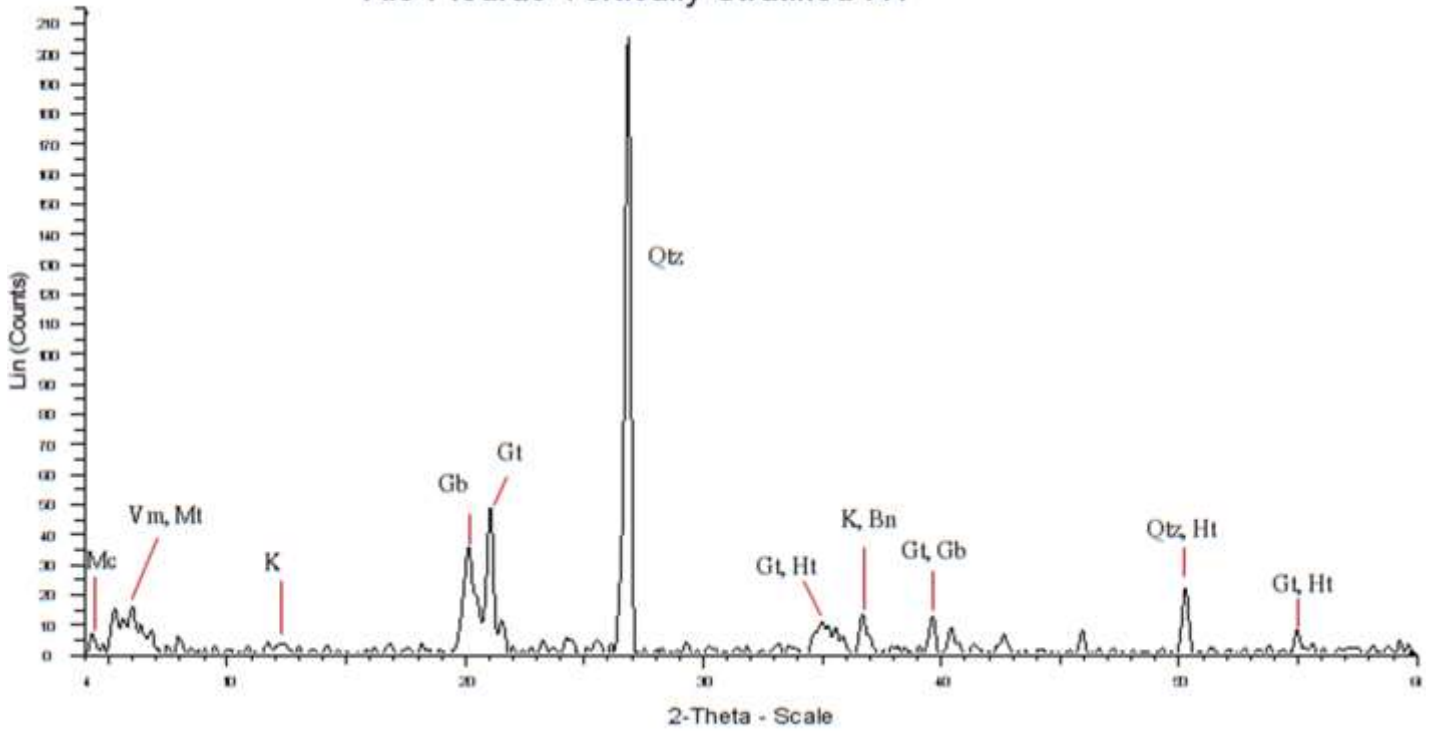
Sample: RP-FT-C2



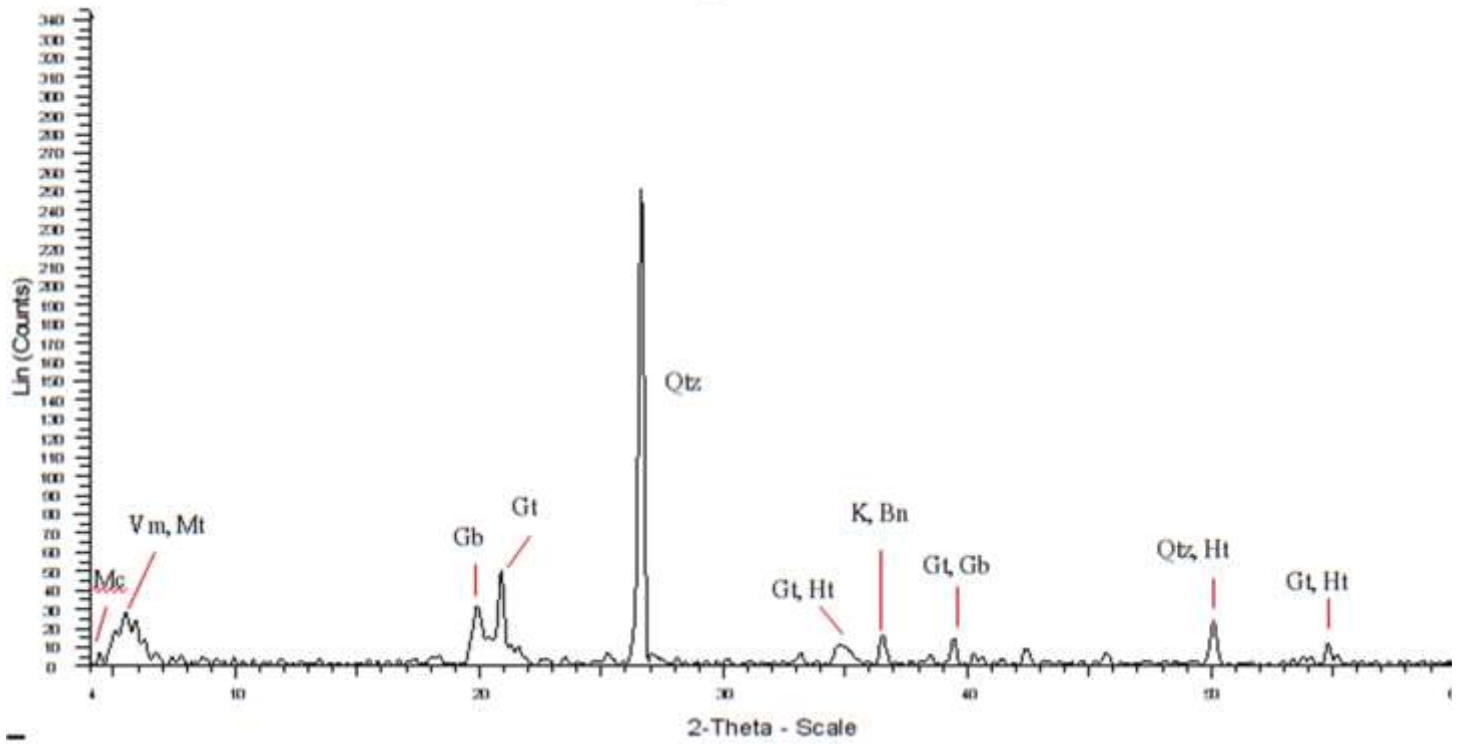
RP FT Saprolite



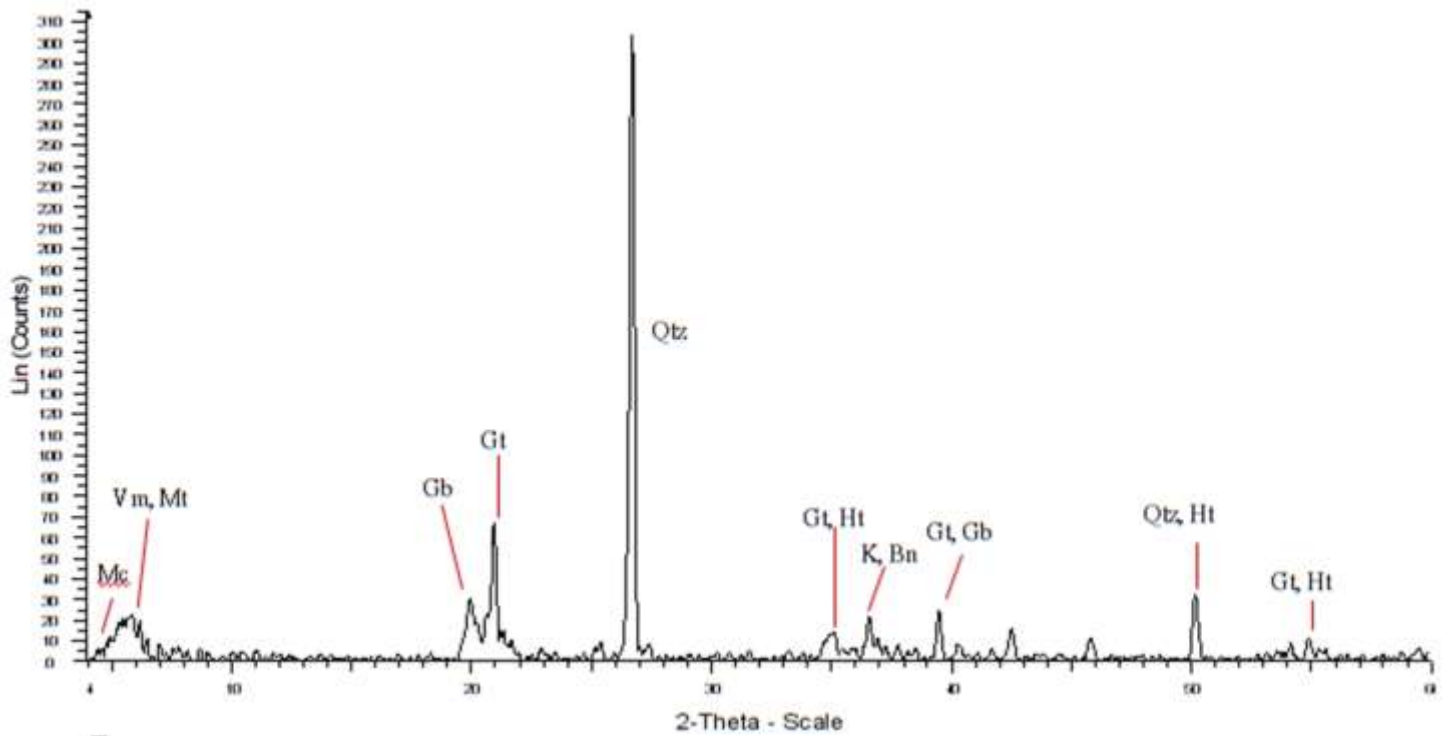
Rio Piedras Vertically Stratified A1



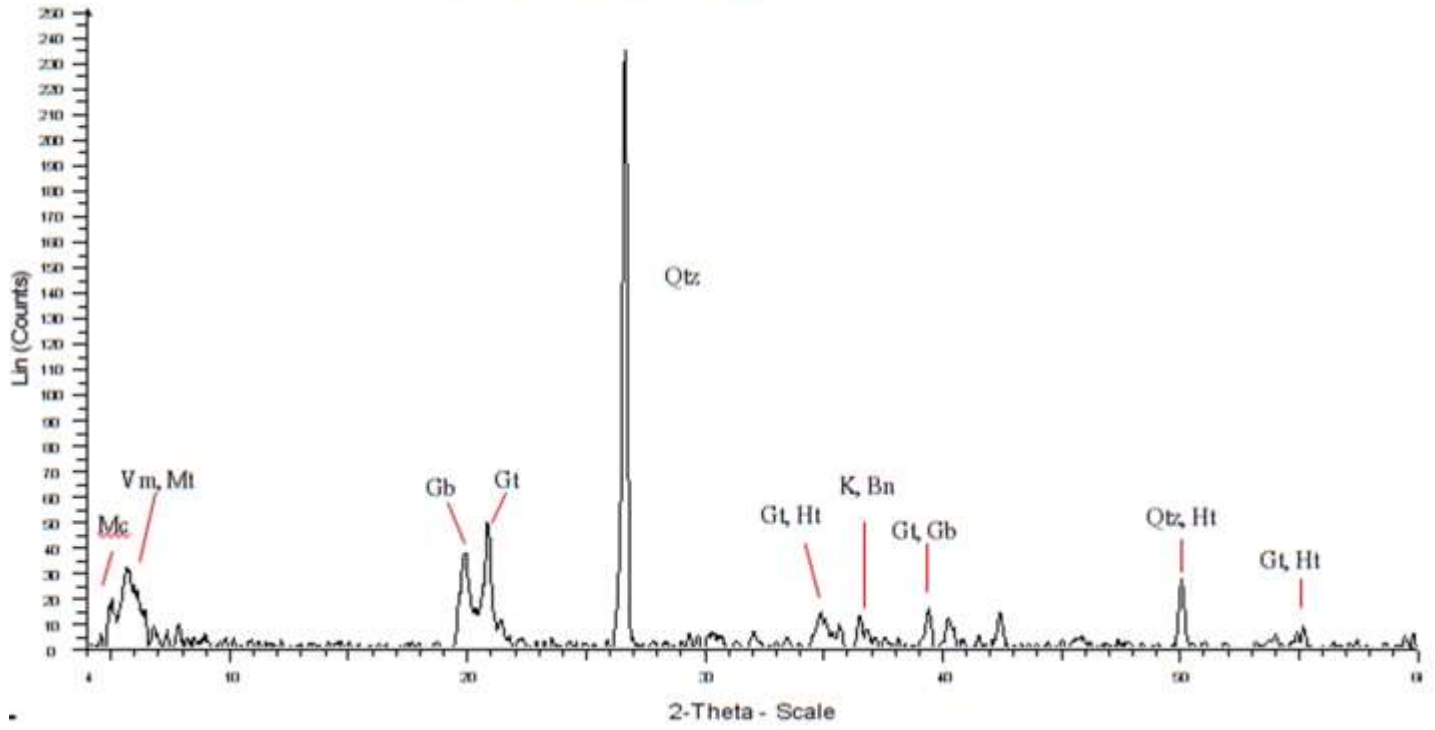
Rio Piedras Vertically Stratified A2



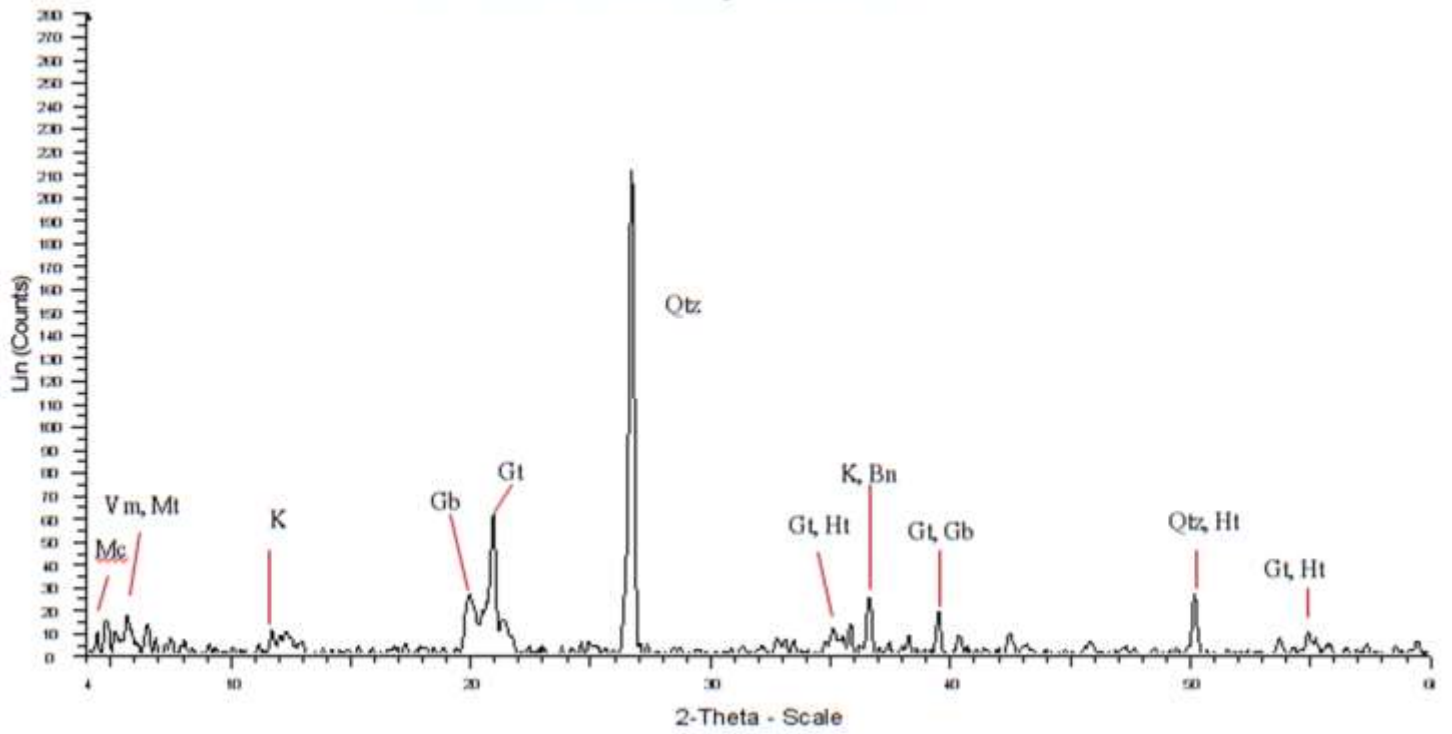
Rio Piedras Vertically Stratified A3



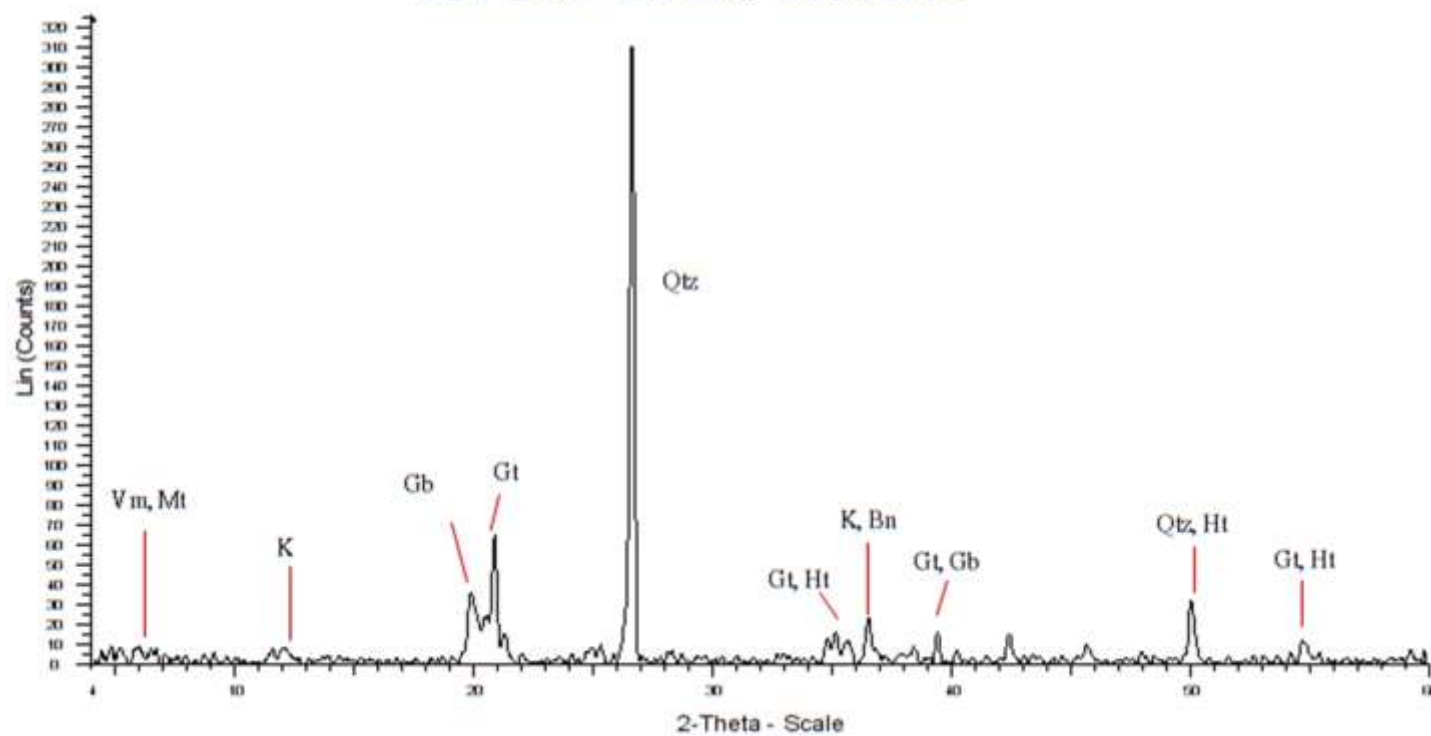
Rio Piedras Vertically Stratified A4



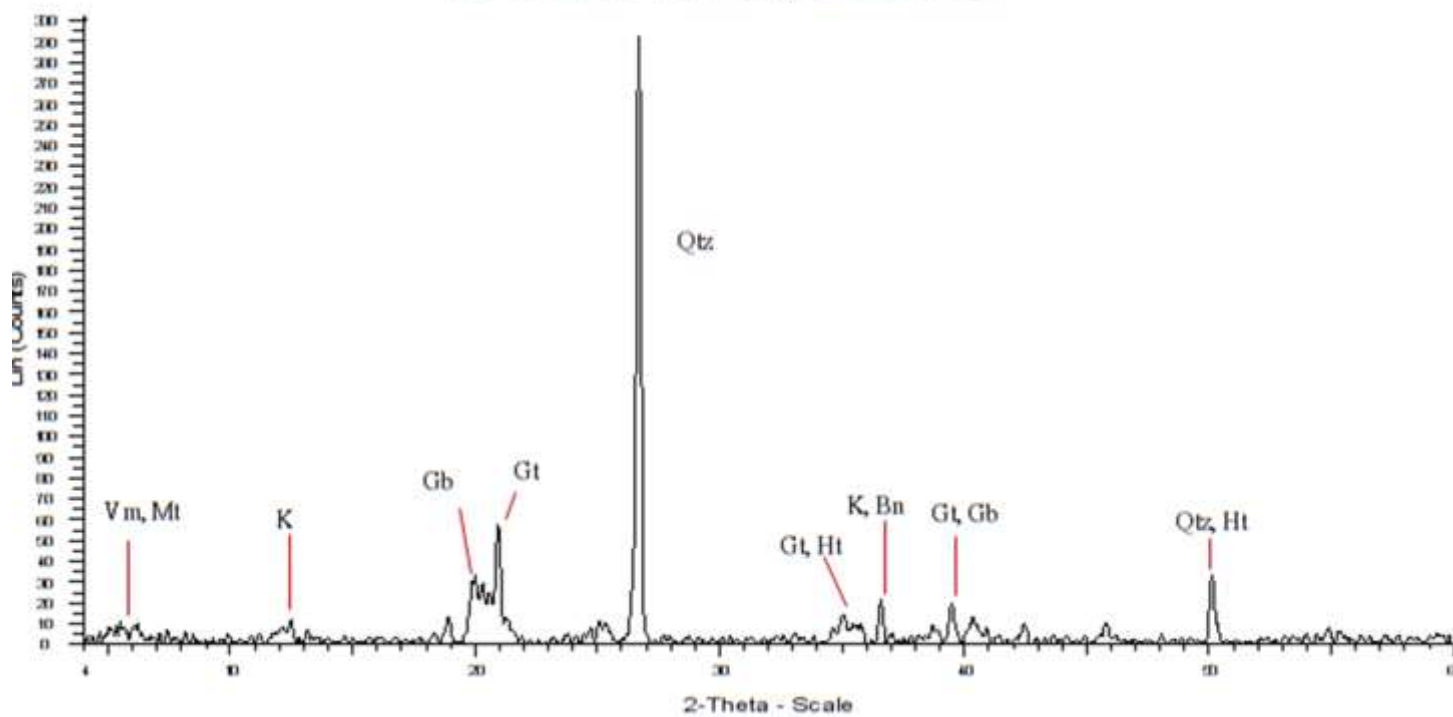
Rio Piedras Vertically Stratified B1



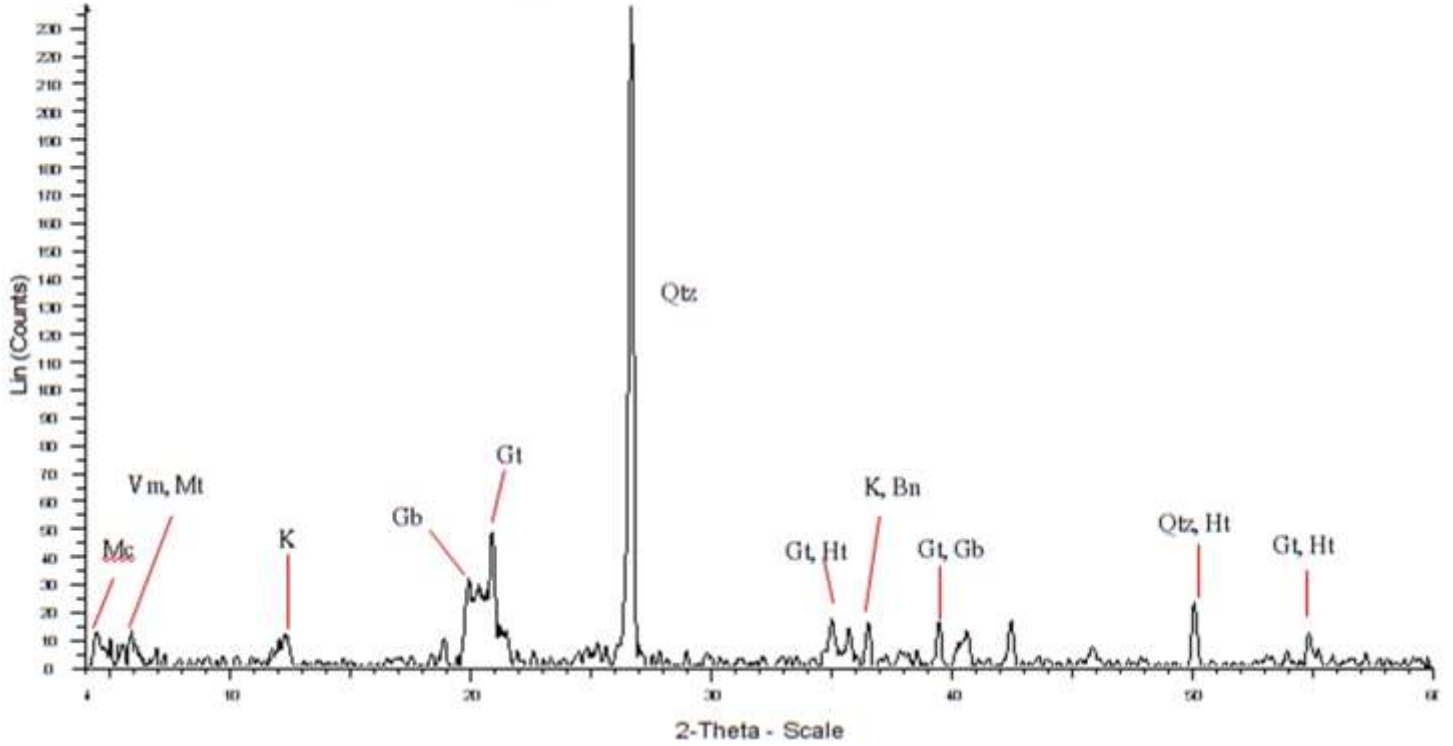
Rio Piedras Vertically Stratified B2



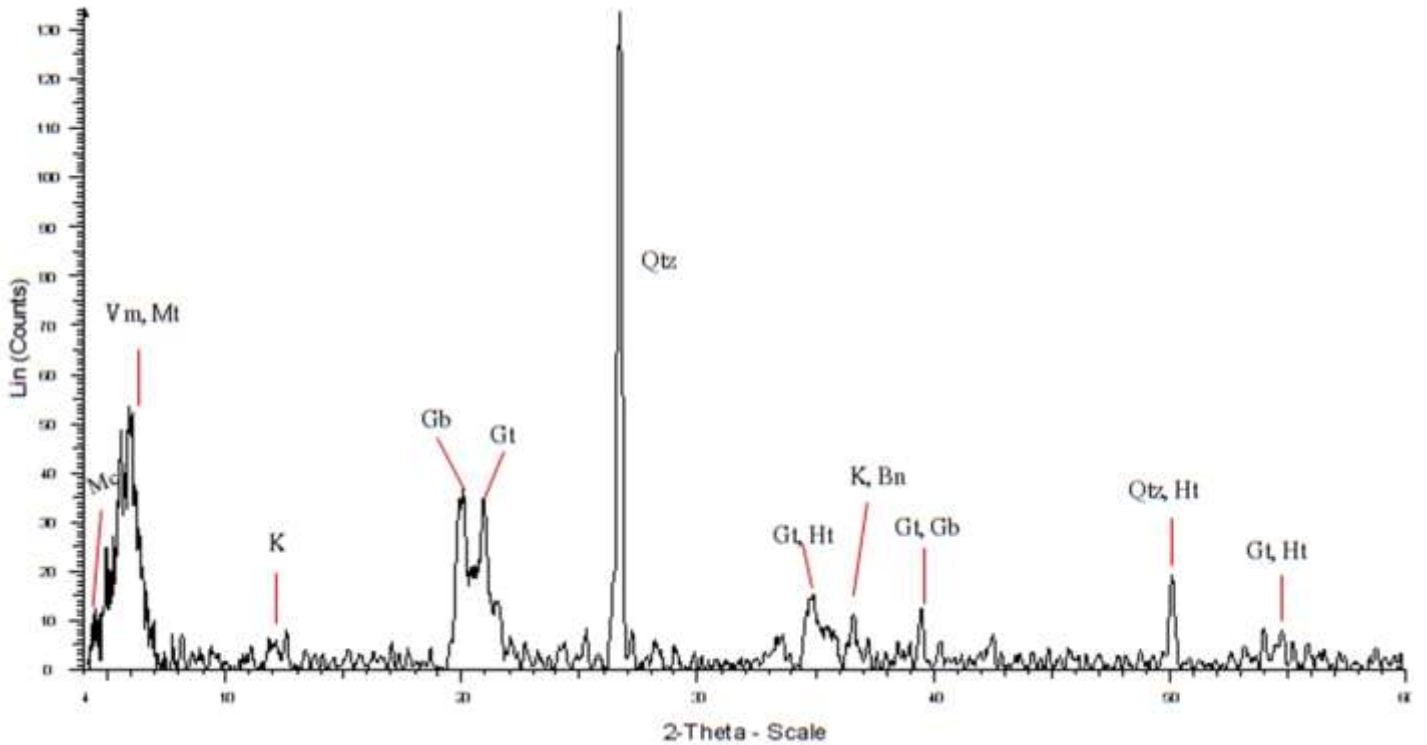
Rio Piedras Vertically Stratified B3



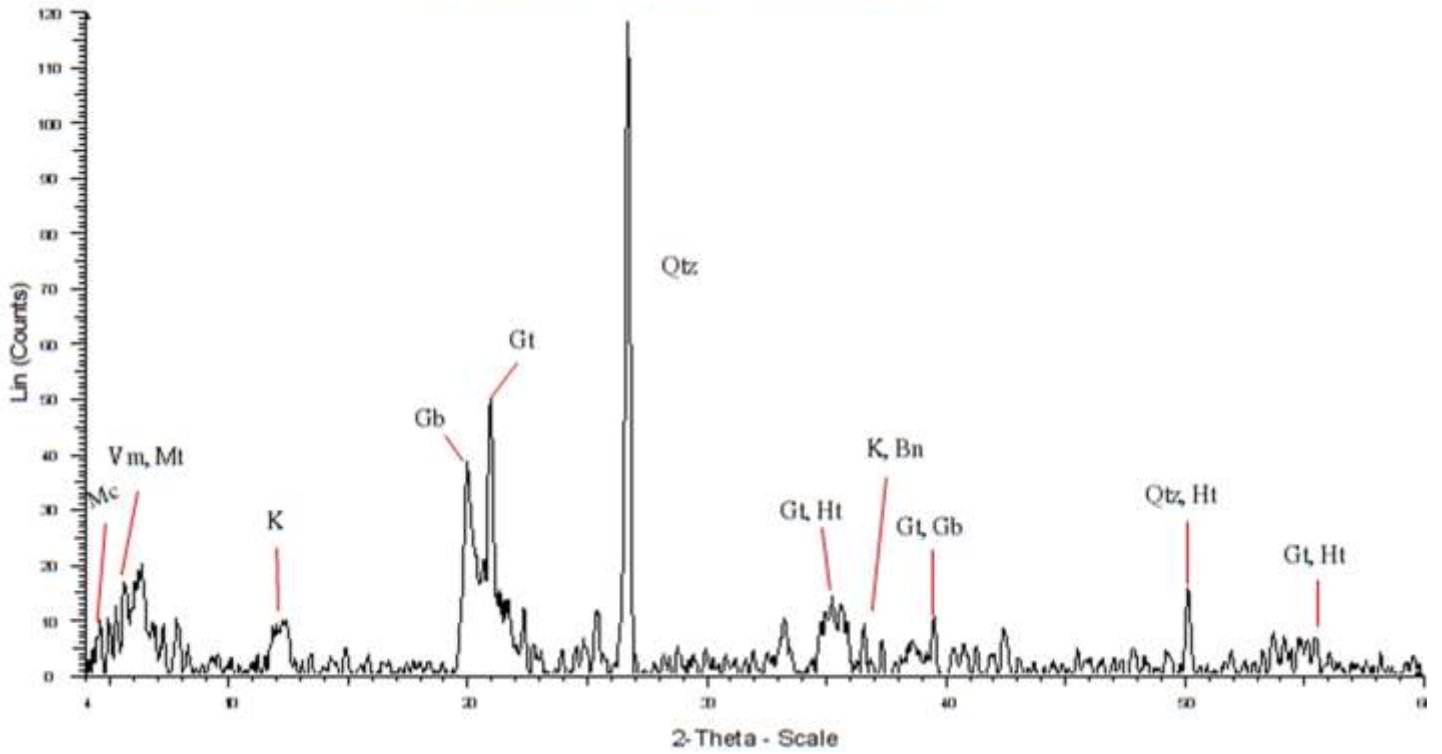
Rio Piedras Vertically Stratified B4



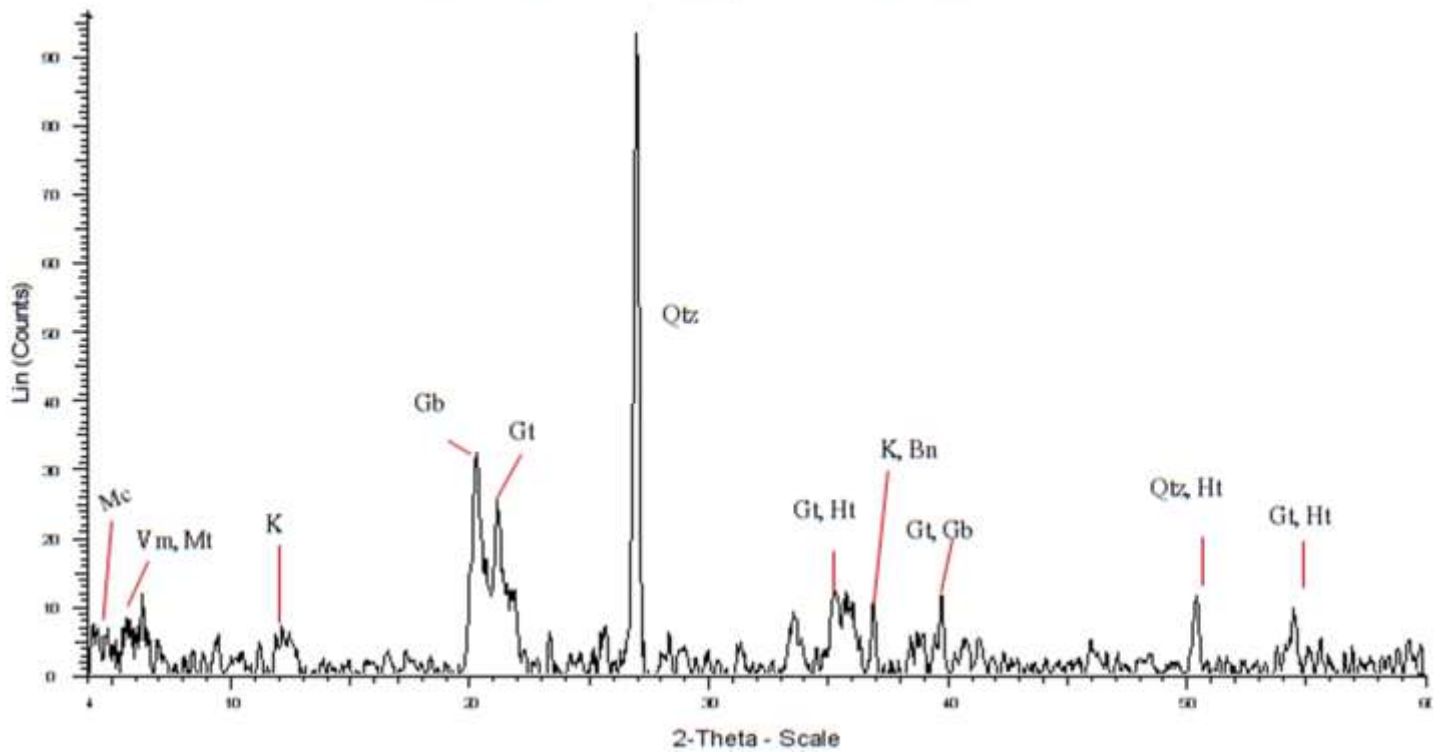
Rio Piedras Vertically Stratified CTop



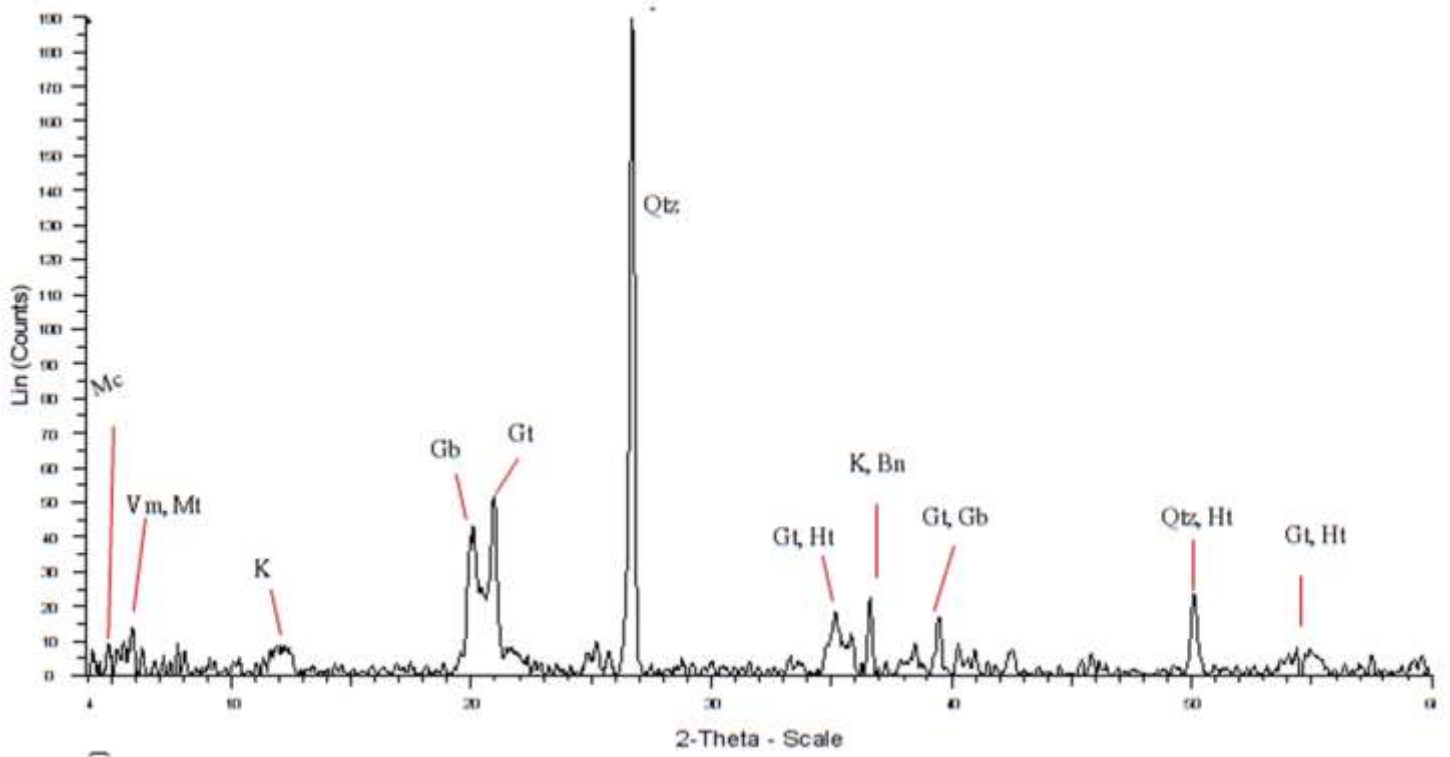
Rio Piedras Vertically Stratified C1



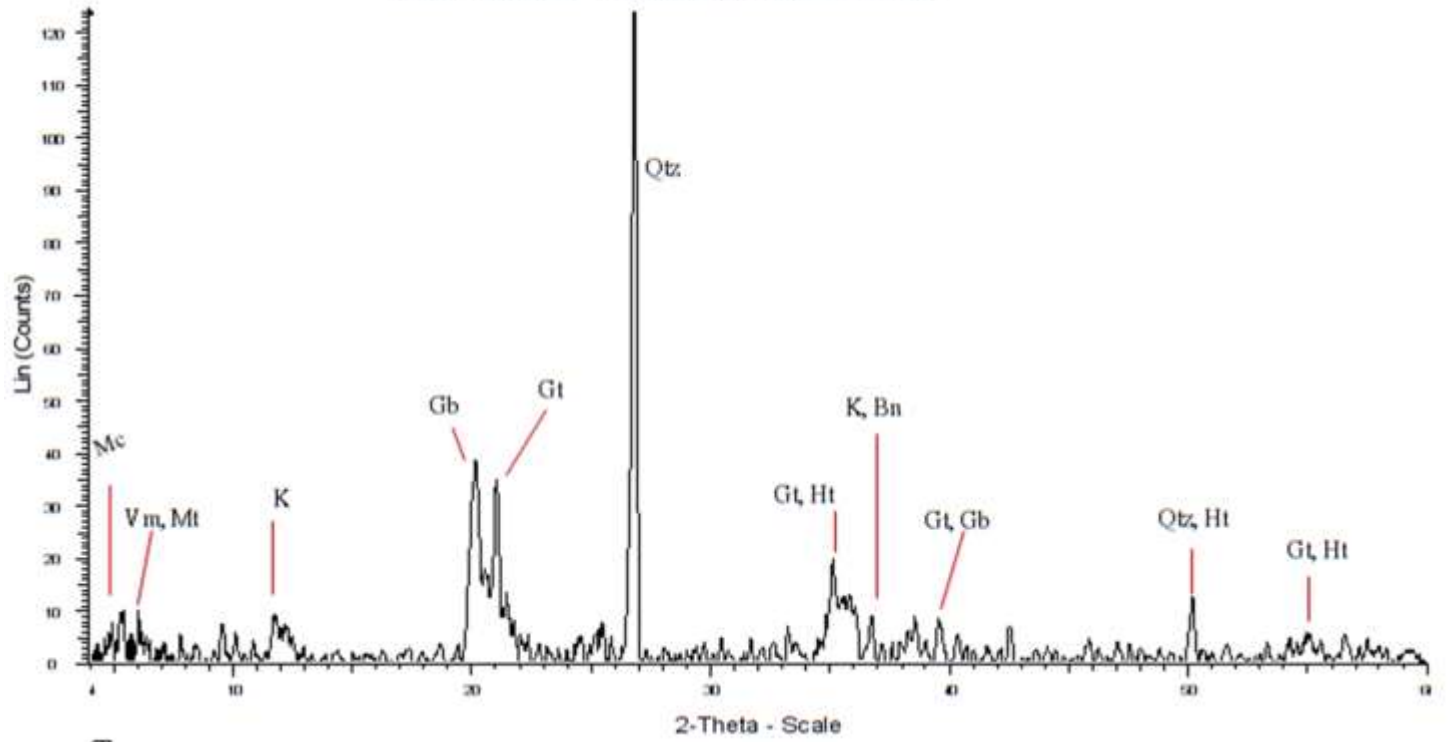
Rio Piedras Vertically Stratified C2



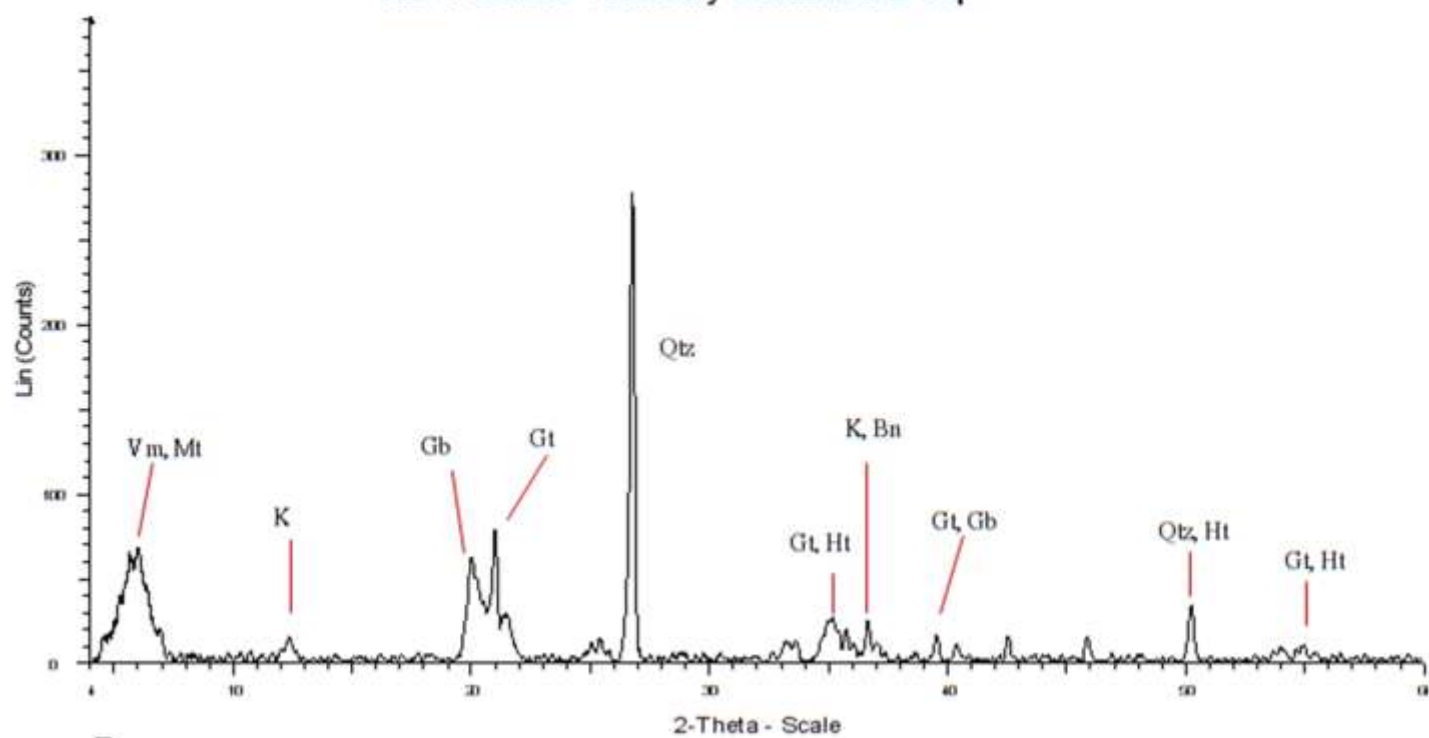
Rio Piedras Vertically Stratified C3



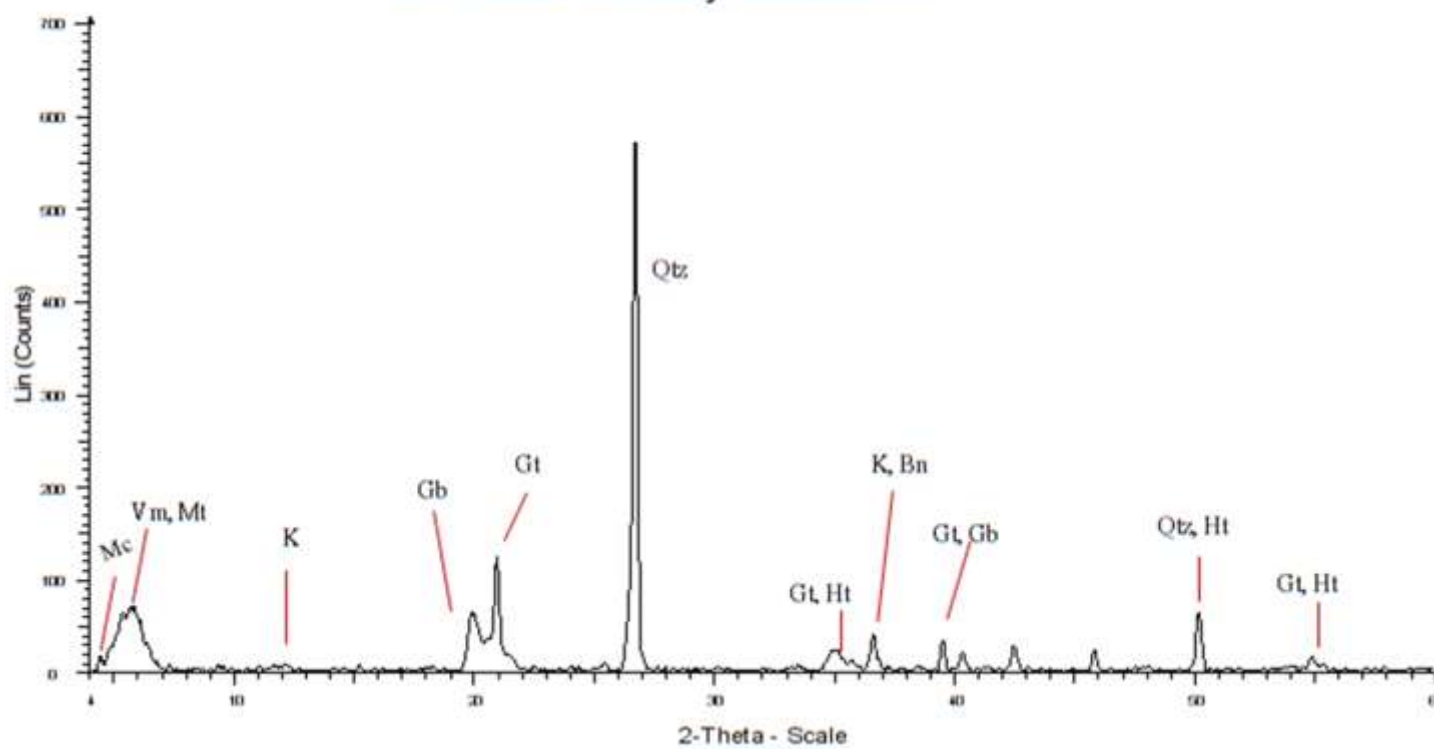
Rio Piedras Vertically Stratified C4



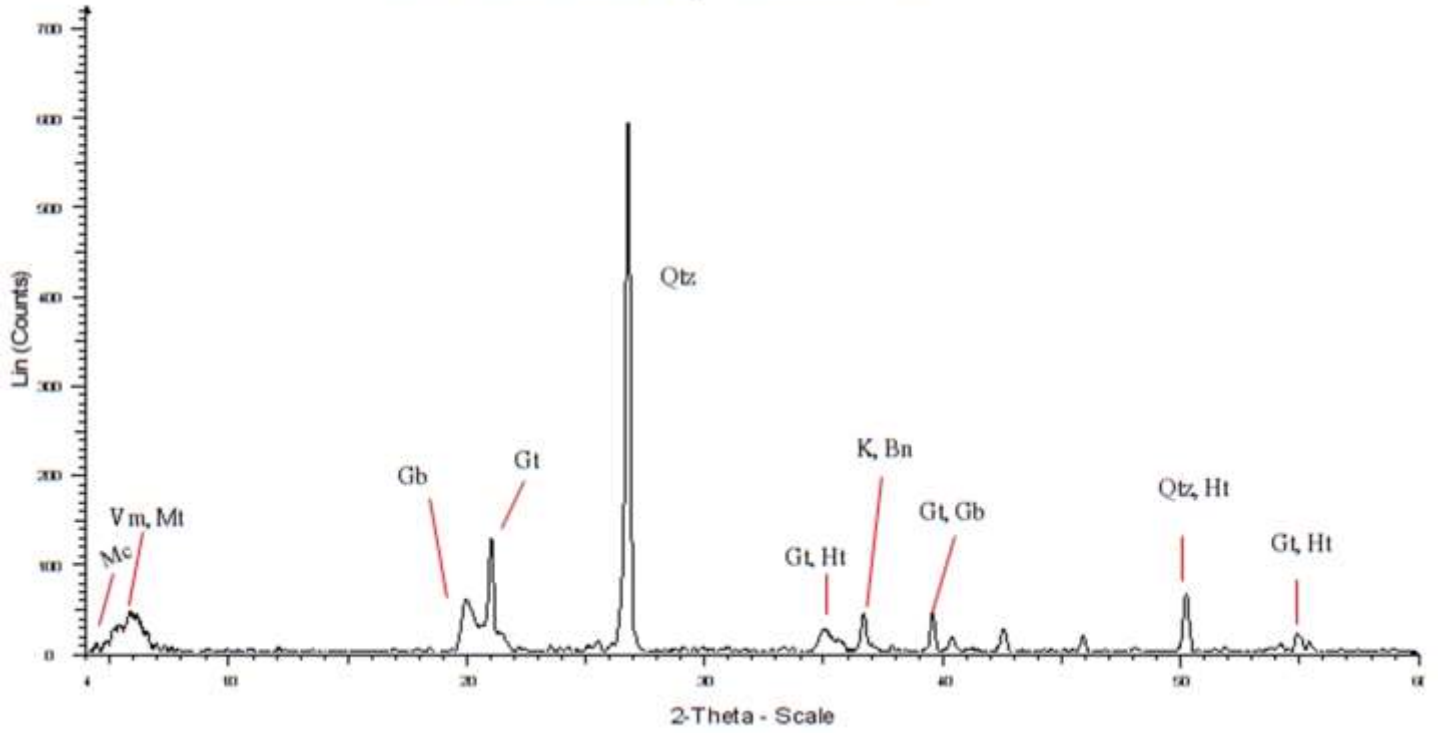
Rio Piedras Vertically Stratified DTop



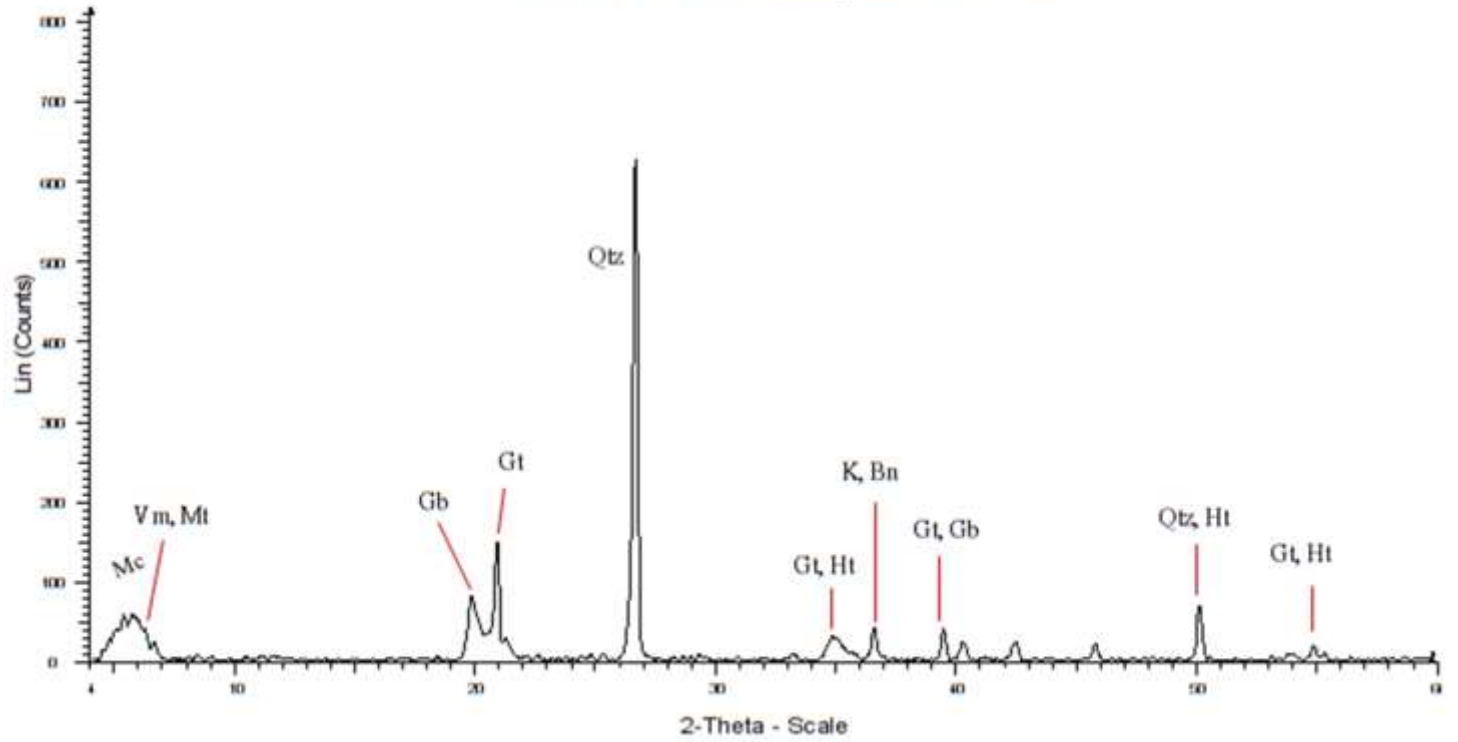
Rio Piedras Vertically Stratified D1



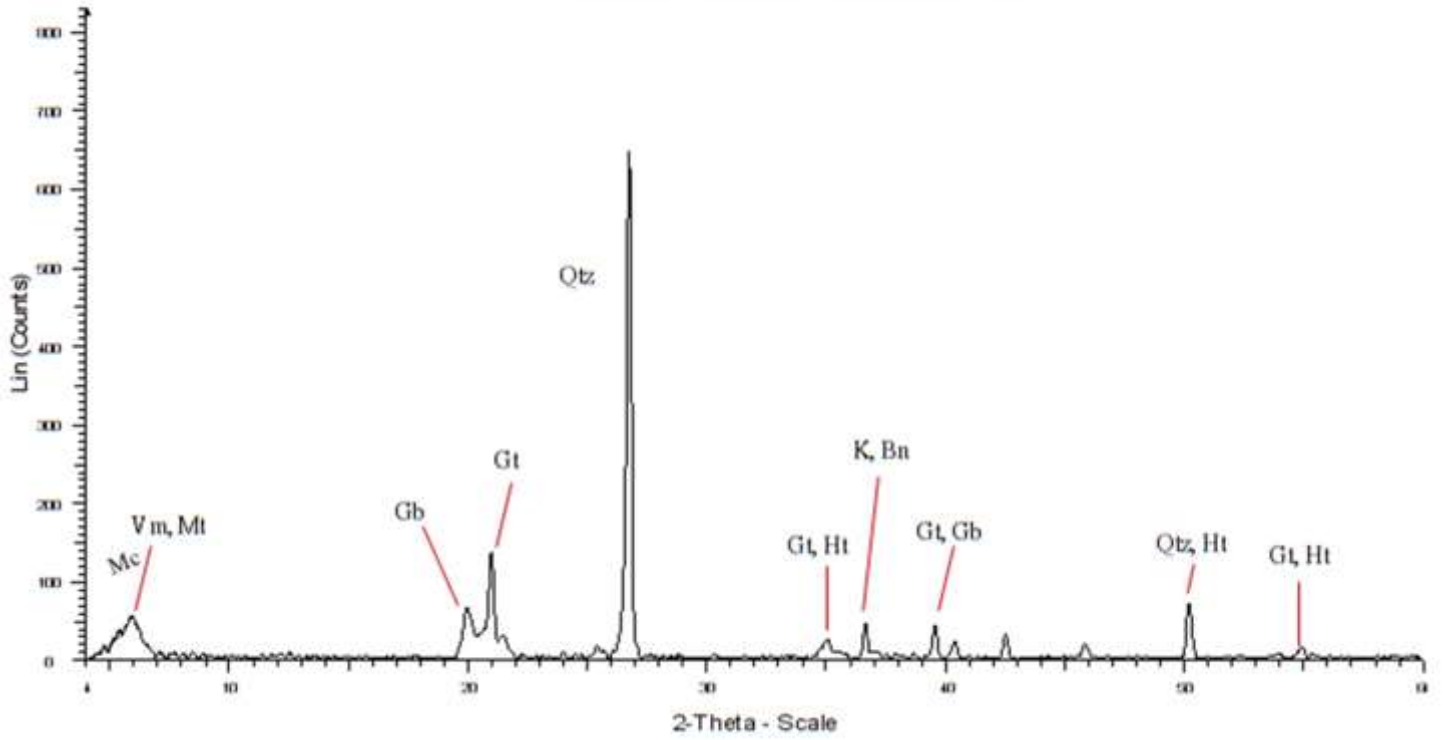
Rio Piedras Vertically Stratified D2



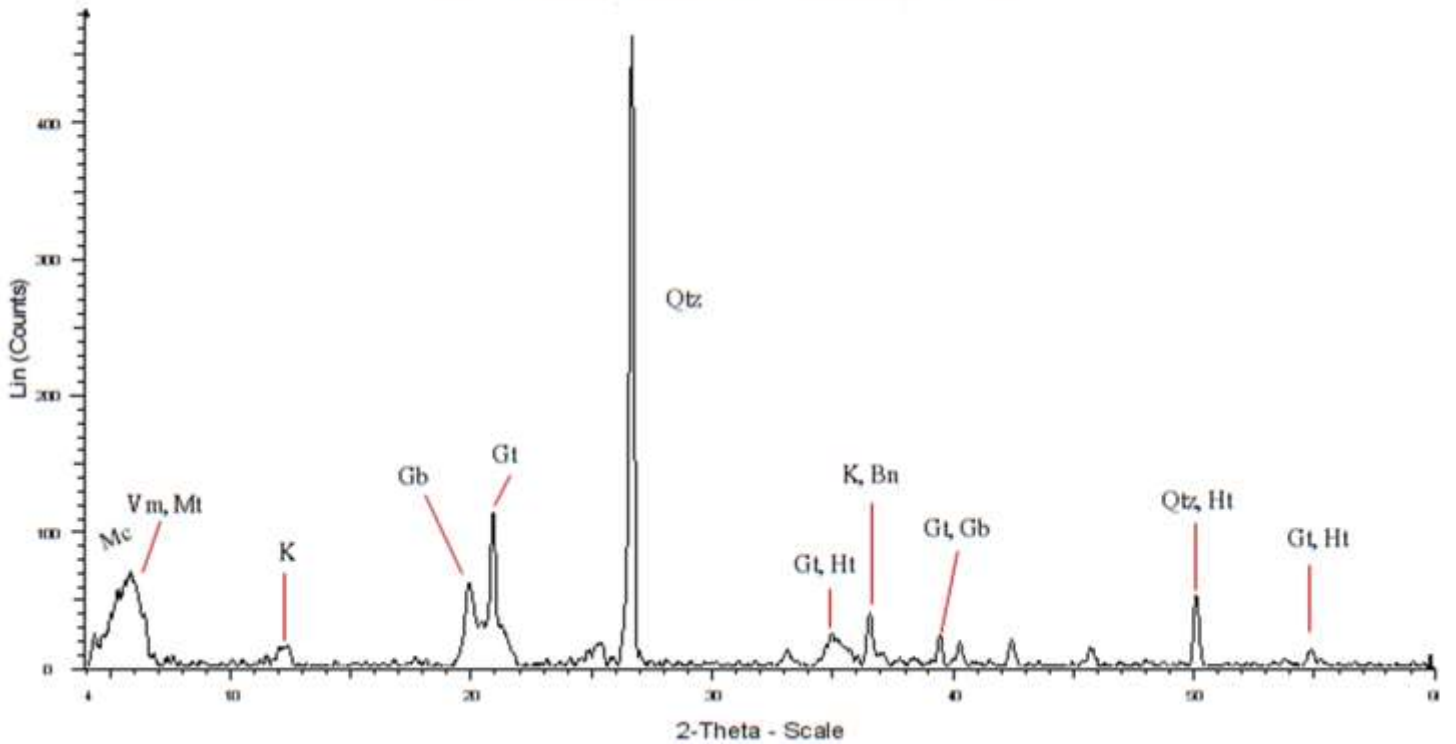
Rio Piedras Vertically Stratified D3



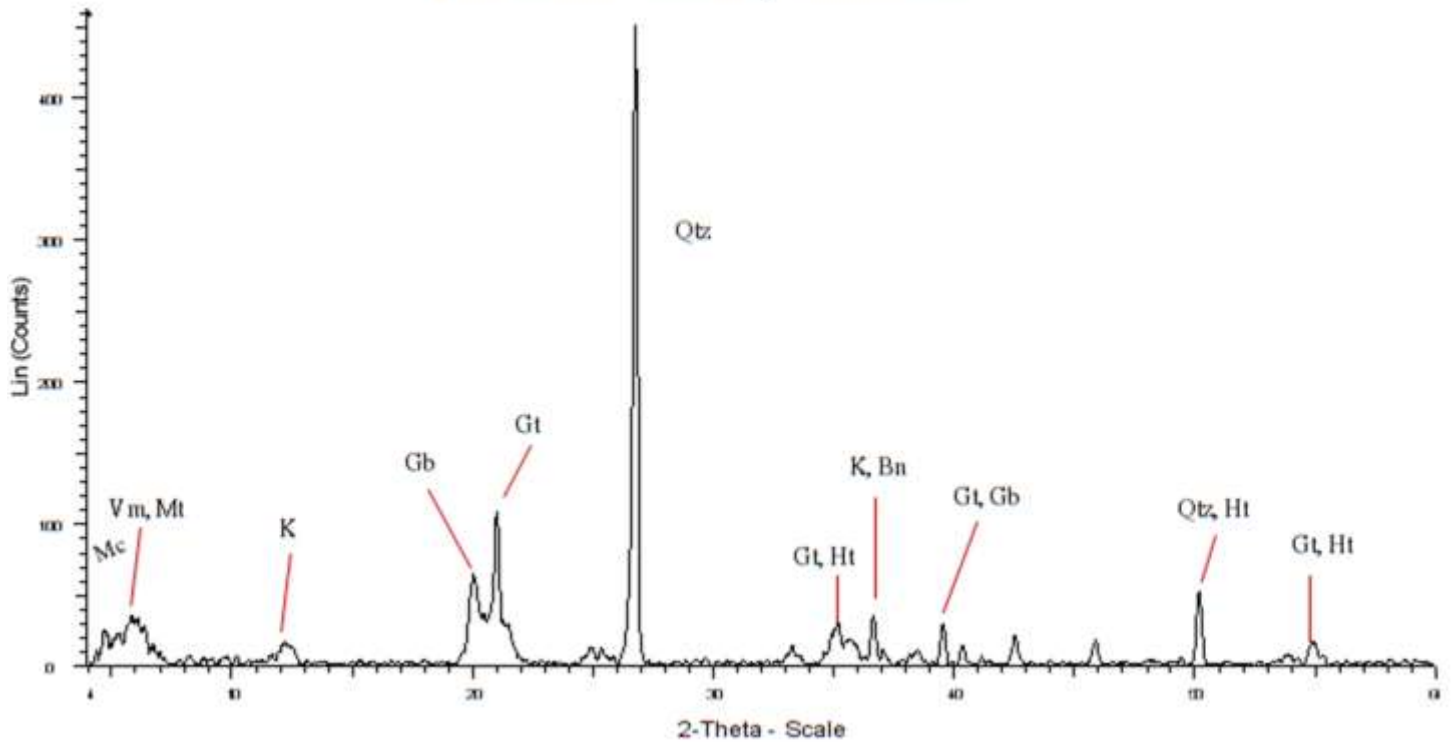
Rio Piedras Vertically Stratified D4



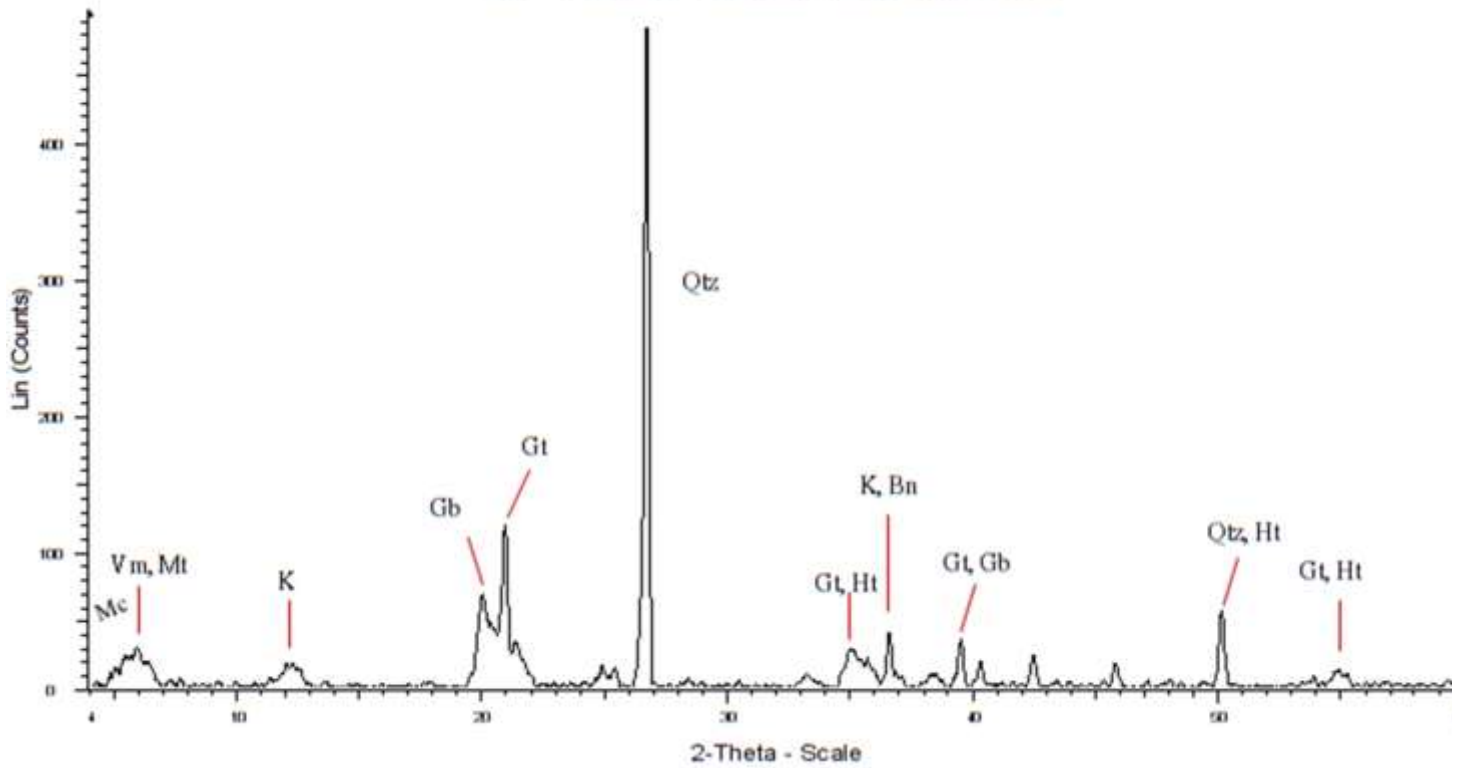
Rio Piedras Vertically Stratified ETop



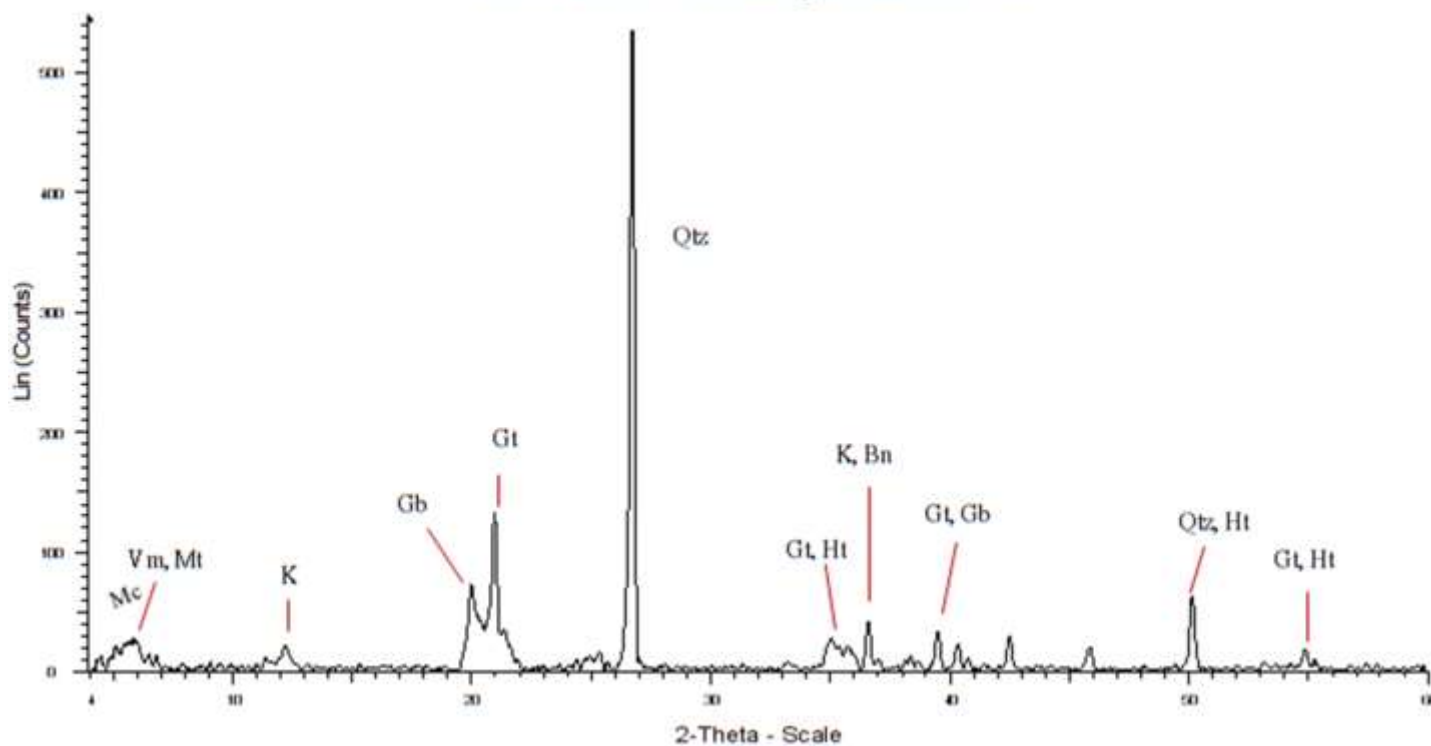
Rio Piedras Vertically Stratified E1



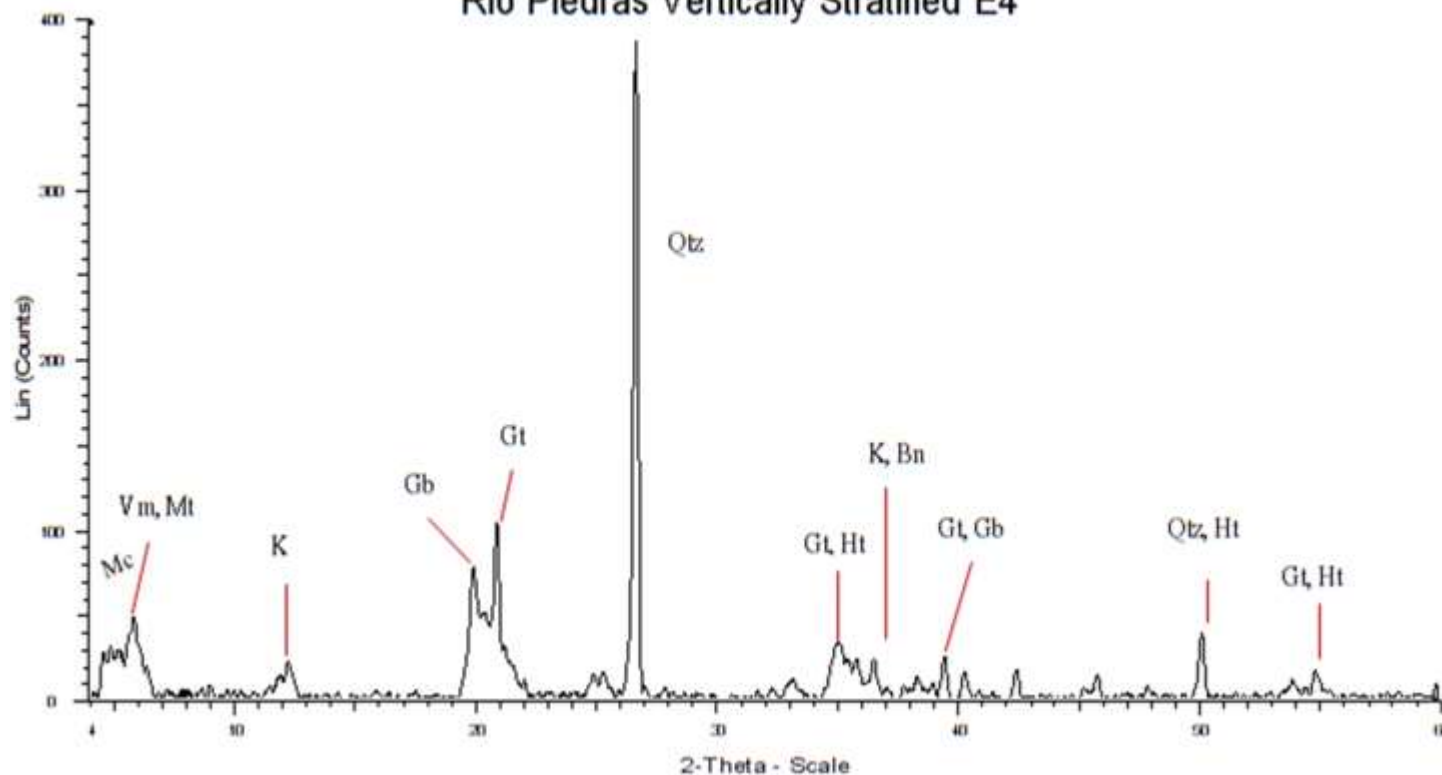
Rio Piedras Vertically Stratified E2



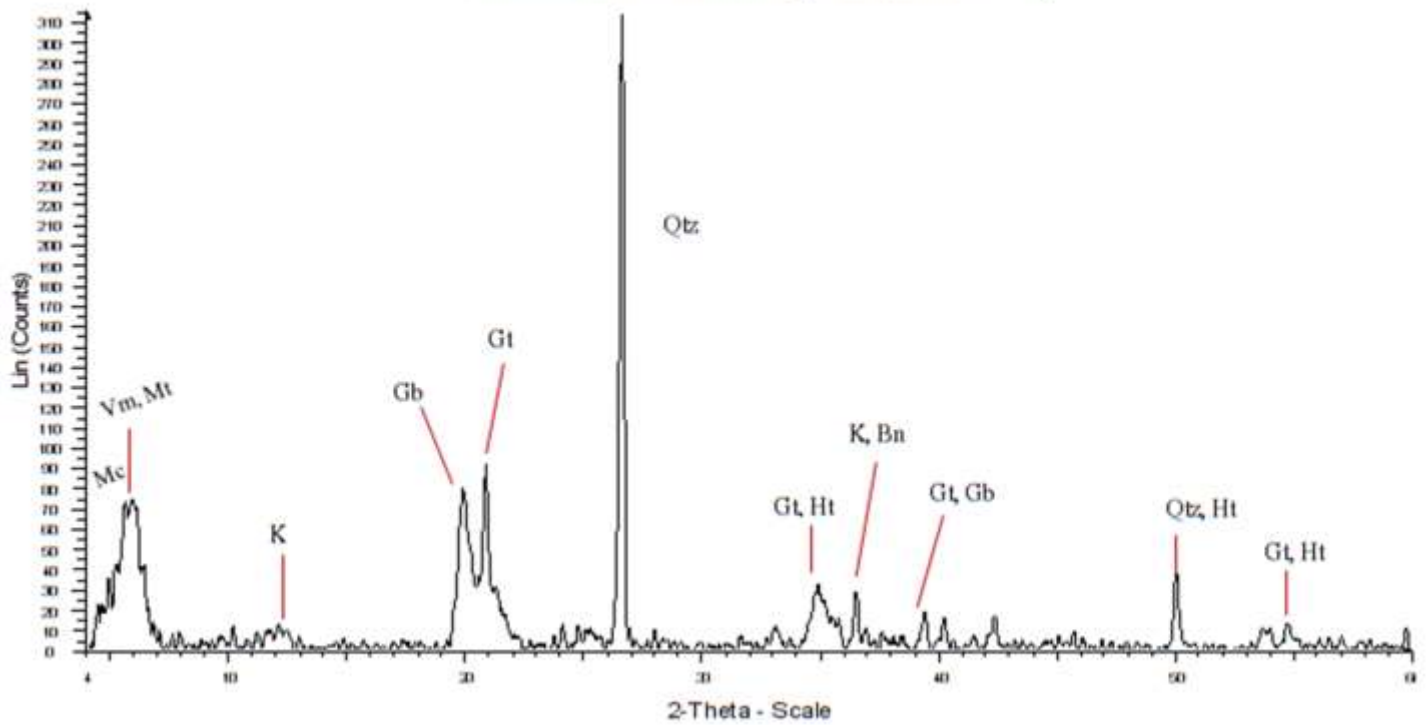
Rio Piedras Vertically Stratified E3



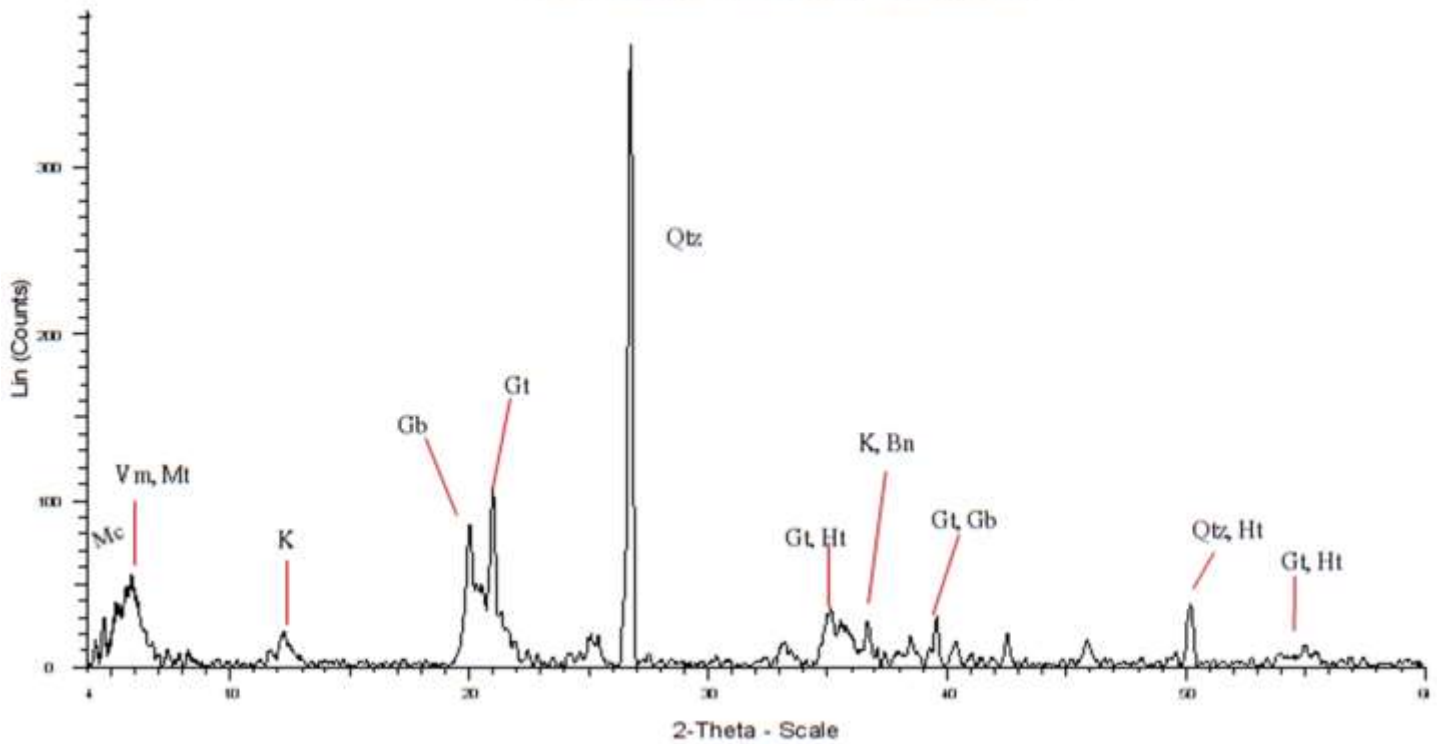
Rio Piedras Vertically Stratified E4



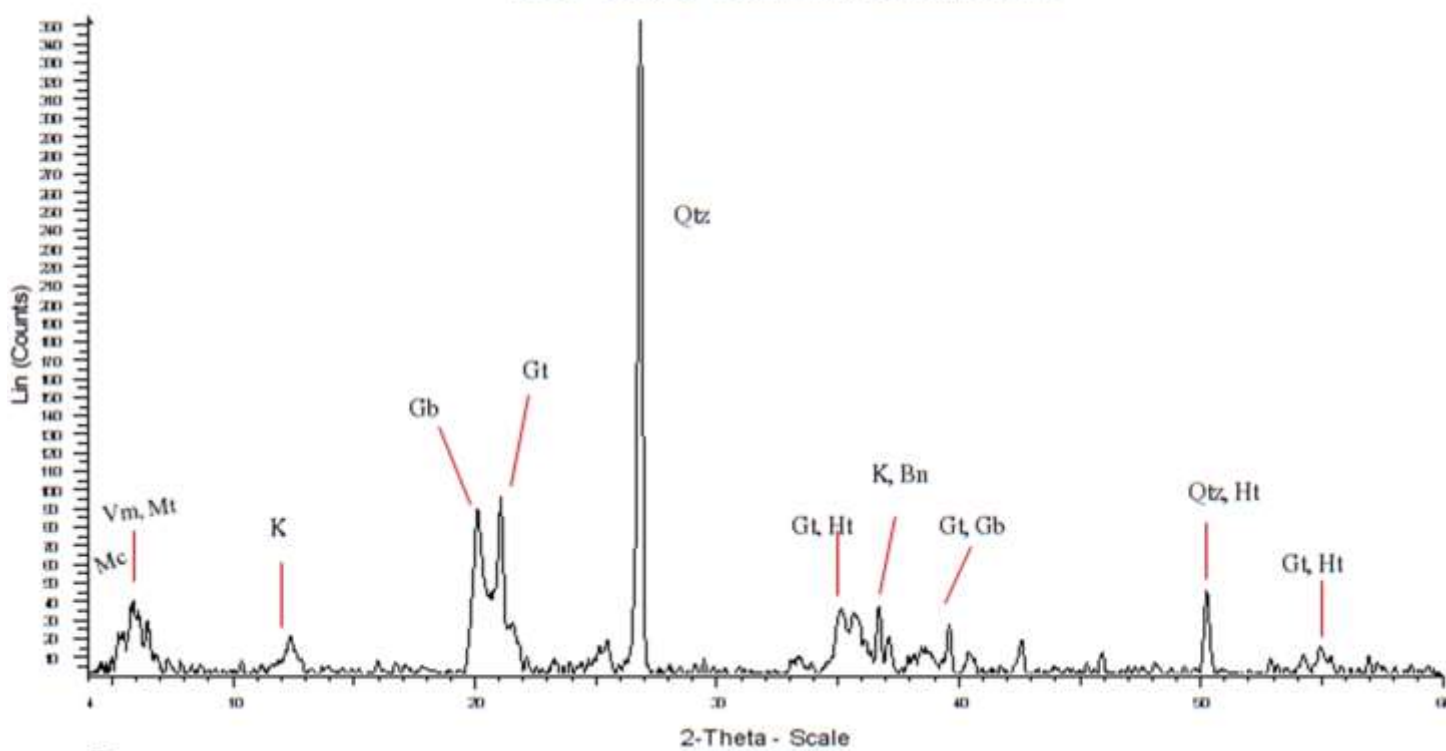
Rio Piedras Vertically Stratified FTop



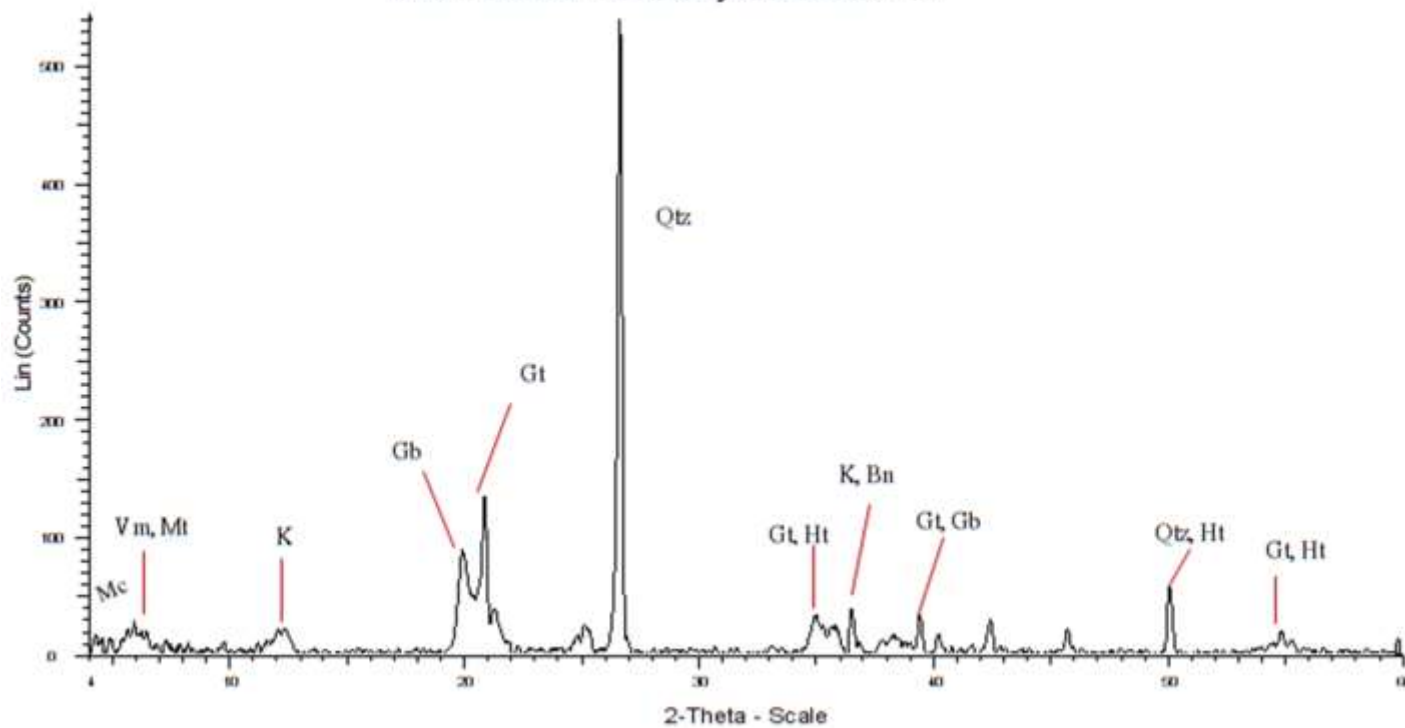
Rio Piedras Vertically Stratified F1



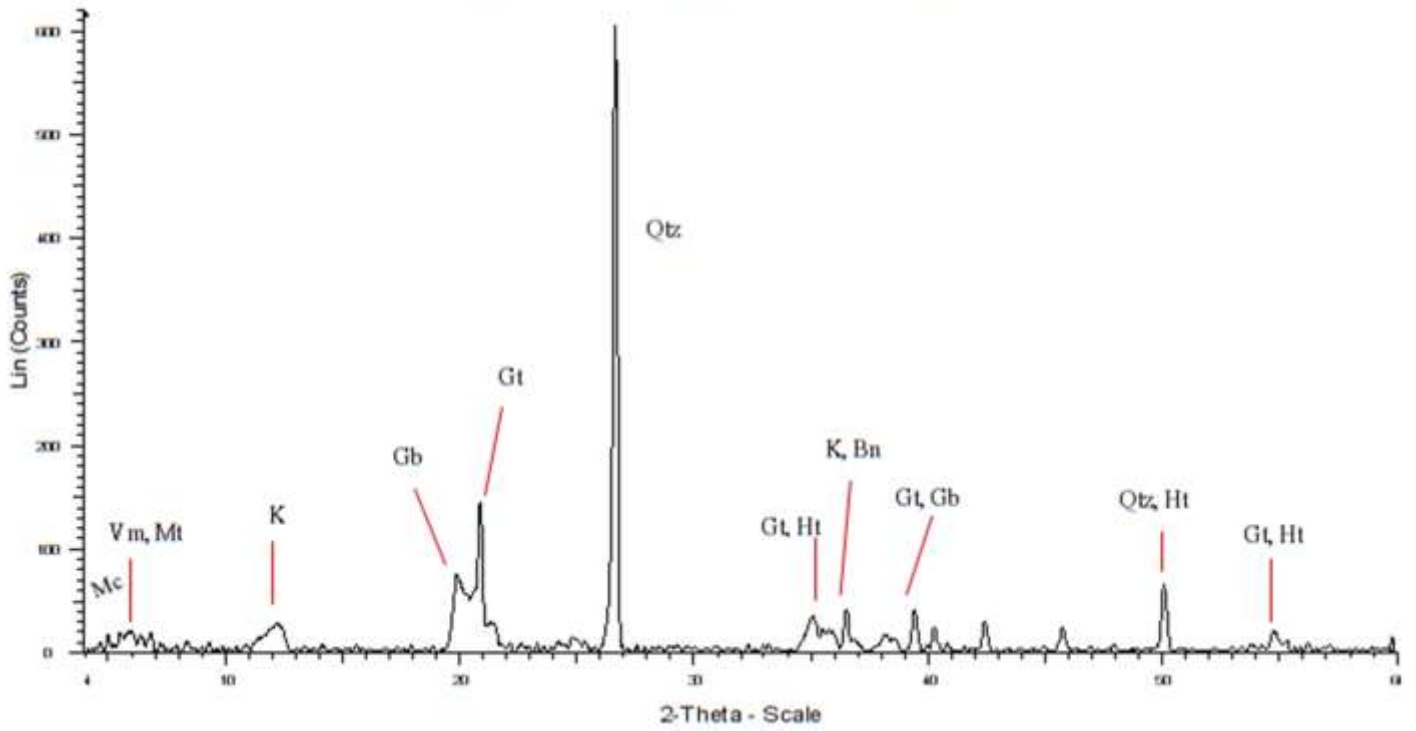
Rio Piedras Vertically Stratified F2



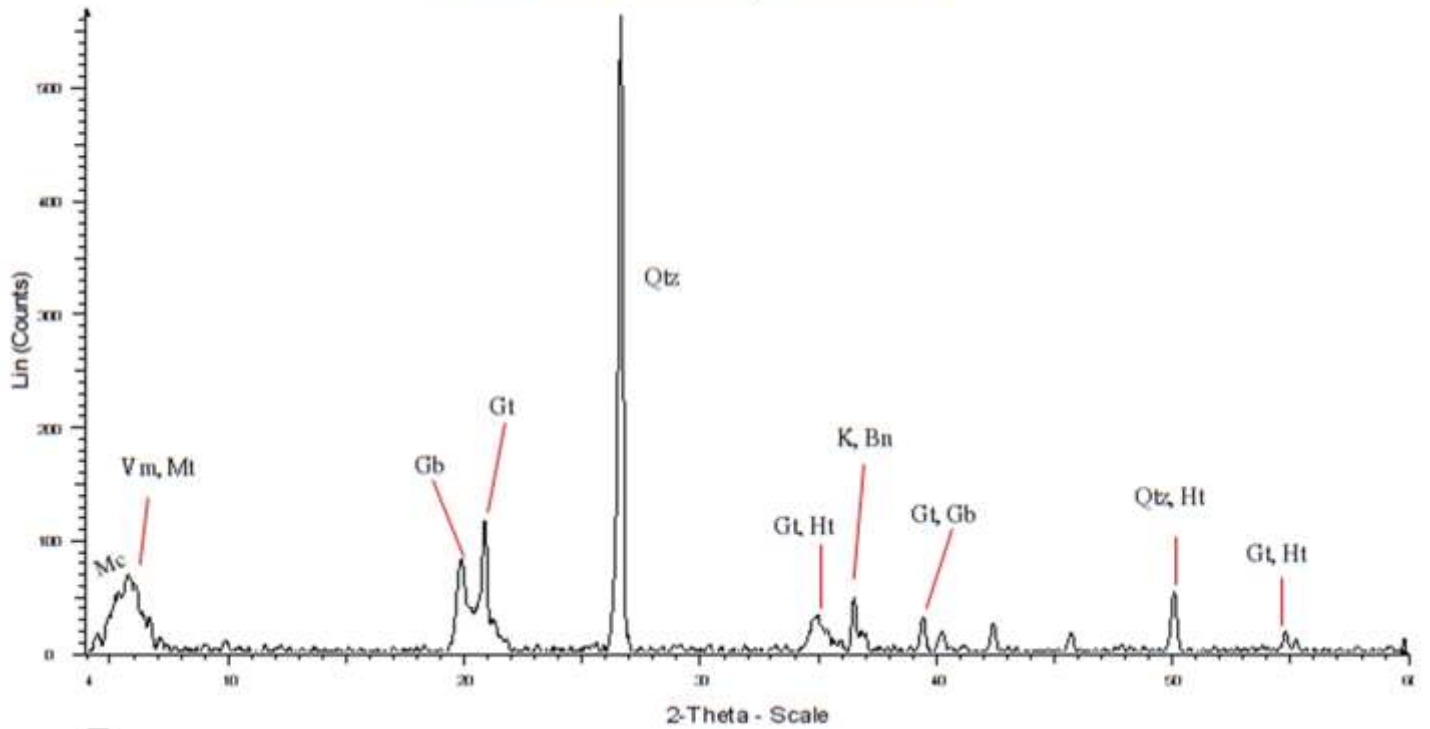
Rio Piedras Vertically Stratified F3



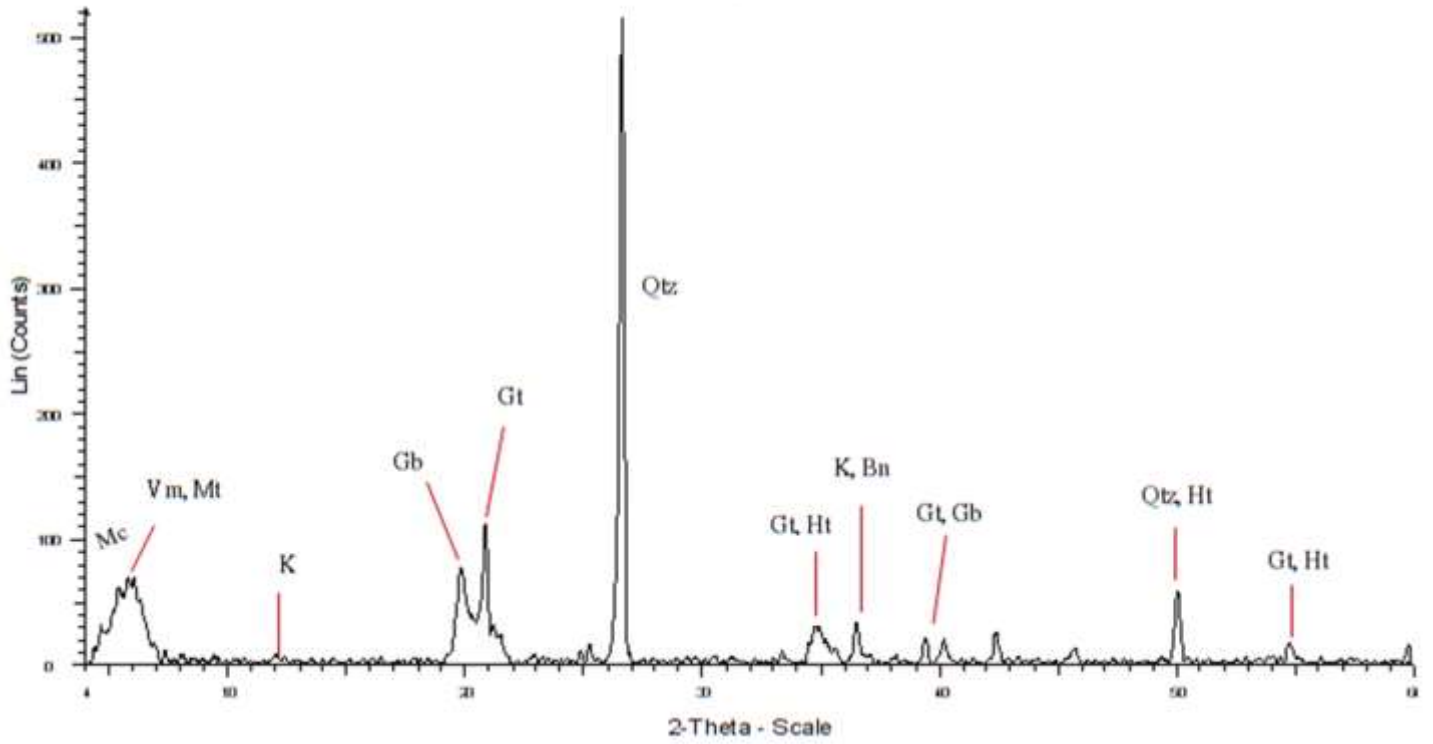
Rio Piedras Vertically Stratified F4



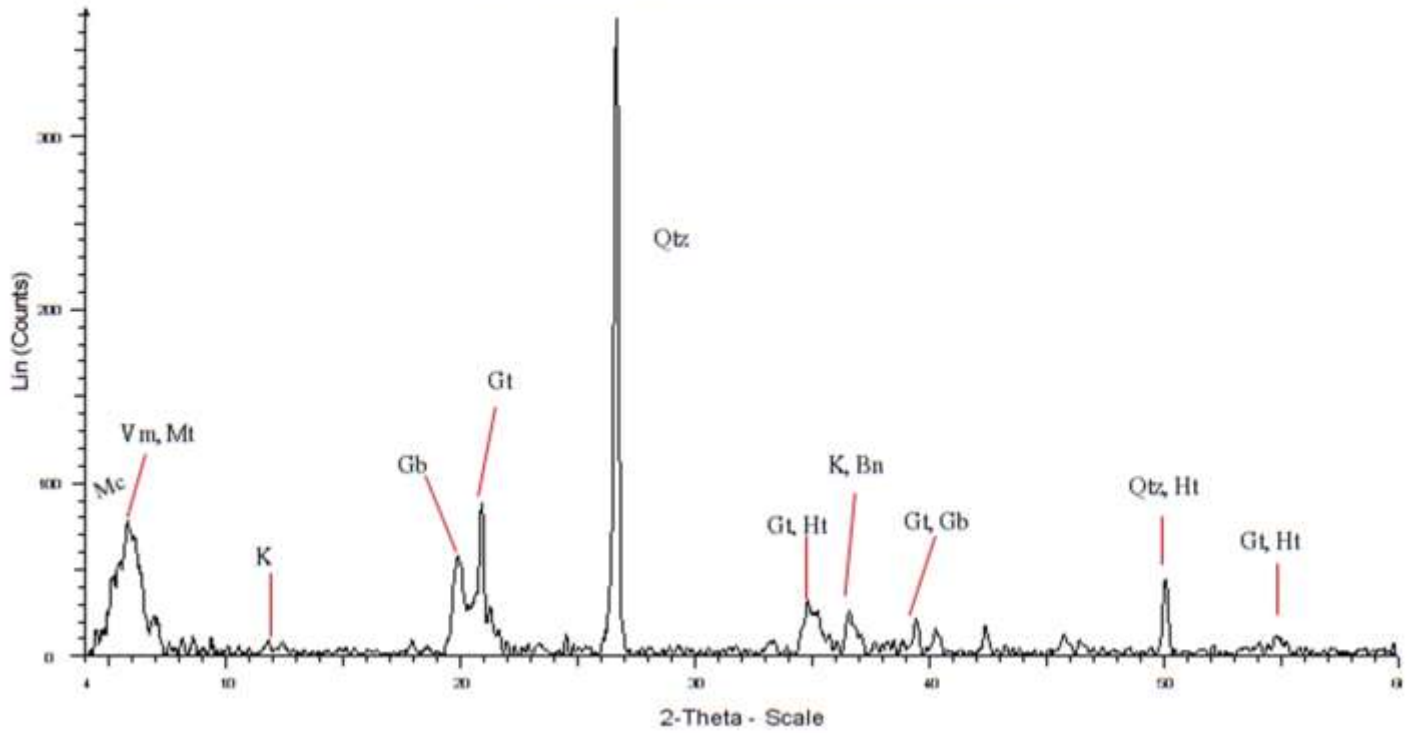
Rio Piedras Vertically Stratified G1



Rio Piedras Vertically Stratified G2



Rio Piedras Vertically Stratified G3



Rio Piedras Vertically Stratified G4

